



NATIONAL CENTER FOR EARTHQUAKE
ENGINEERING RESEARCH

State University of New York at Buffalo

Closed-Loop Modal Testing of a 27-Story
Reinforced Concrete Flat Plate-Core Building

by

H. R. Somaprasad, T. Toksoy, H. Yoshiyuki and A. E. Aktan

Department of Civil and Environmental Engineering

University of Cincinnati

Cincinnati, Ohio 45221-0071

Technical Report NCEER-91-0016

July 15, 1991

REPRODUCED BY
U.S. DEPARTMENT OF COMMERCE
NATIONAL TECHNICAL
INFORMATION SERVICE
SPRINGFIELD, VA 22161

This research was conducted at the University of Cincinnati and was partially supported by the National Science Foundation under Grant No. ECE 86-07591.

NOTICE

This report was prepared by University of Cincinnati and Takenaka Corporation as a result of research sponsored by the National Center for Earthquake Engineering Research (NCEER). Neither NCEER, associates of NCEER, its sponsors, the University of Cincinnati, Takenaka Corporation, nor any person acting on their behalf:

- a. makes any warranty, express or implied, with respect to the use of any information, apparatus, method, or process disclosed in this report or that such use may not infringe upon privately owned rights; or
- b. assumes any liabilities of whatsoever kind with respect to the use of, or the damage resulting from the use of, any information, apparatus, method or process disclosed in this report.

REPORT DOCUMENTATION PAGE	1. REPORT NO. NCEER-91-0016	2.	3. PB92-129980
4. Title and Subtitle Closed-Loop Modal Testing of a 27-Story Reinforced Concrete Flat Plate-Core Building			5. Report Date July 15, 1991
7. Author(s) H.R. Somaprasad, T. Toksoy, H. Yoshiyuki and A.E. Aktan			6.
9. Performing Organization Name and Address Department of Civil and Environmental Engineering University of Cincinnati Cincinnati, Ohio 45221-0071			8. Performing Organization Rept. No.
12. Sponsoring Organization Name and Address National Center for Earthquake Engineering Research State University of New York at Buffalo Red Jacket Quadrangle Buffalo, N.Y. 14261			10. Project/Task/Work Unit No.
			11. Contract(C) or Grant(G) No. (C) 88-0015 and 89-1007 (G) ECE 86-07591
15. Supplementary Notes This research was conducted at the University of Cincinnati and was partially supported by the National Science Foundation under Grant No. ECE 86-07591			13. Type of Report & Period Covered Technical Report
			14.
16. Abstract (Limit: 200 words) Modal testing of a 27-story reinforced concrete flat plate building with concrete cores was performed to identify a reliable analytical model. Closed-loop modal tests were performed to acquire reliable data by utilizing a linear inertia-mass exciter capable of generating a higher level of force to overcome the influence of wind excitation. Furthermore, the level of force permitted the observation of rocking. Recently developed HP SINE signal processing software with an HP-3565S measurement hardware was utilized in a close-loop test setup to control the excitation and to acquire and process the data. The natural frequencies, damping, and modal vectors were determined by post processing the measured data. It was possible to determine the mass-orthonormal modal vectors and flexibility without assuming a mass matrix. The rotational flexibility of the core foundation due to rocking was also quantified. A comparison of the current and previous modal test results is presented. An increase in the level of excitation force resulted in variations in the dynamic characteristics and lateral flexibility of the building. The performance of the hardware and software and the difficulties encountered during the test are detailed in this report. Critical parameters governing the data acquisition, signal processing, and excitation generation, which may have implications on structural control applications, are discussed.			
17. Document Analysis a. Descriptors			
b. Identifiers/Open-Ended Terms EARTHQUAKE ENGINEERING. CLOSED LOOP MODAL TESTS. DAMPING. FULL SCALE TESTS. FIELD INVESTIGATIONS. MULTISTORY BUILDINGS, REINFORCED CONCRETE BUILDINGS. FLAT PLATE CORE BUILDINGS STRUCTURAL IDENTIFICATION. NATURAL FREQUENCIES.			
c. COSATI Field/Group			
18. Availability Statement Release Unlimited		19. Security Class (This Report) Unclassified	21. No. of Pages 148
		20. Security Class (This Page) Unclassified	22. Price



**Closed-Loop Modal Testing of a 27-Story
Reinforced Concrete Flat Plate-Core Building**

by

H.R. Somaprasad¹, T. Toksoy², H. Yoshiyuki³ and A.E. Aktan⁴

July 15, 1991

Technical Report NCEER-91-0016

NCEER Project Numbers 88-0015 and 89-1007

NSF Master Contract Number ECE 86-07591

- 1 Graduate Student, Department of Civil and Environmental Engineering, University of Cincinnati
- 2 Graduate Student, Department of Mechanical, Industrial, and Nuclear Engineering, University of Cincinnati
- 3 Research Engineer, Vibration Engineering Unit, Takenaka Corporation, Tokyo, Japan
- 4 Professor and Director of Cincinnati Infrastructure Institute, Department of Civil and Environmental Engineering, University of Cincinnati

NATIONAL CENTER FOR EARTHQUAKE ENGINEERING RESEARCH
State University of New York at Buffalo
Red Jacket Quadrangle, Buffalo, NY 14261

PREFACE

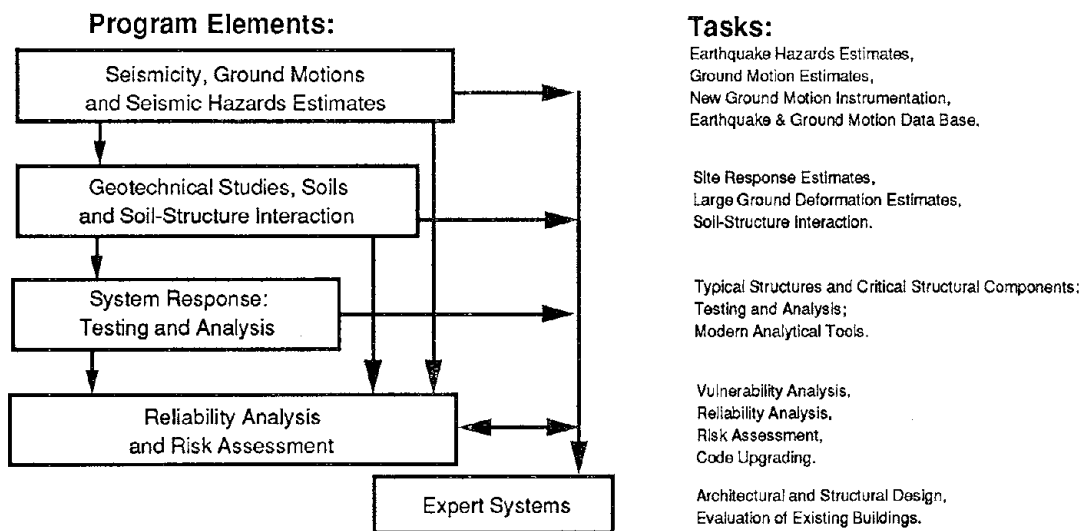
The National Center for Earthquake Engineering Research (NCEER) is devoted to the expansion and dissemination of knowledge about earthquakes, the improvement of earthquake-resistant design, and the implementation of seismic hazard mitigation procedures to minimize loss of lives and property. The emphasis is on structures and lifelines that are found in zones of moderate to high seismicity throughout the United States.

NCEER's research is being carried out in an integrated and coordinated manner following a structured program. The current research program comprises four main areas:

- Existing and New Structures
- Secondary and Protective Systems
- Lifeline Systems
- Disaster Research and Planning

This technical report pertains to Program 1, Existing and New Structures, and more specifically to system response investigations.

The long term goal of research in Existing and New Structures is to develop seismic hazard mitigation procedures through rational probabilistic risk assessment for damage or collapse of structures, mainly existing buildings, in regions of moderate to high seismicity. The work relies on improved definitions of seismicity and site response, experimental and analytical evaluations of systems response, and more accurate assessment of risk factors. This technology will be incorporated in expert systems tools and improved code formats for existing and new structures. Methods of retrofit will also be developed. When this work is completed, it should be possible to characterize and quantify societal impact of seismic risk in various geographical regions and large municipalities. Toward this goal, the program has been divided into five components, as shown in the figure below:



System response investigations constitute one of the important areas of research in Existing and New Structures. Current research activities include the following:

1. Testing and analysis of lightly reinforced concrete structures, and other structural components common in the eastern United States such as semi-rigid connections and flexible diaphragms.
2. Development of modern, dynamic analysis tools.
3. Investigation of innovative computing techniques that include the use of interactive computer graphics, advanced engineering workstations and supercomputing.

The ultimate goal of projects in this area is to provide an estimate of the seismic hazard of existing buildings which were not designed for earthquakes and to provide information on typical weak structural systems, such as lightly reinforced concrete elements and steel frames with semi-rigid connections. An additional goal of these projects is the development of modern analytical tools for the nonlinear dynamic analysis of complex structures.

The proper modeling of buildings is an important part of dynamic analysis, yet the properties of actual buildings are often not well known. This report summarizes closed-loop modal testing of a 27-story building. State-of-the-art equipment was developed and assembled for the testing, including a linear inertia-mass exciter. Nine modes were measured and the contributions of foundation rocking were identified. The performance of the exciter, and the data-aquisition and signal processing equipment is discussed in detail for the benefit of engineers interested in modal testing and active control.

ABSTRACT

Modal testing is explored as an effective tool for the structural identification of constructed facilities. Modal testing of a 27-story reinforced concrete flat plate building with concrete cores was performed to identify a reliable analytical model.

Modal tests of this building were previously carried out by utilizing a low capacity exciter and early 1980's signal processing software and hardware. The acquired data was not accurate due to a low level of excitation force which could not overcome the influence of wind excitation and due to many other limitations. Moreover, the level of excitation force was insufficient to activate the foundation rocking. Therefore, closed-loop modal tests were performed to acquire reliable data by utilizing a linear inertia-mass exciter capable of generating a higher level of force to overcome the influence of wind excitation. Furthermore, the level of force permitted the observation of rocking. Recently developed HP SINE signal processing software with an HP 3565S measurement hardware was utilized in a close-loop test setup to control the excitation and to acquire and process the data.

The natural frequencies, damping, and modal vectors were determined by post processing the measured data. It was possible to determine the mass-orthonormal modal vectors and flexibility without assuming a mass matrix. The rotational flexibility of the core foundation due to rocking was also quantified. A comparison of the current and previous modal test results is presented. An increase in the level of excitation force resulted in variations in the dynamic characteristics and lateral flexibility of the building.

The performance of the hardware and software and the difficulties encountered during the test are detailed in this report. Critical parameters governing the data acquisition, signal processing, and excitation generation, which may have implications on structural control applications, are discussed.



ACKNOWLEDGEMENTS

The research described in this report was sponsored by the National Science Foundation through the National Center for Earthquake Engineering Research, Buffalo, N.Y., Project Nos: 88-1015 and 89-1007.

Dr. D. Brown of the Structural Dynamics Research Laboratory (SDRL) at the University of Cincinnati made significant contributions to the research. His invaluable guidance is gratefully acknowledged. Drs. M. Baseheart of the Department of Civil and Environmental Engineering and R. Allemang of SDRL are faculty associates whose collaboration is acknowledged.

Contributions to all phases of the modal testing from graduate student Chuan Chuntavan, Mr. Charles Young, Development Engineer of the CEE Department, and Mr. Don Strunk, CEE Department technician, are deeply appreciated. Graduate students Messrs. I-Kang Ho, Chen Maosheng, Madwesh Raghavendrachar, and Michael Zwick assisted in various phases of the work. Their contributions are acknowledged.

Data Acquisition and signal processing equipment was provided by SDRL of the University of Cincinnati. Ms. Nancy Hall, Messrs. F. Deblauwe, Allyn Phillips, and S. Shelley of SDRL provided assistance.

The servo-controlled linear inertia-mass exciter for this test was developed by the MANTA Corporation. Mr. Michael Carlier of MANTA assisted in operating the excitation system during the tests. His contribution is acknowledged.



TABLE OF CONTENTS

<u>SECTION</u>	<u>PAGE</u>
1. INTRODUCTION -----	1-1
1.1 General -----	1-1
1.1.1 Global Objectives of Research -----	1-1
1.1.2 Definition of Structural Identification and Related Terms-----	1-1
1.1.3 Need for Structural Identification to Evaluate Capacities of Constructed Facilities -----	1-3
1.1.4 Role of Modal Testing in Structural Identification ---	1-5
1.1.5 Comparison of Modal Testing to Early Forced-Vibration Testing-----	1-6
1.1.6 Need for the Current Modal Test -----	1-8
1.2 Objectives and Scope of the Report -----	1-9
2. DESCRIPTION OF THE TEST BUILDING AND REVIEW OF THE PREVIOUS MODAL TEST -----	2-1
2.1 General -----	2-1
2.2 Description of the Test Building -----	2-1
2.3 Seismic Attributes of the Building -----	2-5
2.4 Description of the Previous Modal Test -----	2-6
2.5 Results of the Previous Test -----	2-8
2.6 Limitations and Shortcomings -----	2-11
3. AMBIENT RESPONSE STUDIES -----	3-1
3.1 General -----	3-1
3.2 Test Setup -----	3-1
3.3 Monitoring the Ambient Conditions -----	3-2

TABLE OF CONTENTS (CONTD)

<u>SECTION</u>	<u>PAGE</u>
3.4 Data Acquisition and Storage -----	3-2
3.5 Ambient Test Results -----	3-5
4. CLOSED-LOOP MODAL TEST -----	4-1
4.1 General -----	4-1
4.2 Test Setup -----	4-1
4.2.1 Exciter Location -----	4-4
4.2.2 Sensor Locations -----	4-4
4.3 Significant Characteristics of the Test Setup -----	4-11
4.4 Description of the Equipment -----	4-12
4.4.1 Excitation System -----	4-12
4.4.1.1 Exciter and Hydraulic Pump -----	4-12
4.4.1.2 Servo-Controller -----	4-16
4.4.1.3 Verifying the Excitation System -----	4-16
4.4.2 Data Acquisition System -----	4-18
4.4.2.1 Work Station -----	4-18
4.4.2.2 Signal Processing Hardware -----	4-18
4.4.2.3 Signal Processing Software -----	4-21
4.4.2.4 Analog Filters -----	4-21
4.4.2.5 Amplifiers -----	4-21
4.4.2.6 Accelerometers -----	4-21
4.4.2.7 Cables -----	4-22
4.5 Execution of the Modal Test -----	4-22

TABLE OF CONTENTS (CONT'D)

<u>SECTION</u>	<u>PAGE</u>
4.5.1 General -----	4-22
4.5.2 Data Acquisition and Storage -----	4-22
4.5.3 Frequency Domain Measurements -----	4-26
4.5.4 Response Time Histories -----	4-26
5. POST PROCESSING -----	5-1
5.1 General -----	5-1
5.2 Algorithm -----	5-1
5.2.1 Significance of the Algorithm -----	5-1
5.2.2 Description of the Algorithm -----	5-2
5.2.3 Complex Modes vs Normal Modes -----	5-3
5.2.4 Residual Terms -----	5-4
5.3 Filtering -----	5-7
5.3.1 Filter Characteristics -----	5-7
5.3.2 Correction for the Filter Effect -----	5-7
5.3.3 Effect of Filtering on the Modal Vectors and Flexibility -----	5-7
5.4 Discussion of Errors -----	5-10
6. RESULTS OF MODAL TEST -----	6-1
6.1 Natural Frequencies and Damping -----	6-1
6.2 Mode Shapes Including Foundation Displacements -----	6-1
6.3 Mass-Orthonormal Modal Vectors and Flexibility -----	6-10
6.4 Assessment of Differences Between the Results of Current Test, Previous Test, and Ambient Test -----	6-12

TABLE OF CONTENTS (CONT'D)

<u>SECTION</u>	<u>PAGE</u>
7. TEST FOLLOWING PARTIAL REMOVAL OF EXTERIOR CLADDING -----	7-1
7.1 General -----	7-1
7.2 Test Setup and Data Acquisition -----	7-1
7.3 Test Results -----	7-4
8. DIAPHRAGM DISTORTION TEST -----	8-1
8.1 General -----	8-1
8.2 Test Setup -----	8-1
8.3 Test Results and Conclusions -----	8-3
8.3.1 Excitation in the EW Direction -----	8-3
8.3.2 Excitation in the NS Direction -----	8-3
8.3.3 Conclusions -----	8-3
9. SYSTEM PERFORMANCE AND CONTROL IMPLICATIONS -----	9-1
9.1 General -----	9-1
9.2 Conclusions Regarding System Performance -----	9-3
10. CONCLUSIONS AND RECOMMENDATIONS -----	10-1
10.1 Conclusions -----	10-1
10.2 Recommendations -----	10-4
11. REFERENCES -----	11-1
APPENDIX A: SPECIFICATIONS OF THE HARDWARE AND SOFTWARE USED FOR THE MODAL TEST -----	A-1
APPENDIX B: NORMALIZED MODAL VECTORS AND FLEXIBILITY -----	B-1

LIST OF FIGURES

<u>FIGURE</u>		<u>PAGE</u>
1-1	Typical Limit-States and Corresponding supplies -----	1-2
1-2	Changes in Mechanical Characteristics Due to Changes in Stress Levels -----	1-10
2-1	Photographs of the Test Building -----	2-2
2-2	Plan of the Typical Floor of the Test Building -----	2-3
2-3	3D Isometric View of the Structure-Foundation System -----	2-4
2-4	Details of the Cores at the Basement -----	2-7
2-5	Flow Chart of the Instruments Used in the Previous Test for Excitation Generation -----	2-9
2-6	Flow Chart of the Instruments Used for the Data Acquisition in the Previous Test -----	2-9
2-7	Comparison of Responses Obtained in the Previous Test Under Both Ambient and Random Forced Excitation -----	2-10
2-8	Coherence Between Excitation and Diaphragm Response at the Roof Level Obtained in the Previous Test -----	2-10
2-9	Mode Shapes and Natural Frequencies Obtained From the Previous Test -----	2-12
2-10	Lateral Flexibility of the Building Obtained from the Previous Test -----	2-15
3-1	Block Diagram of the Test Setup for the Ambient Test -----	3-3
3-2	Photograph of the Weather Station Display Unit -----	3-4
3-3	Power Spectra of Response at the 26th Floor due to Ambient Wind Excitation in NS and EW directions -----	3-6
4-1	Block Diagram of the Closed-Loop Test Setup -----	4-2
4-2	Block Diagram of the Swept Sine Excitation Control -----	4-3

LIST OF FIGURES (CONT'D)

<u>FIGURE</u>	<u>PAGE</u>
4-3 Block Diagram of Hardware and Software for Data Acquisition --	4-3
4-4 Photograph of the Linear Inertia-Mass Exciter Mounted on the RC Column at the 25th Floor -----	4-5
4-5 Instrumented Floors and Location of Accelerometers -----	4-6
4-6 Location of the Exciter and Accelerometers at the Test Floor (Floor 25) -----	4-8
4-7 Photographs of Accelerometers Mounted on the Core at the Basement and on the RC Column at the 26th Floor -----	4-9
4-8 Location of Accelerometers at the Basement -----	4-10
4-9 Photographs of the Linear Inertia-Mass Exciter and the Hydraulic Pump -----	4-13
4-10 Photograph of the Digital Servo-Controller -----	4-14
4-11 Block diagram of the Excitation System -----	4-15
4-12 Comparison of Specified and Actual Dynamic Force Capacity Spectrum of the Exciter -----	4-17
4-13 Photograph of the Data Acquisition Equipment Used for the Closed-Loop Modal Test -----	4-19
4-14 Block Diagram of Modules of the Measurement Hardware -----	4-20
4-15 Typical Plan-Time Schedule Used to prepare for the Test -----	4-23
4-16 Power Spectrum of the Input Force due to Excitation in NS and EW Directions -----	4-27
4-17 Frequency Response Function at the Driving-Point -----	4-28
4-18 Frequency Response Functions at Different Floors due to Excitation in the EW Direction -----	4-29
4-19 Time Histories (Filtered) of the Excitation Signal and Driving-Point at the First EW Mode -----	4-30

LIST OF FIGURES (CONTD)

<u>FIGURE</u>	<u>PAGE</u>
4-20 Time Histories of Responses (Unfiltered) at Different Floors at the First EW Mode -----	4-31
5-1 Comparison of Complex Curve Fitting with Normal Curve Fitting -----	5-5
5-2 Comparison of Curve fitting with and without including Residual Terms -----	5-6
5-3 Frequency Response Function of Filtered Channel with Reference to Unfiltered Channel (Magnitude and Phase) -----	5-8
5-4 Comparison of Flexibility Obtained with and without Correction for Filter -----	5-9
6-1 Comparison of the First Nine Mode Shapes obtained from the Previous and Current Modal Tests -----	6-3
6-2 Location of Accelerometers at the Basement for Measuring Foundation Displacements -----	6-7
6-3 Phase Difference Between Responses on Either Side of the Core (Between V_1 and V_2 in Fig. 6-2) at the Third EW Mode ----	6-8
6-4 Imaginary Part of Frequency Response Functions Measured on Either Side of the Core in the EW Direction in the Frequency Range of 0.5625 Hz to 0.84375 Hz -----	6-9
6-5 Comparison of the Lateral Flexibility Coefficients of the Building Obtained When Loaded at the 26th Floor from the Previous and Current Modal Tests -----	6-11
6-6 Time Histories of Response at the 26th Floor due to Different Wind Levels and Forced Excitation at the First NS Mode -----	6-13
6-7 Effect of Type and Level of Force on the First Natural Frequency of the Building -----	6-14
7-1 Photographs of the Building Before and After Removal of Some of the Exterior Cladding -----	7-2
7-2 Block Diagram of the Test Setup for Tests Following Asbestos Removal -----	7-3

LIST OF FIGURES (CONT'D)

<u>FIGURE</u>		<u>PAGE</u>
8-1	Location of the Exciter and Accelerometers for the Diaphragm Distortion Test -----	8-2
8-2	Diaphragm Displacement at Torsional Modes due to the Excitation Force in EW and NS Directions -----	8-4

LIST OF TABLES

<u>TABLE</u>		<u>PAGE</u>
3-1	Variations in Natural Frequencies due to Variations in Levels of Wind Excitation in the NS Direction -----	3-7
4-1	Data Acquisition Settings Used in the Closed-Loop Modal Test --	4-24
6-1	Comparison of Natural Frequencies and Damping Obtained from Previous and Current Tests -----	6-2
7-1	Comparison of Natural Frequencies Measured by Different Tests -----	7-5



SECTION 1

INTRODUCTION

1.1 General

1.1.1 Global Objective of Research

The global objective of the research reported herein is to seek means of reliably evaluating the existing stiffness, strength, and energy dissipation supplies of constructed facilities. Unless the SUPPLIES or CAPACITIES of a constructed facility (building-foundation-soil-piles or bridge deck-piers-piles-abutments-soil, etc.,) in its existing state are estimated with a reasonable confidence (say 85%), it is not possible to reliably evaluate its resistance against earthquakes or other demands. Also, proper understanding of the capacities is essential in order to reliably design maintenance or upgrade for a constructed facility.

The supplies or capacities of a constructed facility have been defined (Aktan and Ho, 1990) based on the limit states of performance (Fig. 1-1). The limit states are broadly defined as serviceability, damageability (or ultimate), and failure limit states. At the serviceability limit state, critical capacities would include stiffness, inertia, damping, geometric stability, and fatigue. At the damageability limit state, critical capacities are yielding strength, hardening, deformability, hysteretic energy dissipation, geometric stability, and stability of hysteresis. At the failure limit state, critical capacities would include mode of failure and post failure reserves.

1.1.2 Definition of Structural Identification and Related Terms

Structural identification is defined as the application of system identification technique to solve structural engineering problems. System identification is a process for constructing a mathematical description or model of a physical system when both the input (forcing function) to the system and the corresponding output (displacements or other

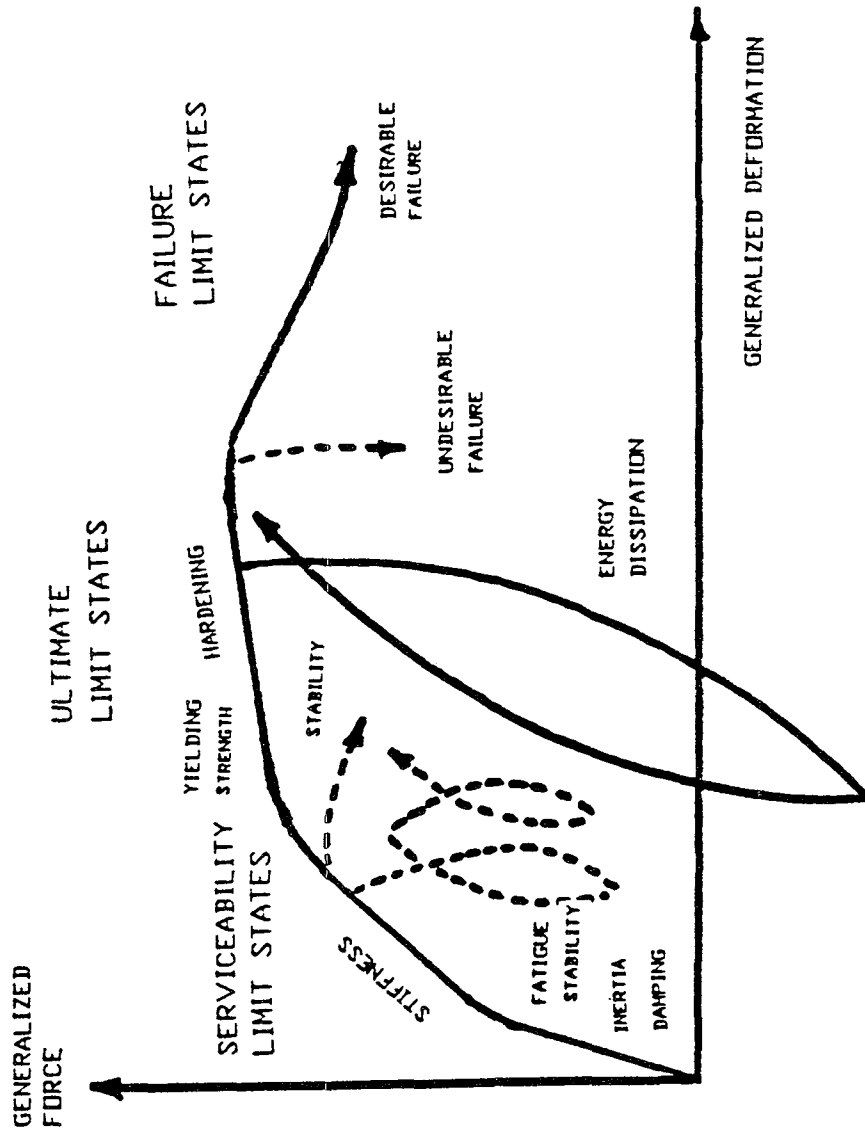


Figure 1-1 Typical Limit-States and Corresponding supplies.

motions of the structure subjected to these forces), are known (Yao, 1985). System identification technique is applied in structural engineering to obtain an analytical model which can best represent the characteristics of constructed facilities.

A rigorous definition of the identification of constructed facilities has been offered: "Constructed facility identification is to conceptualize a soil-foundation-super structure and to quantify, test, improve, and validate the resulting analytical model by correlating its predicted, measured, and simulated responses. The identification of a constructed facility should lead to an understanding of: (a) All the critical mechanisms of inertia and flexibility; (b) the 3D response kinematics; (c) the resistance mechanisms (load paths); (d) the critical regions; and, (e) localized force, deformation and accumulated damage states at the critical regions" (Hogue, Aktan and Hoyos, 1991).

1.1.3 Need for Structural Identification to Evaluate Capacities of Constructed Facilities

The structural engineering profession has been utilizing analytical modeling and analysis procedures for evaluating the supplies of existing constructed facilities. These evaluation techniques are similar to those applied in designing new facilities. There is evidence, however, that the reliability of capacity estimates based on analytical models and analysis procedures used in new design may not be acceptable in evaluating existing facilities. This is especially true if a facility is aged and deteriorated due to previous overloads, damage, or simply designed and constructed with undesirable attributes. The only means to improve the reliability in evaluation and upgrade design is to improve the reliability of analytical prediction. Hence, practical global and regional structural identification is needed in order to construct reliable analytical models and bound the supplies of an existing facility with a level of confidence needed for effective upgrading (Aktan, 1988).

A methodology incorporating structural identification has been formulated to reliably establish the existing capacities of a constructed facility (Aktan and Ho, 1990). This

methodology includes: (a) Fact-finding, generating a data base, and conceptualizing the facility which is being evaluated; (b) linearized 3D analytical modeling of the facility and its experimental identification; (c) establishing the critical regions, elements, and response mechanisms by studying the identified model; (d) localized in-situ experimental identification of the critical regions by appropriate non-destructive techniques and sampling and testing of materials; (e) estimating local capacities at all the limit states by incorporating the experimentally determined existing conditions; (f) establishing region-site-and-facility-specific critical demands; and, (g) transforming the identified linearized model into a nonlinear model by incorporating the estimated local capacities, followed by 3D step-by-step collapse analyses. These analyses should provide bounds of the system supplies and local demands for estimated global demands.

Although identifying a linearized analytical model is a key step for reliably bounding the capacities of a constructed facility, there are considerable difficulties in achieving this model. Certain obstacles may entail (Hogue, Aktan and Hoyos, 1990): (a) Lack of a coordinated effort by the profession towards a standardized methodology; (b) many of the mechanisms which influence responses of irregular or aged constructed facilities are not yet understood; (c) problems in mechanical, numerical, and computational modeling of mechanisms which are known to influence responses; (d) problems in reliable experimentation; (e) failure to integrate the existing analytical research on identification with experimentation; and, (f) failure to transfer the existing knowledge-base in modal testing of mechanical structures to constructed facility identification.

Identifying a linearized analytical model of a building-foundation-soil does not directly permit estimating supplies of strength, deformability, and energy dissipation at the advanced limit states. However, by improving and calibrating a linearized analytical model and by quantifying the critical mechanical characteristics, a reliable starting point for the nonlinear analyses of a constructed facility can be obtained (Aktan, 1988). After all, the most critical requirement of an analytical model, whether it is to be used for linear or

nonlinear analysis, is to simulate the 3D geometry, displacement kinematics, force-paths, and critical/local response mechanisms of a structure-foundation-soil system.

Unfortunately, the present analytical modeling techniques fail to accomplish this for many constructed facilities due to: (a) Certain complex mechanisms such as foundation rocking/uplift, foundation distortions at the base of the walls, out-of-plane and in-plane distortions of diaphragms, etc., influence the 3D kinematics of the complete structure. Conceptualizing these mechanisms, which are typically omitted in modeling, is not easy. Although this task is difficult, simulation of these mechanisms is important during all limit state responses of large-scaled test specimens (Aktan and Bertero, 1987) and therefore, should not be overlooked; (b) difficulties in modeling irregular architectural attributes, nonstructural and secondary elements, soil-foundation flexibility, and 3D loading (Aktan and Nelson, 1988); (c) problems in estimating the material characteristics of different structural elements; and, (d) problems in discretizing large facilities into a manageable number of coordinates and parameters.

The difficulties listed above, as well as ignorance of many other response mechanisms which influence the kinematics of a structure, compound the uncertainties in analytical modeling. Therefore, conceptualizing and experimental verification afforded by structural identification becomes a necessity for reliable modeling.

1.1.4 Role of Modal Testing in Structural Identification

Modal testing has emerged as the most powerful tool for the experimental component of linearized structural identification in the mechanical and aerospace engineering disciplines. The experimentally identified natural frequencies, mode shapes, mass-orthonormal modal vectors, and damping factors are used as a basis for improving and calibrating analytical models of structures in geometric coordinates, i.e. finite-element models. Therefore, the writers have concentrated their research into exploring how the expertise accumulated in modal testing of mechanical structures may be imported to modal

testing of constructed facilities.

Although modal testing of structures has evolved over the past decade into a well established application area, some problems are still encountered in its applications. Common problems faced in the experimental modal analysis were synthesized by Ibrahim (1988): (a) The number of measurement degrees of freedom and test coordinates in modal testing is limited and also is different from those of the analytical model; (b) some modes of the test structure may not be excited or may be weakly excited; (c) some modes may not be identified by the modal test and the number of those modes that are identified is limited; (d) the modal vectors derived from the data processing algorithms are typically complex whereas the structural analysis is based on the normal modes; (e) errors are involved in the measured data; and, (f) the algorithms, used to refine the analytical model from the modal test results, are not sufficiently rigorous and lack physical justification or meaning.

1.1.5 Comparison of Modal Testing to Early Forced-Vibration Testing

Since the 1960's, forced-vibration tests of more than thirty full scale buildings were conducted to determine their dynamic characteristics. While rotating-weight type exciters were commonly administered, there have also been reported attempts to develop and use a rectilinear force generator.

In the early sixties, tests were conducted on buildings by using a counter-rotating eccentric weight type vibration generator which was designed and developed jointly by the California Institute of Technology and the University of California, Berkeley. The details of the exciter and tests are given by Hudson (1964) and Nielsen (1966). The rotating-weight exciter found continued use for forced-vibration tests in the seventies and eighties in U.S. with additional applications in Europe and Japan (Hudson, 1977, Jeary et al, 1981, Beliveau, 1981, Aktan et al, 1983, Neuss et al, 1983 and Stephen et al, 1985, etc.,).

Although forced-vibration tests using a rectilinear force generator were conducted on several buildings (Hudson, 1977, and Craig and Lewis, 1981), applications with this type

of exciter did not continue. A rectilinear exciter developed by the Georgia Institute of Technology was based on an electro-hydraulic actuator capable of generating random and sinusoidal types of excitation. However, this exciter had such problems as oscillatory instability and chatter in the air bearings (Craig and Lewis, 1981). Installation was also difficult due to its large size.

Regardless of the type of exciter employed, the purpose of forced-vibration tests reported in the seventies and early eighties was to measure a small number of structural responses (typically lateral accelerations of floors) and to calculate the dynamic characteristics from these responses. The linear spectra of the time histories of responses, commonly termed as resonance curves, were typically used to determine the natural frequencies, damping, and mode shapes without fitting a mathematical model to the measured data. The frequencies were found by picking the peaks, and damping was calculated from the band-width of the resonance curves. As for the mode shapes, relative floor response amplitudes at the resonances were measured and plotted. Typically, floor responses were not measured simultaneously due to a lack of capable dynamic data-acquisition hardware. The accuracy of the results was often questionable due to many sources of error involved in dynamic testing (Aktan, 1986). Furthermore, mass-orthonormal modes and the lateral flexibility could not be obtained without assuming a mass matrix.

The limitations of the earlier forced-vibration tests may be overcome by modal tests using servo-controlled linear-mass exciters that can be integrated with recently developed multi-channel signal processing software and hardware. Modal testing involves the measurement of frequency response functions, which requires the measurement of input force as well as response. This type of testing is based on the assumptions and governing principles of the modal theory which transforms physical coordinates into modal space. Rigorous post-processing of the data is required to obtain the damped natural frequencies, damping ratios, and mass-normalized modal vectors. The frequency band of interest is typically wider than what has been considered in the forced-vibration tests of the early

eighties. Scaled modal vectors (mass-orthonormal modal vectors) and flexibility can be derived without assuming a mass matrix. Furthermore, since all the data is measured and processed together, the identified properties correspond to a rationally linearized modal model of the complete facility. This approach in determining dynamic properties of structures has been proven to be a more accurate and reliable method than the earlier forced-vibration tests. Therefore, it is now being adapted to testing large-scale constructed facilities.

1.1.6 Need for the Current Modal Test

Previous modal tests of a 27-story building, located at the University of Cincinnati campus, were conducted by utilizing the modal test hardware and software available since the early eighties (Ho and Aktan, 1989). Using a 1500 lbf linear inertia-mass exciter, the lower modes could be only weakly excited. The responses due to forced excitation and wind were of similar magnitude. Since the influence of the wind excitation was significant relative to the forced excitation responses, reliability of the modal parameters derived from this test became questionable. Furthermore, researchers observed many limitations and shortcomings in applying 1980's vintage data acquisition hardware and software to reliable testing of buildings in the 1990's as discussed in detail in Section 2. These limitations and shortcomings indicated the need to repeat the modal tests to acquire more reliable data.

A new servo-controlled linear inertia-mass exciter was developed especially for the current modal tests. This new exciter could generate a force at the fundamental frequency of the building six times higher than that of the exciter used in the previous test. In addition, state-of-the-art signal processing hardware and software developed in the last several years were utilized in a closed-loop test setup for the current modal tests.

1.2 Objectives and Scope of the Report

The specific objectives of the work described in this report are as follows:

- (1) To obtain more reliable data by repeating modal tests, exploring the newly developed linear inertia-mass exciter and the latest signal processing hardware and software within a closed-loop test setup. Correlating the results of earlier and current modal tests is expected to reveal any limitations of the earlier tests and possible errors in the results.
- (2) It is well established that mechanical characteristics of buildings depend on test stress level. This is schematized in Fig. 1-2. Changes in initial mechanical characteristics typically occur due to changes in ambient conditions, soil-foundation-structure interactions, nonstructural-structural element interactions, existence and dissipation of initial stresses, and changes in the damping mechanisms. The desired test stress level corresponds to the state at which all the critical service-level response characteristics of the building are activated and stabilized (Fig. 1-2). In this regard, the critical mechanism of foundation rocking and uplift could not be activated in the previous modal test. Hence, an important objective of the current test was to conduct modal tests at stress levels well above those caused by gravity and ambient conditions. With this cause and effect, the kinematics of foundation response due to soil and foundation displacements could be captured and a representative foundation flexibility may be quantified.
- (3) Rigorous closed-loop modal tests of the building were performed in June and July of 1990. A portion of the exterior cladding was subsequently removed from the building to eliminate asbestos before implosion. Another objective was to repeat the forced-vibration tests following the removal of the exterior cladding to investigate possible influence of cladding on the dynamic characteristics of the building.
- (4) In previous tests, variations in the natural frequencies of the building were observed during ambient and forced excitation. Therefore, another objective was to conduct

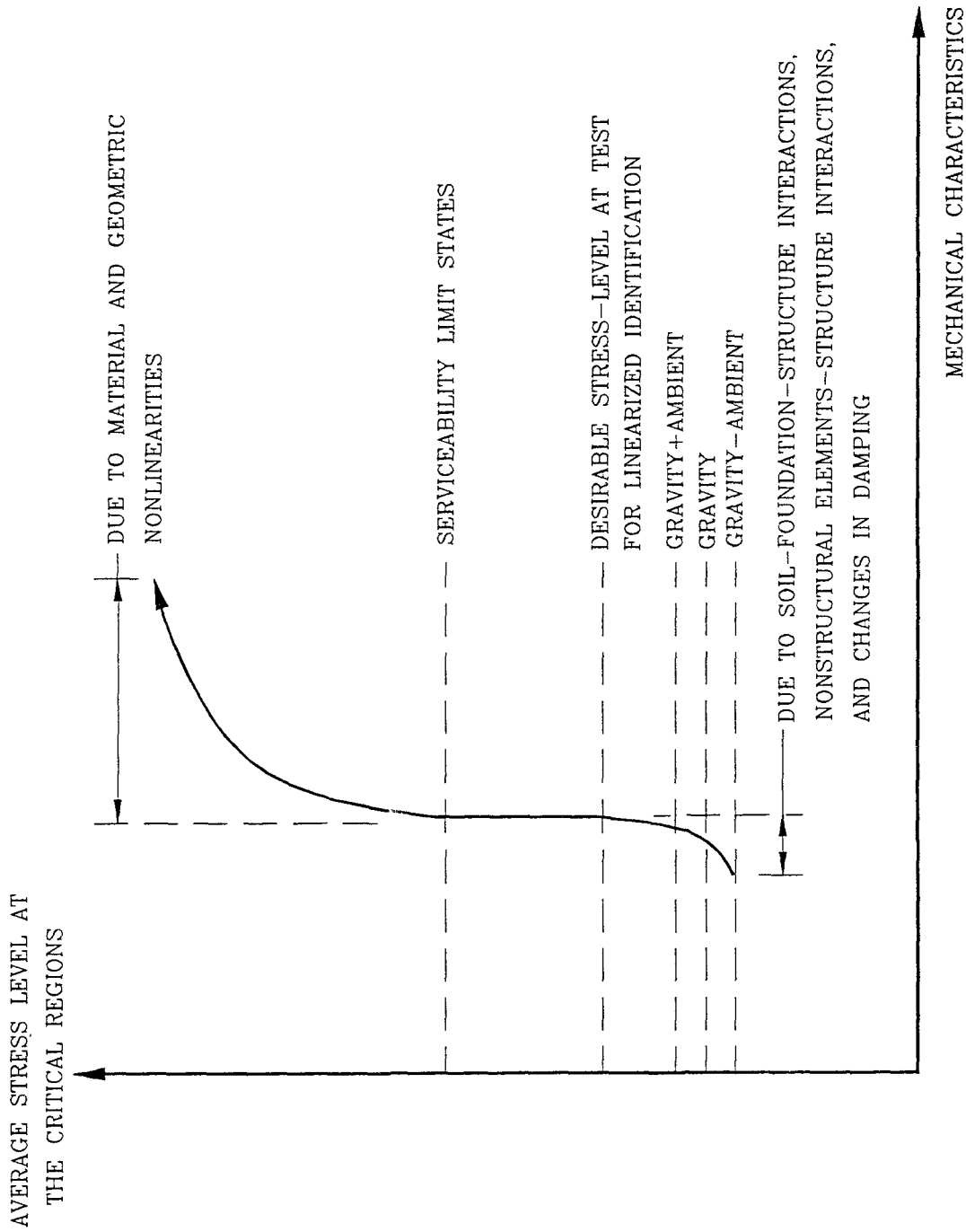


Figure 1-2 Changes in Mechanical Characteristics Due to Changes in Stress Levels.

ambient vibration tests to study the frequency shifts due to fluctuating wind excitation. The frequencies measured from ambient vibration tests were compared with those obtained from the modal test.

- (5) In 3D analysis of buildings, many computer programs neglect in-plane deformations of the diaphragm. However, some of the previous forced-excitation tests indicated in-plane diaphragm distortions in higher modes (Stephen et al, 1985). Conducting modal tests to study in-plane responses of the diaphragm at higher modes was another objective.
- (6) Various algorithms for the active control of buildings have been investigated by many researchers. For structural control implementations, consideration of important factors include the performance of electro-hydro-mechanical actuators, sensors, and data acquisition and processing hardware and software. Understanding the behavior of the hardware and software and the interaction between the components used in the current closed-loop modal test revealed realities which have bearing on structural control applications. Therefore, another objective was to discuss the implications of the current closed-loop modal test on active control implementations in real buildings.

The scope of the report is organized as follows:

Details of the test building, its structural system, and its undesirable attributes are described in Section 2, followed by a description of the previous modal test and observed shortcomings of the equipment utilized in this test.

Details of the test setup, test equipment, and results of the ambient excitation tests are discussed in Section 3.

The closed-loop modal test setup is introduced in Section 4. Significance of the closed-loop test setup, description of the hardware and software administered, and the test procedures are discussed. Execution of the modal test and data acquisition is described.

The post processing of the data to derive modal parameters is described in Section

5, followed by the modal test results which are presented in Section 6. The mass-orthonormal modal vectors and lateral flexibility including the foundation flexibility were obtained without assuming the inertia. The current and previous test results are also compared in Section 6 and the variations in fundamental frequency measured by various procedures are compared.

Details of the test setup and results of modal tests repeated following the removal a portion of the exterior cladding are discussed in Section 7.

The setup and results of the diaphragm distortion test are described in Section 8. The performance of the hardware and software used in the modal test and the implications of these on structural control applications are discussed in Section 9.

The summary, conclusions, and recommendations are presented in section 10.

SECTION 2
DESCRIPTION OF THE TEST BUILDING AND REVIEW OF THE PREVIOUS
MODAL TEST

2.1 General

The most important characteristics of the test building and its seismic attributes are reviewed. In addition, hardware and software, test setup, and results of the previous tests of this building are briefly reviewed. Finally, the limitations and shortcomings of the previous test are discussed.

2.2 Description of the Test Building

Photographs of the 27-story reinforced concrete test building are shown in Fig. 2-1. The building was constructed as an undergraduate residence hall in 1968, and was closed in 1978 due to a lack of adequate fire safety measures. Even after additional fire escapes were provided, social and political constraints would not allow the use of the building as a residence hall. Since the limited elevator facilities and architectural features did not permit the conversion of the building for other purposes, it was imploded in June 1991.

A typical floor plan of the test building is shown in Fig. 2-2. The structural system consists of RC flat-slabs with several peripheral shear walls and two central cores. The cores are coupled by beams at the first four floors and by the flat slab at the remaining floors. The peripheral walls are terminated at the third floor. The total height of the building, including the basement, is 275 feet with the typical story height being 9 feet, except that of five floors indicated in Fig. 2-2. The thickness of the floor slab is 7.25 inches, except for the reduction to 5 inches between the cores. The 3D isometric view of the structure-foundation system is shown in Fig. 2-3.

An elevation difference of 15 feet exists between the grade at the N and S faces (N indicated in Fig. 2-2). The foundation system consists of individual spread footings cast

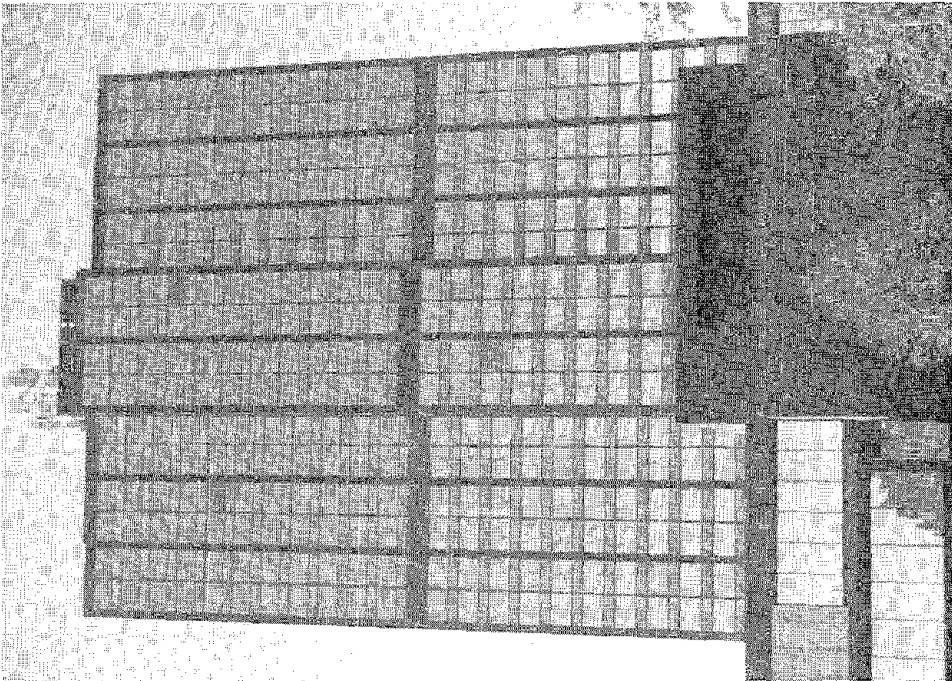
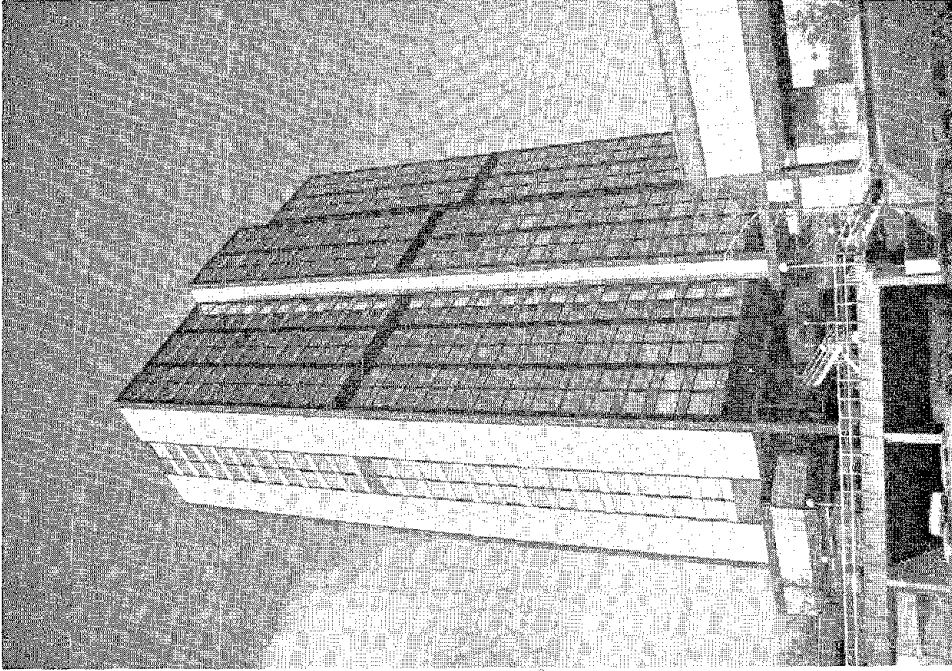


Figure 2-1 Photographs of the Test Building.

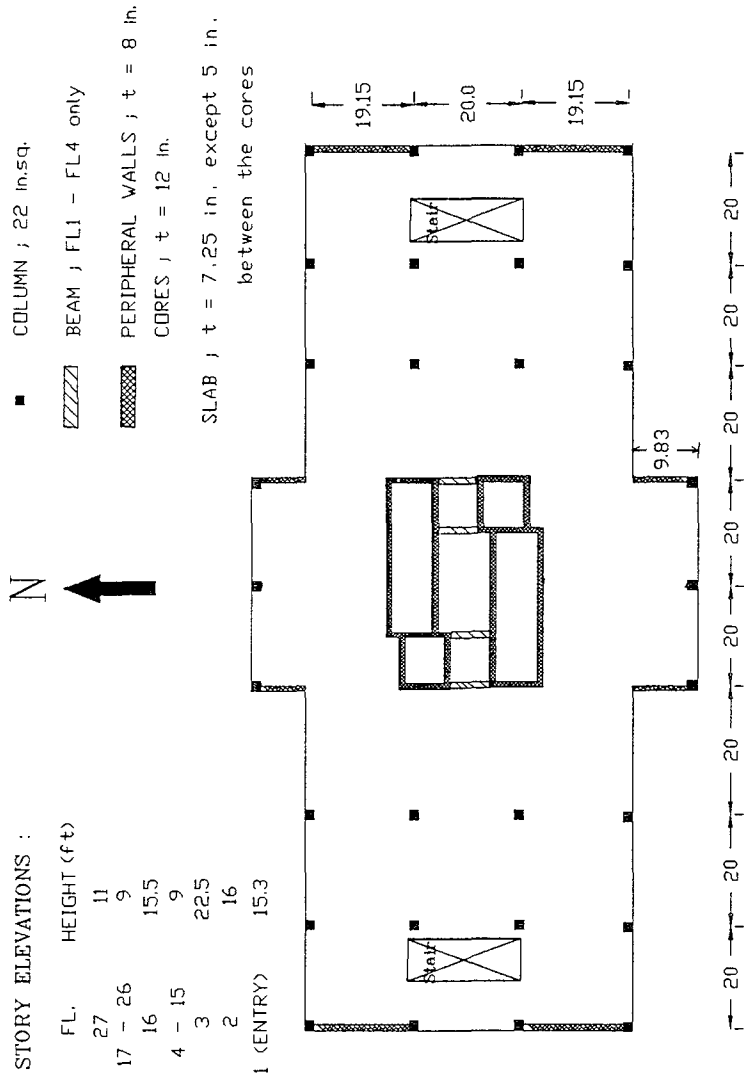


Figure 2-2 Plan of the Typical Floor of the Test Building.

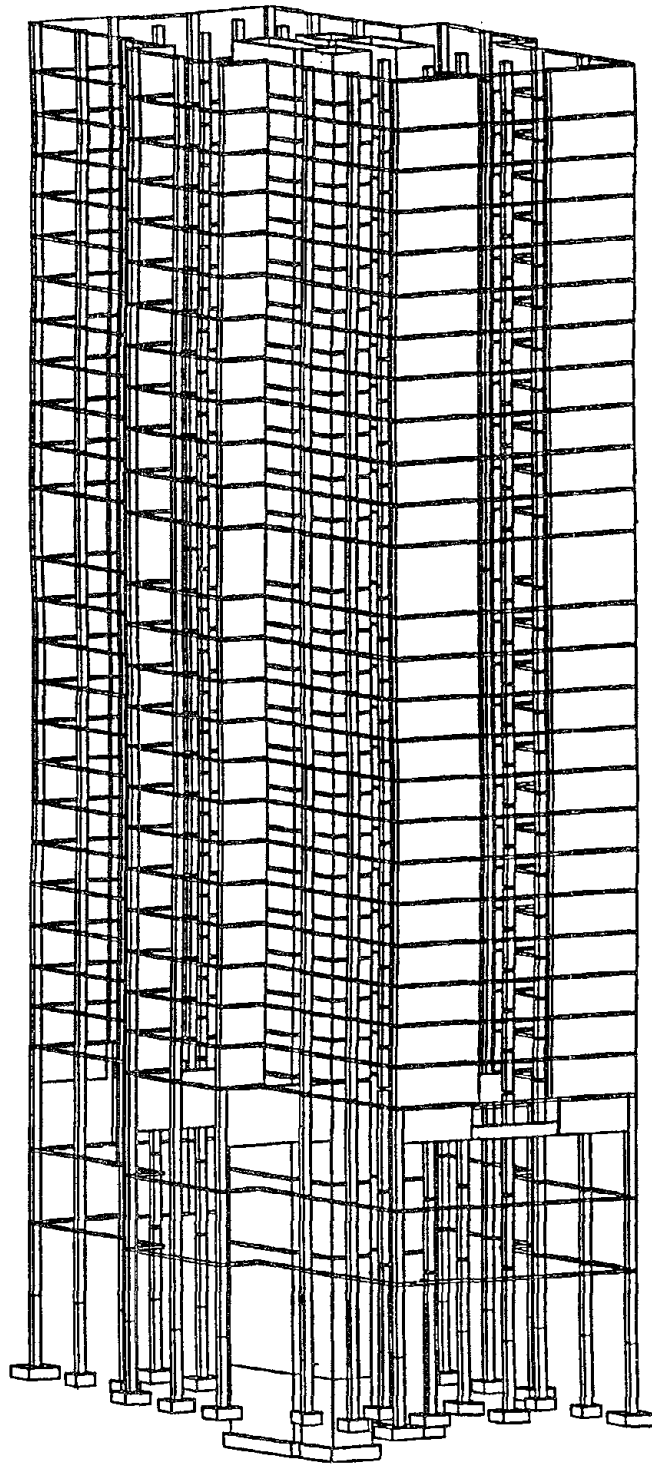


Figure 2-3 3D Isometric View of the Structure-Foundation System.

directly on rock. The column footings have a depth of only 4 feet below the grade and the core foundation is 7 feet deeper than the column footings. The footings of the two cores are at different levels bearing on sloped contours of the excavated rock. Bore tests indicate hard shale with thin layers of limestone, rated for a bearing capacity of more than 25 tons per square foot. The interior nonstructural elements are made of light wood products. Exterior cladding consists of lightweight precast panels nailed on concrete and glass panels mounted with rubber on a flexible aluminum frame. A structural steel appendage of 2400 square feet in plan as well as several microwave antenna towers are located on the roof.

2.3 Seismic Attributes of the Building

The critical attributes of the building make it a challenging test specimen. Some of the features described earlier by Aktan and Ho (1990) are:

- (1) Peripheral RC walls terminate at the third floor leading to significant stiffness discontinuity at this level with a particular reduction in the torsional stiffness.
- (2) Forces from the terminated peripheral walls are transferred to slender corner columns. Therefore, it is reasoned that shear from the peripheral walls would have to be transferred to the core via the diaphragm at the third floor.
- (3) Central core foundations bear on rock at a shallow depth without any anchorage. This raises concern regarding rocking and uplifting and their influence on the overturning resistance of the building.
- (4) 7.25 inch thick diaphragms without thickened edges, in spite of a large plan aspect ratio of 2.7.
- (5) A significant portion of the lateral stiffness is provided by the central cores, however, there is an absence of specially designed details for the most critical connections such as core-wall corners and core-slab interfaces.

Dimensions and reinforcement details of the cores, the first floor diaphragm, and

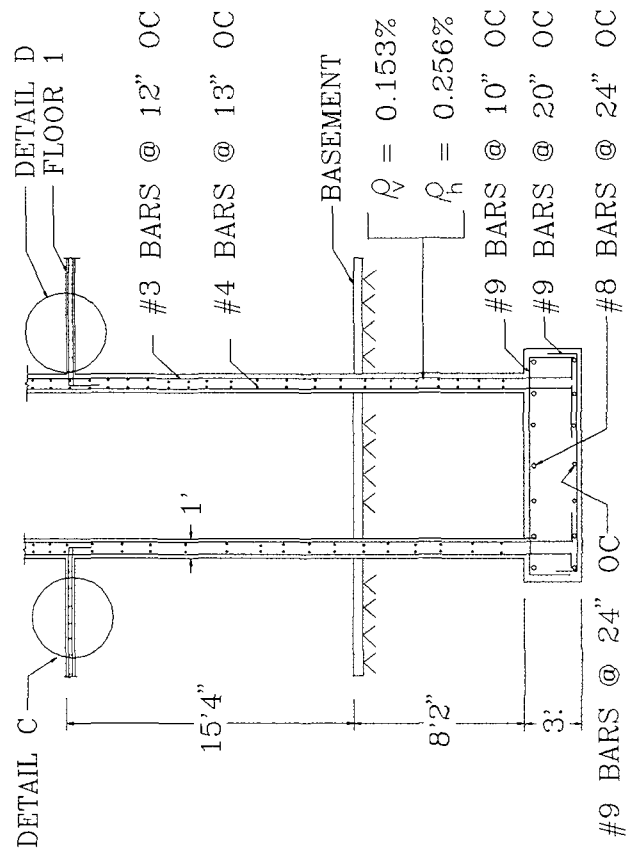
an interior column at the foundation level are shown in Fig. 2-4. The reduction in the diaphragm thickness from 7.25 inches to 5 inches in the regions between the cores decrease effective slab-coupling of the two cores. The capacity of closed-section RC cores under bi-axial-flexural-torsional demands is uncertain, particularly since wall interfaces in the cores are not detailed for such demands. The capacity of slab-wall connections under flexural and torsional moment transfer demands are also quite uncertain, particularly without special detailing. There is also uncertainty in the force transfer demands imposed on the in-plane stiffness and strength capacities of the diaphragm with many openings and without additional stiffness along exterior edges.

Many of the geometric features listed above have been incorporated in a previously developed analytical model of the building (Ho and Aktan, 1989). However, some critical features were not included: (a) The kinematics of foundation displacements including rocking and uplift; (b) elevator door openings in the core; and, (c) in-plane deformations of the diaphragm, in spite of several large openings, have not been incorporated.

2.4 Description of the Previous Modal Test

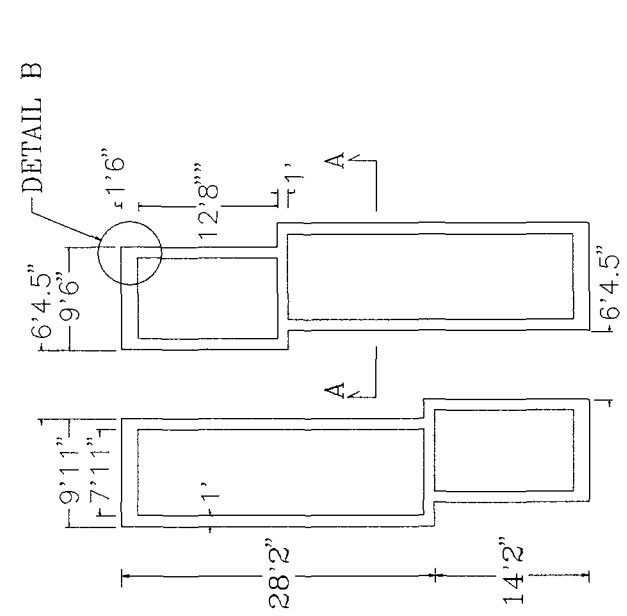
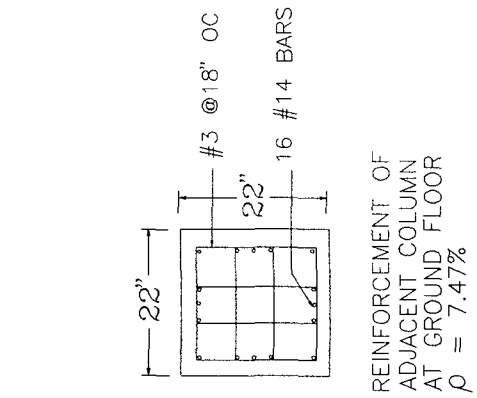
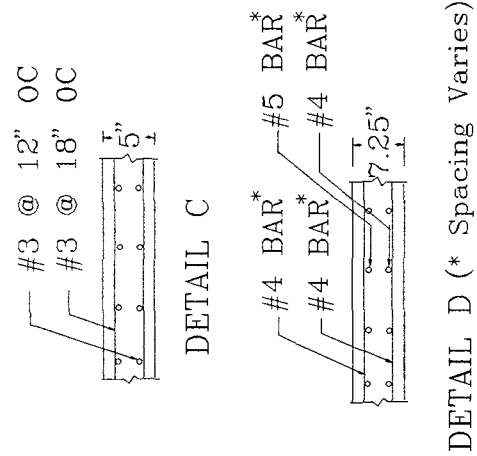
The previous modal test was performed to identify an element-level linearized analytical model of the building. Details of the test are given by Aktan et al (1990) and Ho and Aktan (1989).

A linear 1500 lbf reactive mass actuator with a ± 2 inches useable stroke generating a dynamic force of 75 lbf at 0.5 Hz was utilized. An attempt was made to generate swept-sine excitation using a GenRad 2515 test system, however, the sine software did not track a synchronous signal below 1 Hz. Hence, random excitation had to be administered for the complete modal test. A WAVETEK signal generator generated the random excitation while the GenRad 2515 data acquisition system acquired and processed the data. In order to increase the magnitude of the excitation signal in the lower frequency ranges, there was use of an HP 35651A Spectrum Analyzer which generated additional noise in a bandwidth of



SECTION A-A

PLAN OF CORES AT THE BASEMENT



DETAIL B

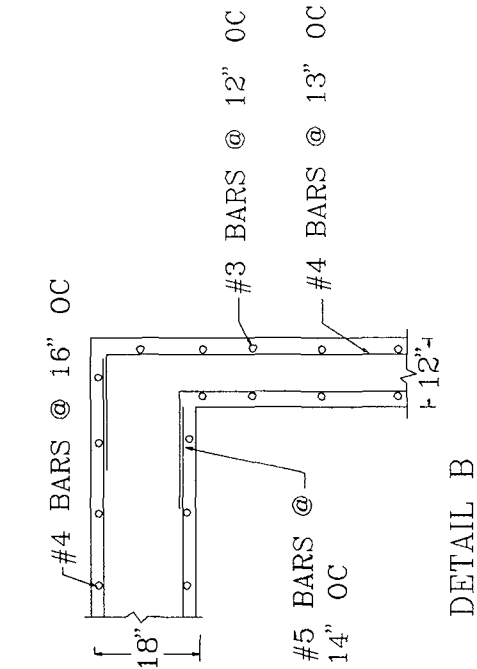


Figure 2-4 Details of the Cores at the Basement.

0.5 Hz-1.0 Hz. The output from the two wave sources were summed increasing the magnitude of the excitation signal in the lower frequency ranges. The summed signal was passed through a Krohn-Hite low-pass filter to improve the response.

Flow-charts of the instruments used for the excitation generation and data acquisition are shown in Figs. 2-5 and 2-6. Due to low excitation capacity, the test was repeated over two frequency ranges, 0 to 4 Hz, to determine the low frequency range characteristics, and 0 to 16 Hz, to determine the higher frequency range characteristics. The GenRad system measured the excitation, driving-point response, and eight accelerometers responses per floor. Since the system had a capacity of 16 channels, the accelerometers were moved from floor to floor while the exciter remained stationary at the 25th floor. Data was collected from nine floors with the approximate data acquisition time being 50 hours. Time histories of responses measured due to forced excitation are compared to those measured due to ambient wind excitation in Fig. 2-7.

Initially, a quadrature fit method was used for post processing the data and anomalies were observed in the lower three modes. This was attributed to the influence of wind on the measured responses and led to a lack of coherence between the applied force and responses below 1 Hz as shown in Fig. 2-8. In order to eliminate the anomalies, the "Response Ratio" algorithm was used. A fixed reference acceleration signal was selected for FRF calculations rather than the excitation force (Aktan et al, 1990).

2.5 Results of the Previous Test

The first nine natural frequencies, damping factors, and modal vectors were obtained as described by Ho and Aktan (1989). The first three predicted frequencies obtained from the Super ETABS analyses were 25% lower than the measured frequencies and the remaining were 5% lower than the measured frequencies. A subtle but consequential error in macro-modeling of the cores was discovered and the analytical model was corrected leading to an accurate simulation of the measured frequencies. It is important to note that

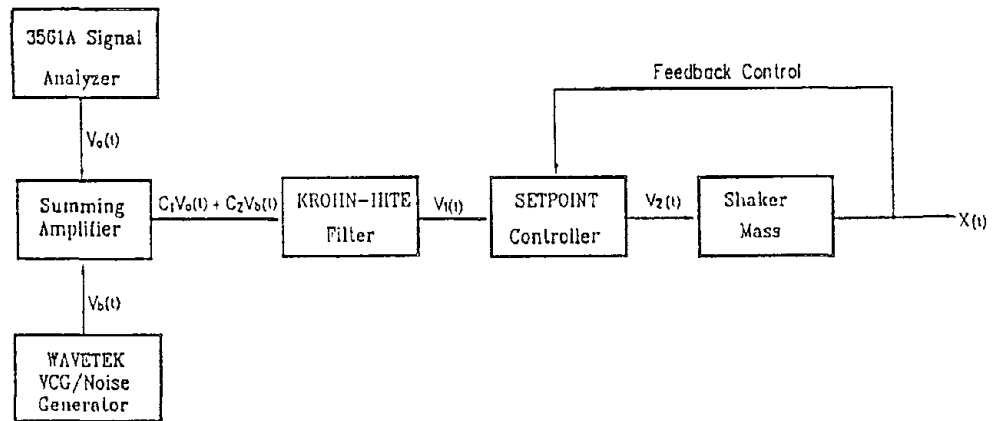


FIGURE 2-5 Flow Chart of the Instruments Used in the Previous Test for Excitation Generation.

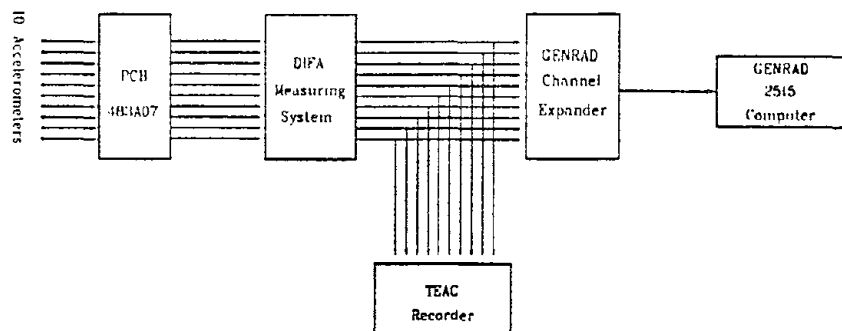


FIGURE 2-6 Flow Chart of the Instruments Used for the Data Acquisition in the Previous Test.

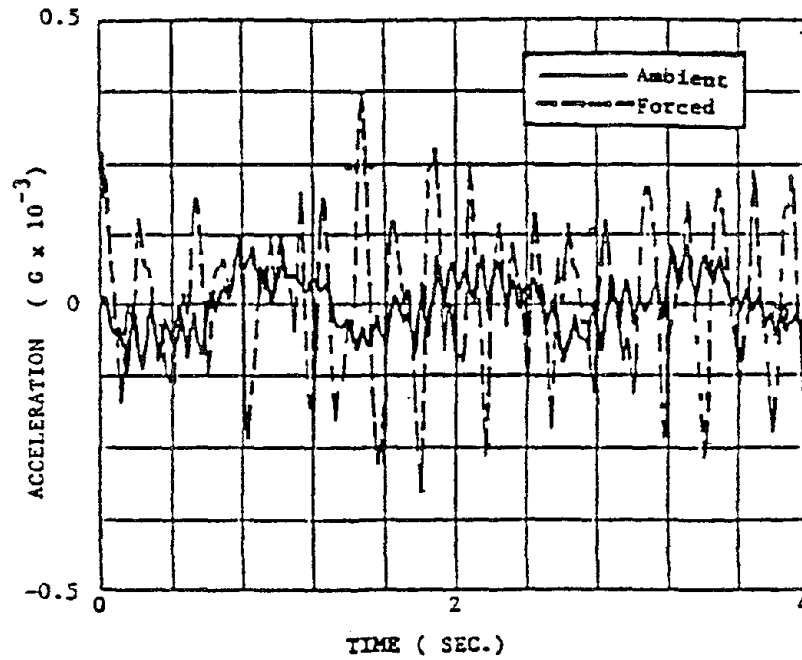


Figure 2-7 Comparison of Responses Obtained in the Previous Test Under Both Ambient and Random Forced Excitation.

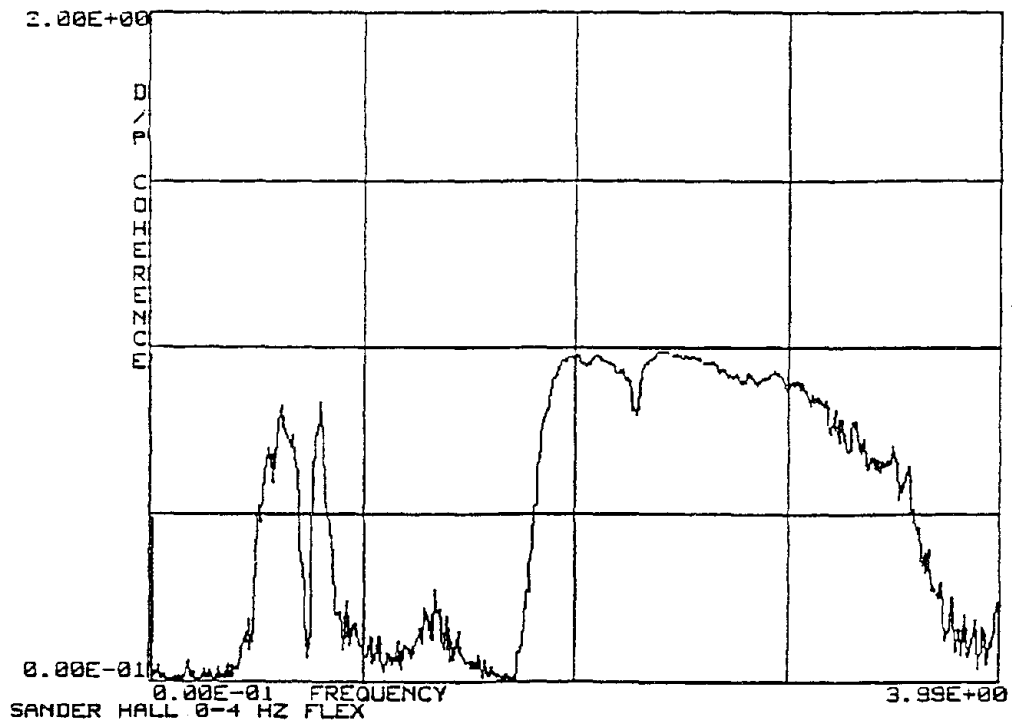


Figure 2-8 Coherence Between Excitation and Diaphragm Response at the Roof Level Obtained in the Previous Test.

the error in analytical modeling could not be avoided and could only have been discovered with this experimentation. The predicted, measured, and simulated frequencies and mode shapes are shown in Fig. 2-9.

The lateral flexibility coefficients of the building were obtained by transforming the mass-orthonormal modal vectors. The predicted, measured, and simulated lateral flexibility are shown in Fig. 2-10. The predicted flexibility was 100% more than the flexibility derived from the modal test. After correcting the analytical model, a difference of less than 5% remained between the simulated and measured flexibility.

2.6 Limitations and Shortcomings

The limitations and shortcomings of the previous modal tests are outlined below.

- (1) The excitation force level (75 lbf at 0.5 Hz, 400 lbf maximum force with a random excitation between 0-4 Hz) excited the modes weakly and at times, the wind excitation overwhelmed the forced excitation. This is shown in Fig. 2-7 and indicates that the data quality for forced excitation was highly dependent on the level of the wind, particularly in the lower frequency ranges.
- (2) Coherence between the excitation and response at the 27th floor was poor. This was true for the first three modes which had frequencies below 2 Hz as shown in Fig. 2-8. Coherence decreased further when the wind speed increased (Aktan and Ho, 1990).
- (3) The accelerometers were moved from floor to floor to acquire the data. Consequently, the data from every floor could not be simultaneously acquired at a particular mode. Due to constant fluctuations in the ambient conditions, the effect of wind force on the data changed from one floor to another. Furthermore, moving the accelerometers compounded the experimental errors.
- (4) The signal-to-noise ratio in the measured data was low in random excitation relative to harmonic excitation. The input energy is distributed throughout the frequency

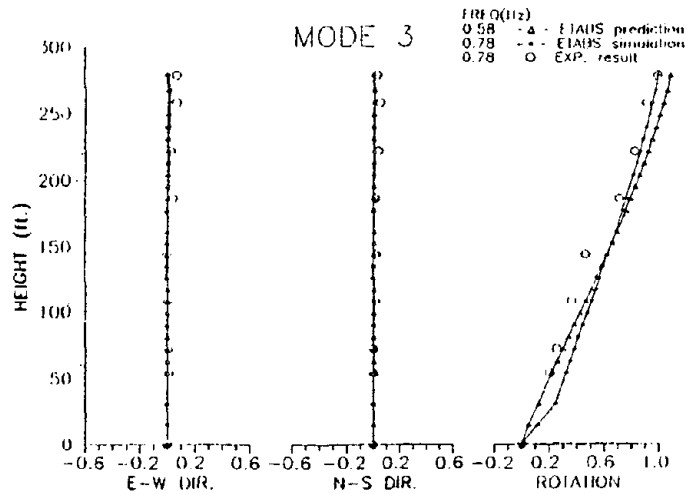
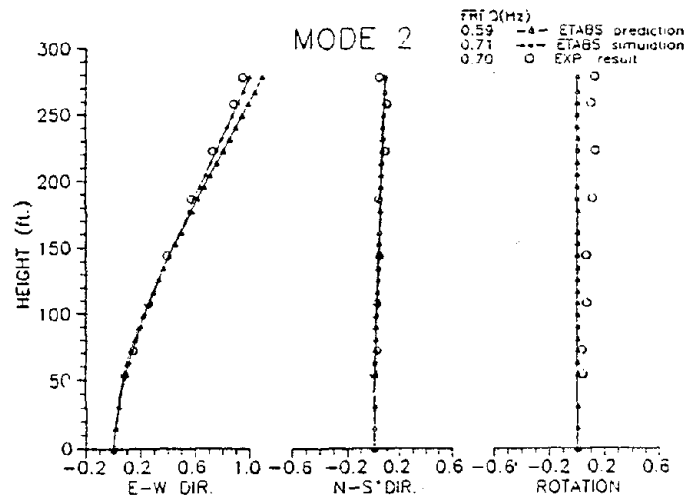
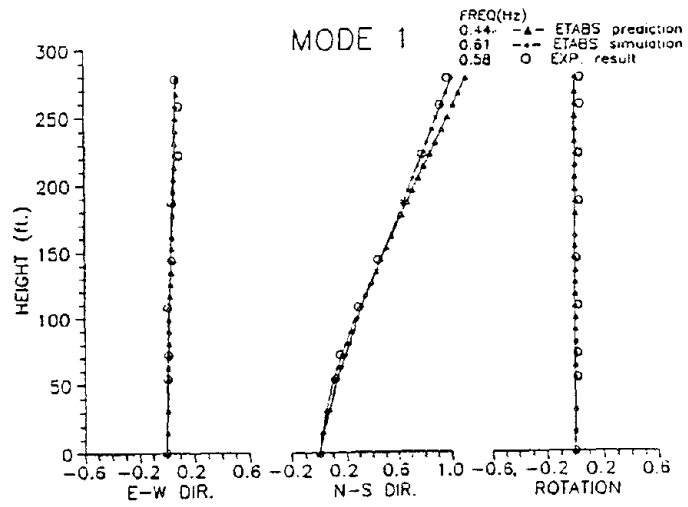


Figure 2-9 Mode Shapes and Natural Frequencies Obtained from the Previous Test.

- Continued

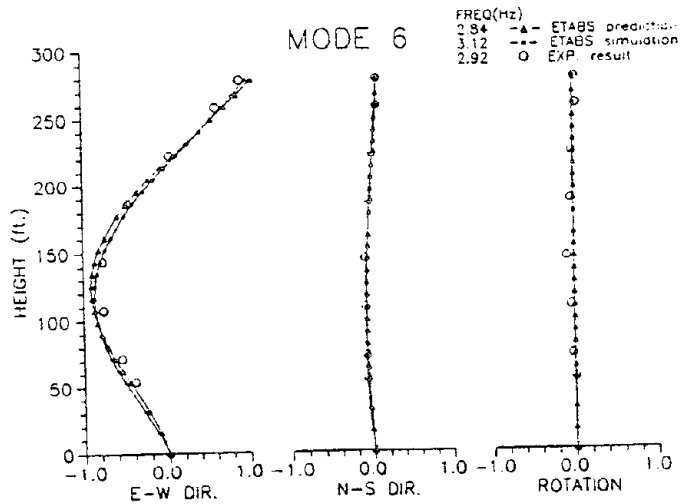
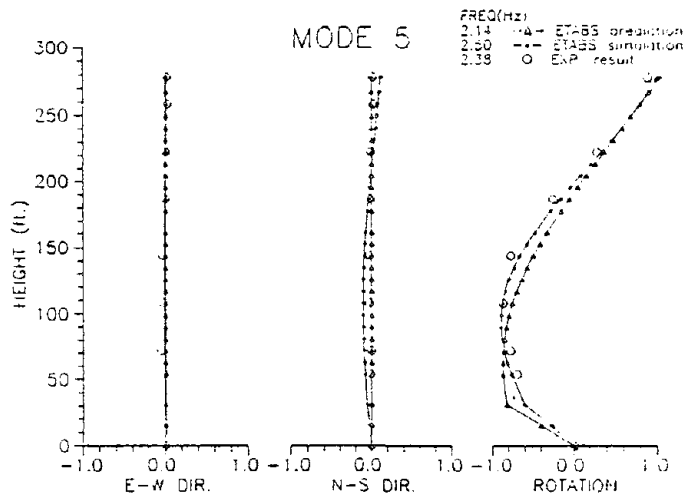
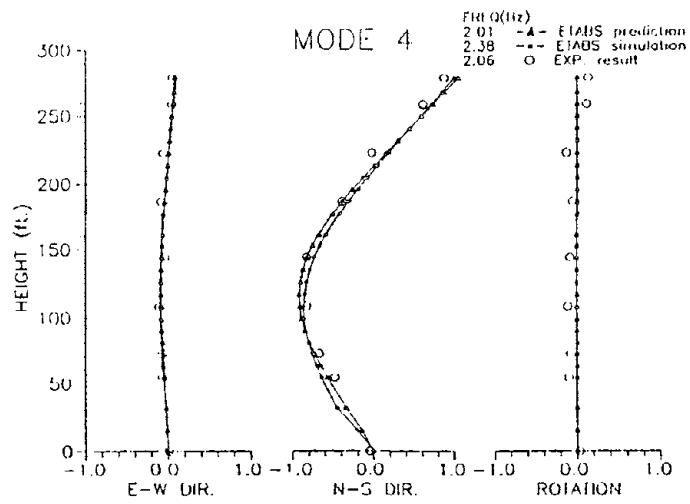


Figure 2-9 Mode Shapes and Natural Frequencies Obtained from the Previous Test.

- Continued

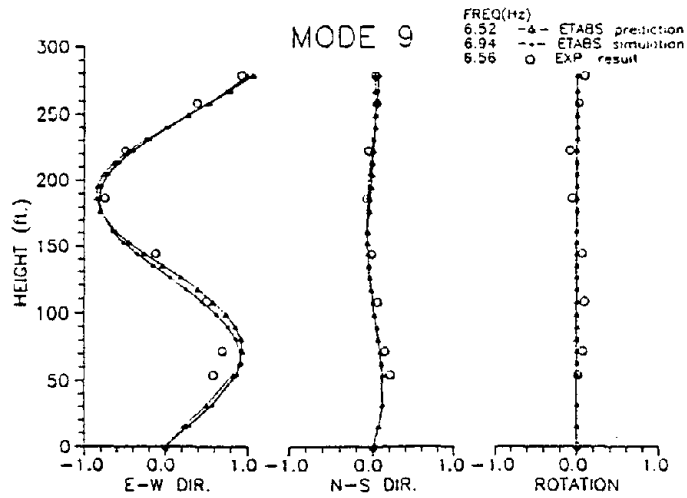
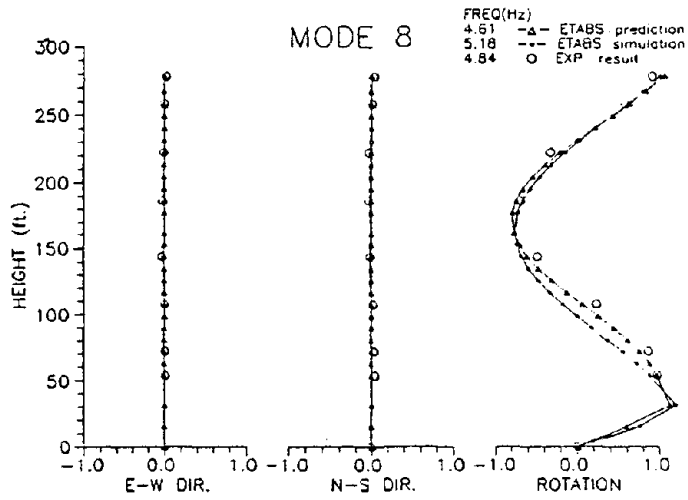
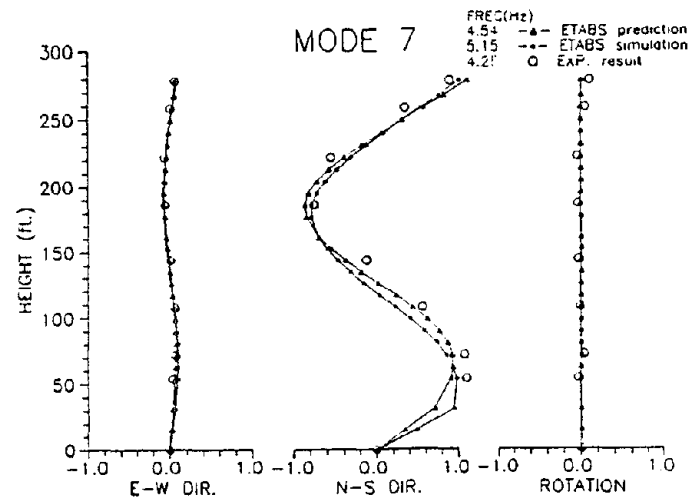


Figure 2-9 Mode Shapes and Natural Frequencies Obtained from the Previous Test.

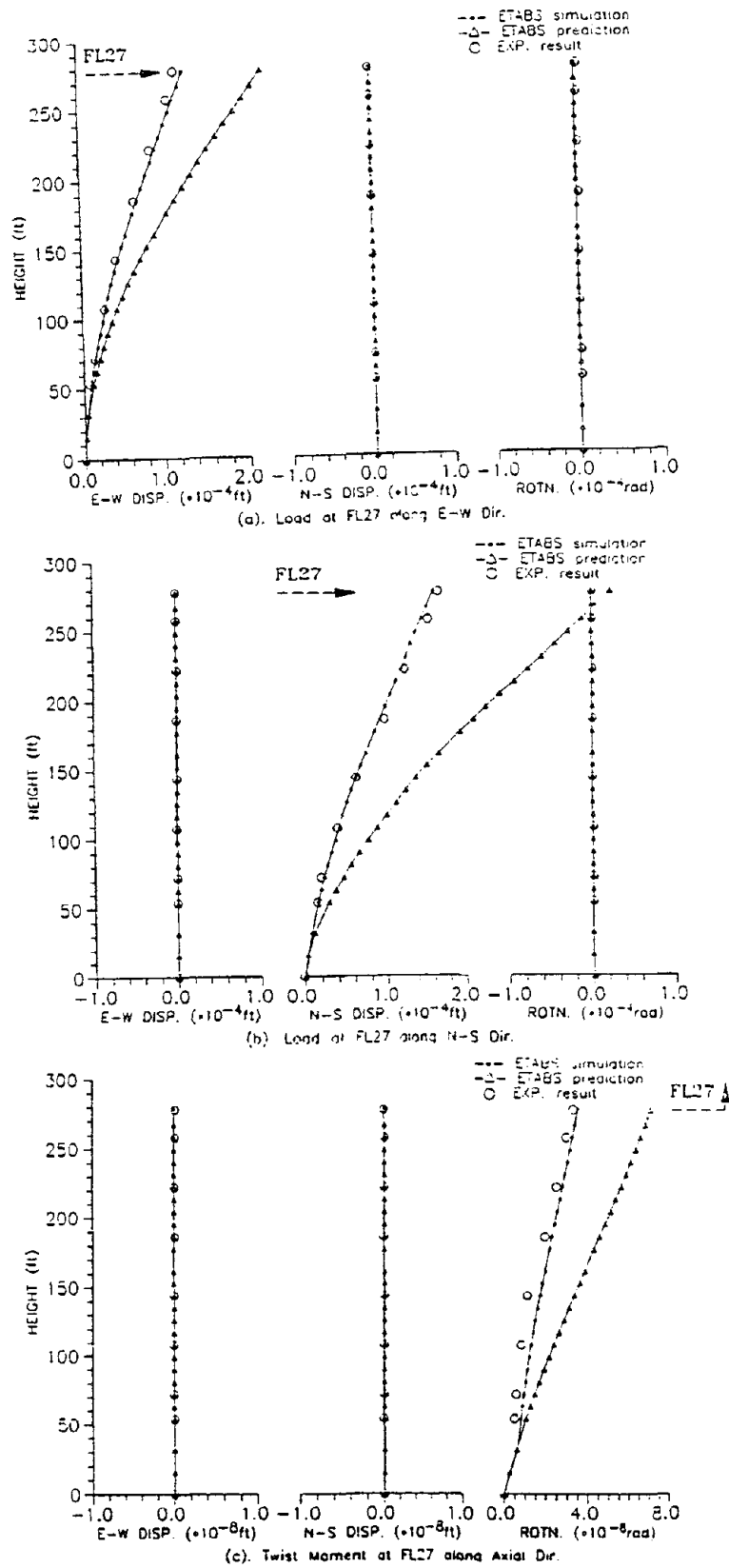


Figure 2-10 Lateral Flexibility of the Building Obtained from the Previous Test.

range in random excitation This is in opposition to its concentration at the frequency of interest in the case of single harmonic force.

- (5) The level of force was insufficient to activate foundation displacements. The effects of this on the dynamic characteristics, displacement kinematics, and lateral flexibility of the building could not be observed. Hence, the analytical model identified based on the previous test could not properly incorporate all of the effects of soil-foundation flexibility.
- (6) The test time was considerable (approximately 50 hours required to acquire the data for the complete test) since a large number of averages were required to improve the signal-to-noise ratio in the data. This duration of time allowed significant changes in ambient conditions and corresponding changes in the mechanical characteristics.

The above listed limitations and shortcomings indicated the need to repeat the modal tests and acquire more reliable data. Increasing the level of excitation force to overcome the wind excitation, and to focus on the soil-foundation flexibility and details of the displacement kinematics at the foundation level, became important needs.

SECTION 3

AMBIENT RESPONSE STUDIES

3.1 General

In the past, numerous wind excitation tests were conducted to determine building dynamic characteristics. Such tests are relatively simple and inexpensive compared to forced excitation tests. However, the wind forces are generally too low to excite all the modes of interest of large scale buildings. Even the lower mode responses of a building are generally low and the dynamic characteristics change due to fluctuating wind. A serious shortcoming is the fact that wind excitation forces cannot be accurately measured or even estimated reliably since wind forces are distributed over a building in very complex manners. Due to these factors, a direct measurement of frequency response functions is not possible and flexibility cannot be obtained directly. Therefore, ambient wind excitation tests are suitable only for approximately determining the natural frequencies of a building.

In earlier tests of buildings, variations in the natural frequencies were observed during ambient and forced excitation (Stephen et al, 1985). Therefore, ambient response studies of the building were performed to investigate the effects of changes in the ambient wind excitation levels on the building's natural frequencies and also to better understand the level of forced excitation relative to the ambient excitation. In addition, the natural frequencies obtained from the ambient excitation were compared to those obtained from the forced excitation modal test.

The test setup, hardware and software employed, data acquisition, and test results are discussed in the following.

3.2 Test Setup

The block diagram of the setup for ambient wind excitation studies is shown in Fig. 3-1. The hardware and software used for this test are a HP 3582A Dynamic Signal Analyzer,

a HP 3565S Measurement Hardware, a HP 9000 Series 300 Computer (model HP 370) with HP-UX operating System, HP VISTA Signal Processing Software, 20 Seismic Accelerometers (model PCB 393 C), and two 12-channel Amplifiers (model Piezotronics 483 B17).

The seismic accelerometers were located on eight floors in addition to the basement as shown in Fig. 3-1. The accelerometer locations correspond to those used for the closed-loop modal test (Section 4). Initially, the accelerometers were oriented along the NS direction to measure the responses along the NS direction. After acquiring the data, the accelerometers were re-oriented along the EW direction. Since the responses were in the order of milli g's, the signals were amplified by 100 times. The HP VISTA software, with measurement hardware, and the HP 370 computer, acquired and processed the data in both the time and frequency domains. The HP VISTA (1987) is a recently developed signal processing software that can be employed as a multi-channel signal analyzer to acquire and process random data (Section 4).

3.3 Monitoring the Ambient Conditions

A weather station (ORACLE 2) monitored and recorded wind speed, wind direction, wind-chill temperature, and interior and exterior temperature. The weather station consisted of a wall-mounted display with magnetic controls that displayed information, a roof top unit that provided information about wind speed and direction, and exterior and interior temperature sensors. The display unit is shown in Fig. 3-2. This was located in a control center at the 25th floor. The wind speed was recorded every five minutes during the ambient excitation test and fluctuated from 0 to 21 mph.

3.4 Data Acquisition and Storage

The power spectra of the acceleration response in NS and EW directions at the 26th floor due to medium wind excitation (wind speed in the range of 6-15 mph) are shown in



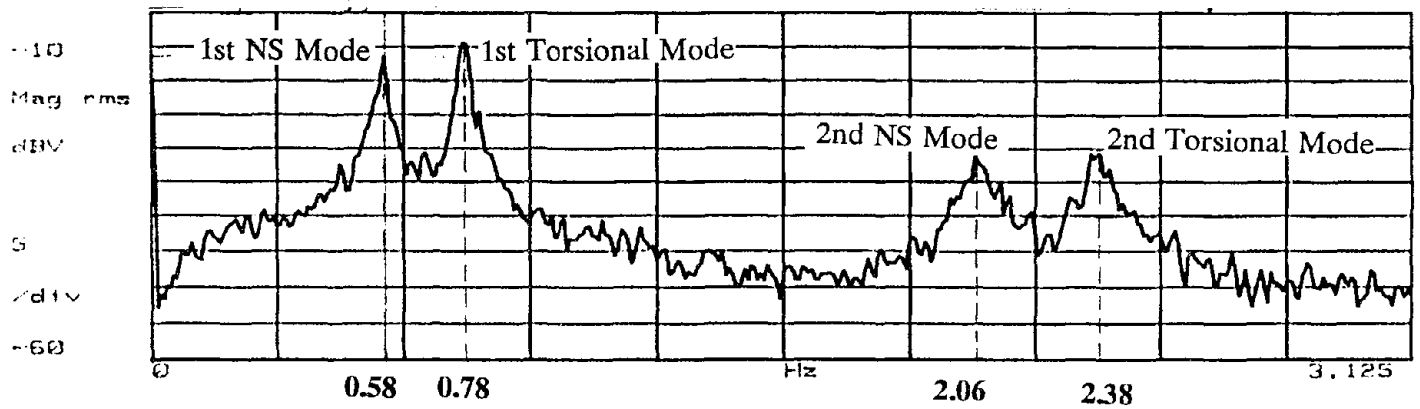
Figure 3-2 Photograph of the Weather Station Display Unit.

Fig. 3-3. Discernible frequencies of the building are marked.

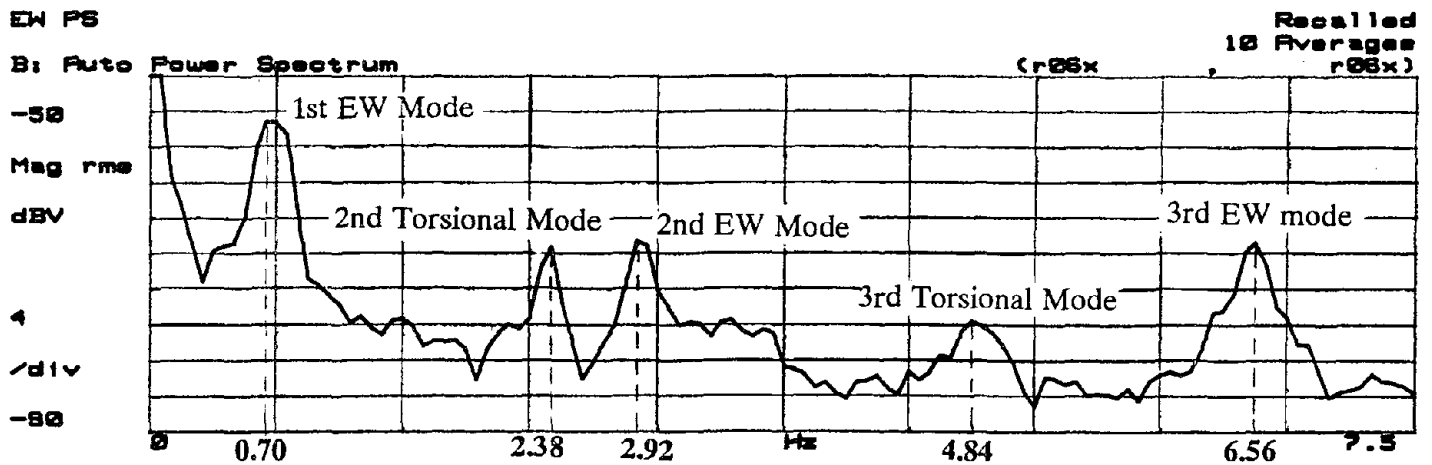
The highest frequency resolution by using the HP VISTA system was 0.015625 Hz. Therefore, a HP 3582A Dynamic Signal Analyzer possessing a frequency resolution of 0.004 Hz was employed to investigate the changes in the natural frequencies due to changes in the level of wind excitation. Due to limitations of this analyzer, responses from only two accelerometers at the 26th floor were measured. Response histories were recorded by a TEAC XR-710 Cassette Data Recorder.

3.5 Ambient Test Results

Data permitted investigating variations in natural frequencies of the first translational (NS) and torsional modes. The frequencies measured by the 2-channel HP 3582A Dynamic Signal Analyzer for different wind speed ranges in the NS direction are shown in Table 3-1. The NS natural frequency decreased from 0.584 Hz to 0.576 Hz and the frequency of the first torsional mode decreased from 0.784 Hz to 0.776 Hz as the wind speed increased from 1 mph to 21 mph. The frequencies obtained from the ambient responses are compared to those obtained from the modal test in Section 6.



(a) NS Direction



(b) EW Direction

Figure 3-3 Power Spectra of Response at the 26th Floor due to Ambient Wind Excitation in NS and EW directions.

TABLE 3-1 Variations in Natural Frequencies due to Variations in Levels of Wind Excitation in the NS Direction.

Different Ranges of Wind Speed (MPH) in the NS Direction	Natural Frequency at the First NS Mode (Hz)	Natural Frequency at the First Torsional Mode (Hz)
1-5 (Low Wind)	0.584	0.784
6-14 (medium Wind)	0.580	0.780
15-21 (High Wind)	0.576	0.776

FREQUENCY RESOLUTION = 0.004 Hz

SECTION 4

CLOSED-LOOP MODAL TEST

4.1 General

State-of-the-art hardware and software recently developed by Hewlett Packard for modal testing of mechanical structures were employed in a closed-loop test setup for the current modal tests. A linear inertia-mass exciter was specially developed for servo-controlled excitation. The closed-loop test setup and the components of the excitation and data acquisition systems are discussed in the following sections. The significance of the closed-loop nature of the test is also addressed.

4.2 Test Setup

A global block diagram of the closed-loop forced excitation test is shown in Fig. 4-1. The following hardware and software were employed: (a) HP 9000 Series Work station model HP 370 with HP-UX Operating System; (b) HP 3565S Measurement Hardware System; (c) HP SINE Signal Processing Software; (d) Linear Inertia-Mass Exciter and its Hydraulic pump; (e) Pegasus 5900 Servo-Controller; (f) 22 PCB 393C Accelerometers; (g) two 12-channel Piezotronics Model 483 B17 Amplifiers; and, (h) DIFA Analog Filter.

The HP SINE software, via the measurement hardware, directed the swept-sine excitation signal to the exciter's servo-controller. Using the same software, the resulting acceleration responses of the building were measured and processed through the measurement hardware. After sending an excitation signal to the servo-controller, the computer waited for the transients to diminish and then stored the steady-state responses. The block diagram of the hardware and software for swept-sine excitation control is shown in Fig. 4-2. The block diagram of the hardware and software used for the data acquisition is detailed in Fig. 4-3.

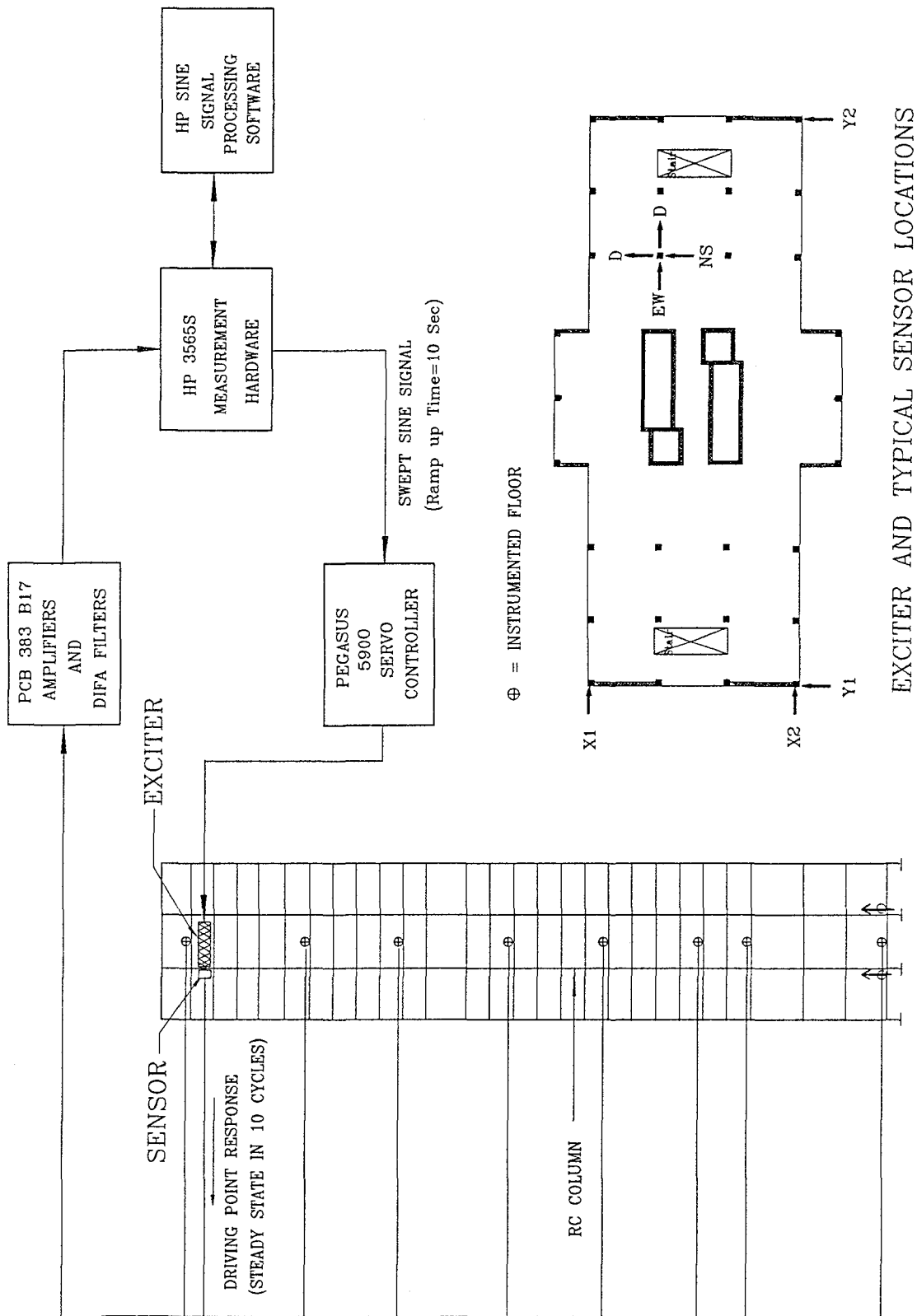


Figure 4-1 Block Diagram of the Closed-Loop Test Setup.

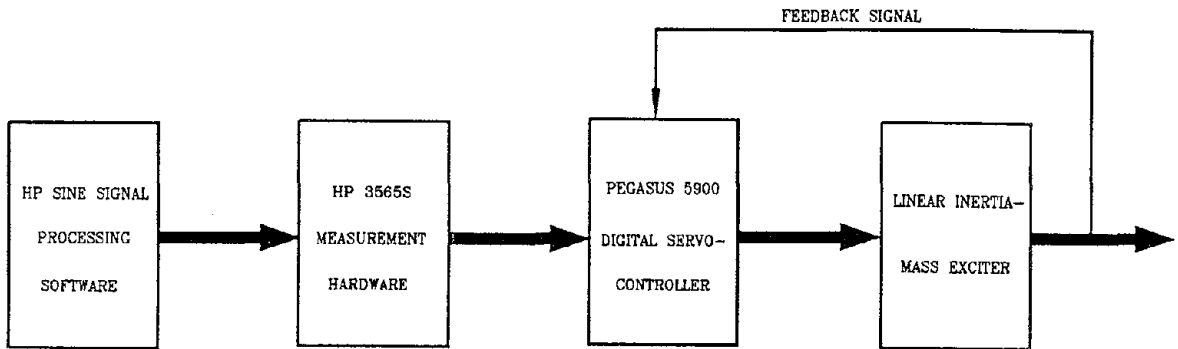


Figure 4-2 Block Diagram of the Swept Sine Excitation Control.

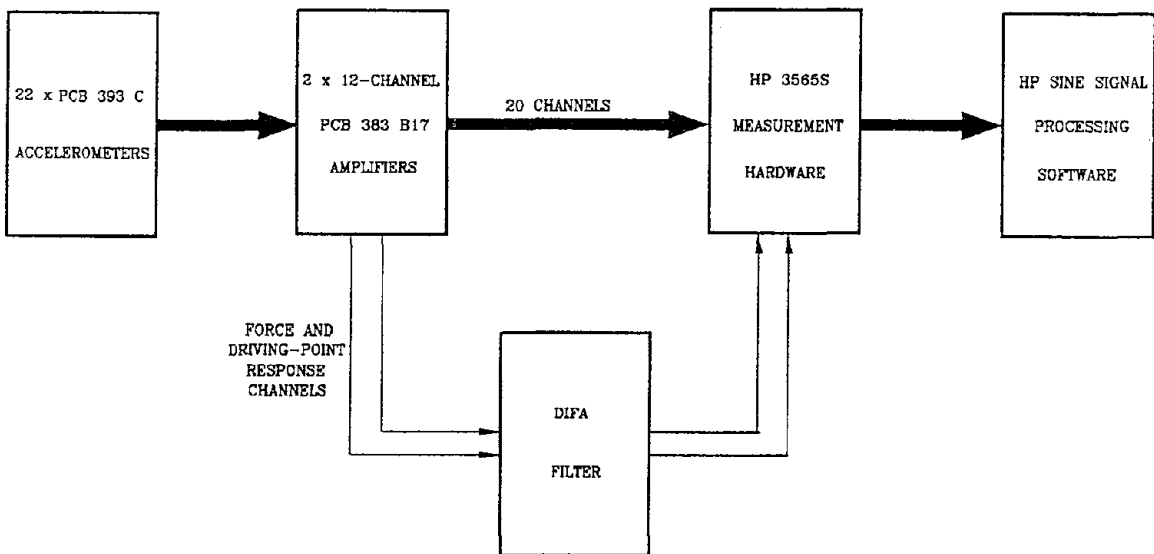


Figure 4-3 Block Diagram of Hardware and Software for Data Acquisition.

4.2.1 Exciter Location

The exciter was mounted against an RC column at the 25th floor as shown in Fig. 4-4 based on the following criteria:

- (1) To provide maximum moment-shear ratio thereby producing maximum overturning at the base;
- (2) To provide eccentric force with respect to floor mass center in order to excite the building in torsional modes as well as translational modes;
- (3) To mount the exciter against an RC column as close as possible to the diaphragm. This attachment will provide a force in the diaphragm plane with minimum column local responses (Photograph in Fig. 4-4); and,
- (4) To obtain a location that did not coincide with any of the nodal points of the first nine mode shapes. The nodal points were obtained from the previous test.

The exciter was initially oriented along the NS direction. After acquiring the data, the exciter was rotated towards the EW direction and the tests were repeated.

4.2.2 Sensor Locations

The accelerometers were located on eight floors to measure horizontal diaphragm responses. They were fixed directly on the concrete of structural elements by hot glue. Accelerometer locations on a typically instrumented floor are shown in Fig. 4-5. Although instrumenting all the floors was not possible due to economic constraints, the available accelerometers (22) were optimally distributed based on the knowledge gained from the previous modal test and after several iterations. The accelerometers were located based on the following criteria:

- (1) To discretize the building into a sufficient number of lateral displacement coordinates in order to capture the amplitudes and nodal points of all the critical

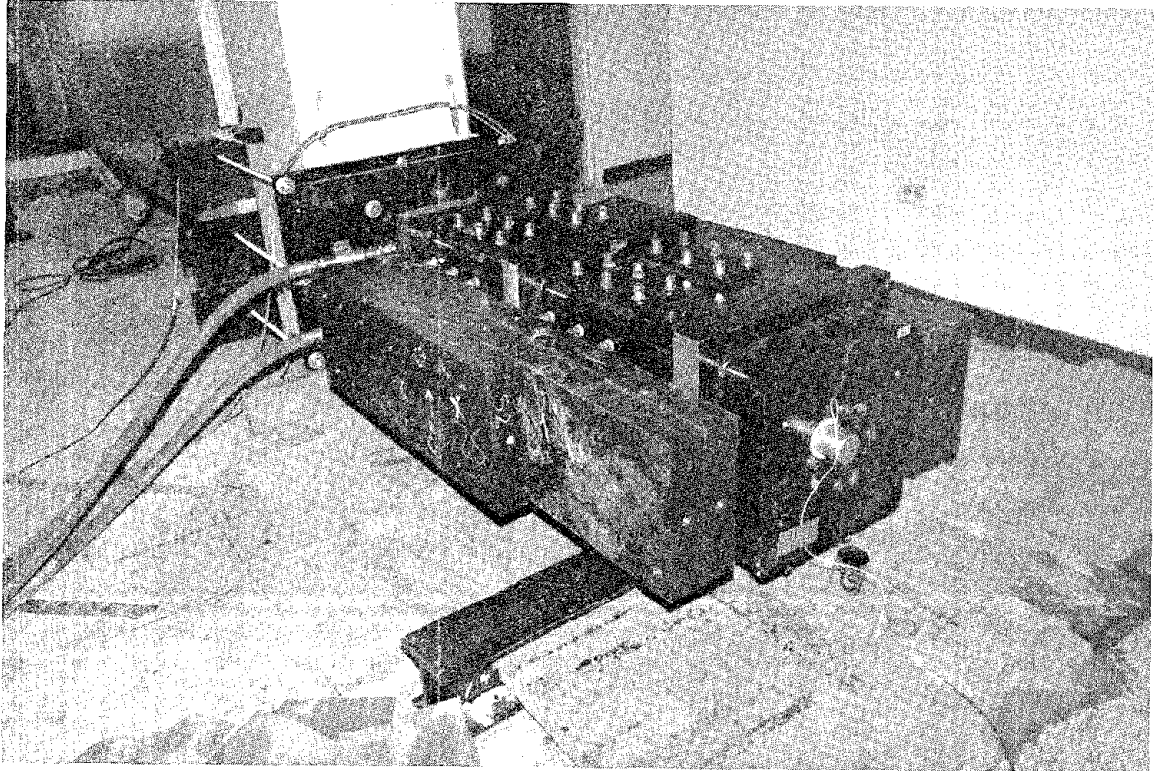
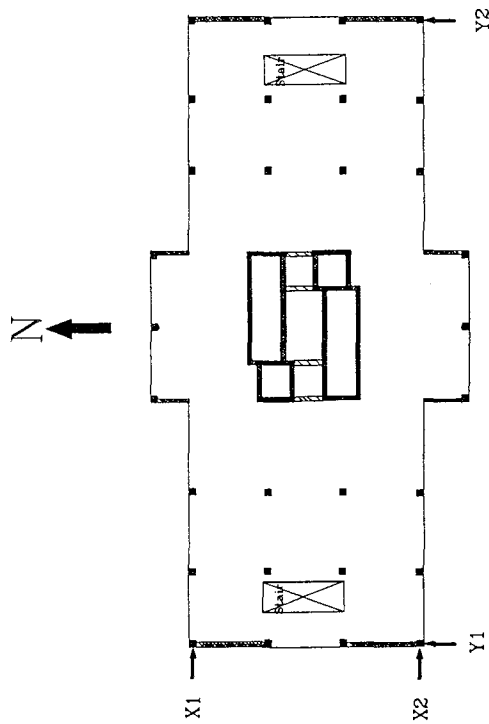
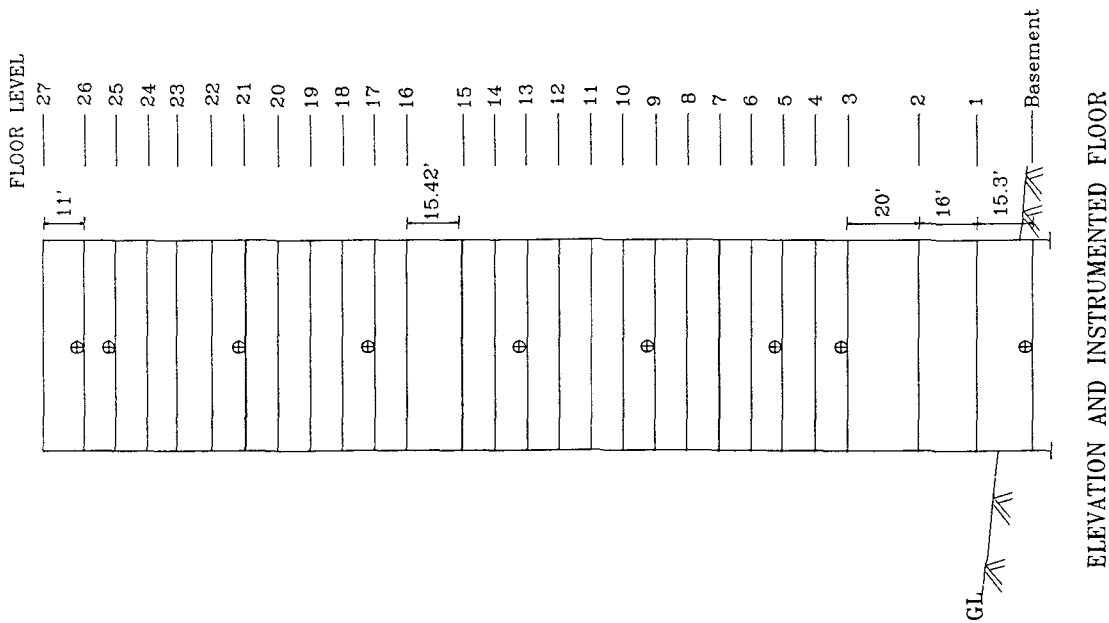


Figure 4-4 Photograph of the Linear Inertia-Mass Exciter Mounted on the RC Column at the 25th Floor.



Y1-Y2 : Responses in the NS Direction due to Excitation in the NS Direction
 X1-X2 : Responses in the EW Direction due to Excitation in the EW Direction

TYPICAL ACCELEROMETER LOCATIONS

Number of Accelerometers at Each Floor = 2
 (Except at the Basement)

Number of Accelerometers at the Basement = 4

Total Number of Accelerometers Used = 20
 (Except Those Used to Measure Input Force
 and Driving Point Response)

⊕ : INSTRUMENTED FLOOR
 TYPICAL STORY HEIGHT : 9 FEET
 GL : GROUND LEVEL

Figure 4-5 Instrumented Floors and Location of Accelerometers.

modes. These modes should account for over 90% of the lateral flexibility*;

- (2) To capture the torsional response characteristics of the building in view of the significant discontinuities in torsional stiffness;
- (3) To capture the responses in regions of lateral stiffness and inertia discontinuity; and,
- (4) To capture the critical response mechanisms which influence response kinematics of the complete building such as foundation distortions and displacements at the soil interface due to soil flexibility and uplift.

The locations of accelerometers on the 25th floor and in the basement were different from that of other floors. The accelerometer locations on the 25th floor are shown in Fig. 4-6 and a photograph of an accelerometer located on a RC column at the 25th floor is shown in Fig. 4-7. An accelerometer was located on the column against which the exciter was mounted to measure the "Driving-Point Response". The driving-point response is required to obtain the unit-mass-normalized modal vectors as explained in Section 6. Another accelerometer was mounted on the moving shell of the exciter to measure its acceleration as a measure of the input force. The output from the latter unit was used as the force-reference channel for calculating the frequency response functions.

In order to understand the kinematics at the foundation level, the horizontal and vertical responses at the basement were monitored. The horizontal responses were insignificant compared to the vertical responses. The accelerometers were located vertically on either side of the cores and also on the extreme columns at either side of the building. A photograph of an accelerometer located on the core is shown in Fig. 4-7 and the location of accelerometers at the basement is shown in Fig. 4-8. The vertical responses revealed

*The modal truncation issues should be studied prior to testing. The concept of modal mass is typically used as a measure of modal contributions to response. In case of irregular structures, however, modal mass may not be an accurate indicator. Hence preliminary analyses are required to check the influence of modes on lateral flexibility and to study the effects of modal truncation. A prior knowledge or estimate of mode shapes and flexibility are therefore needed for optimum locations of measurement points and instrumented floors.

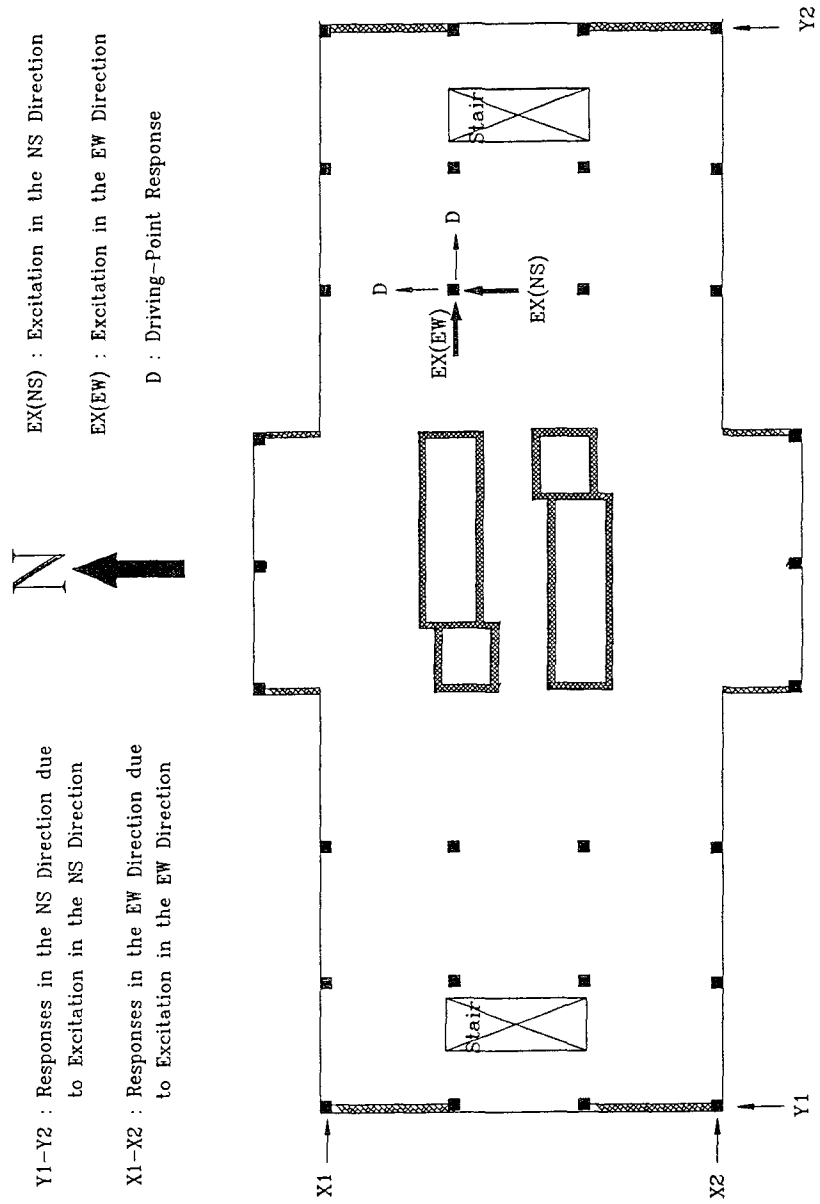
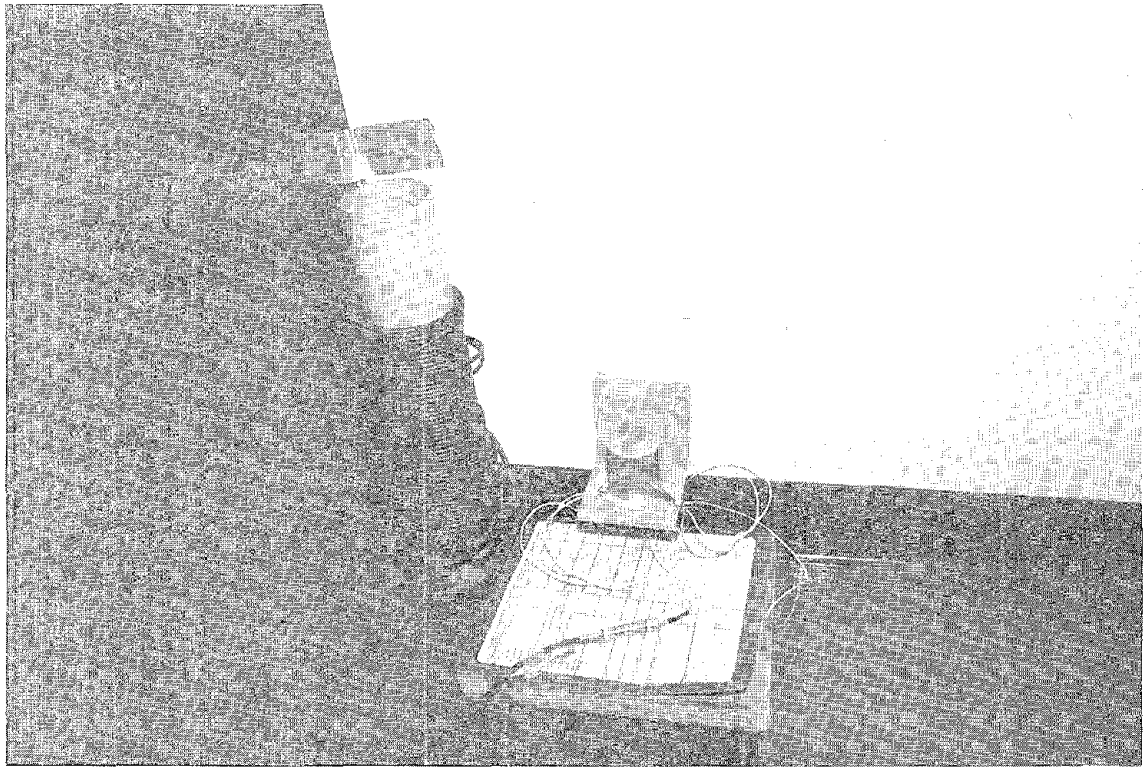
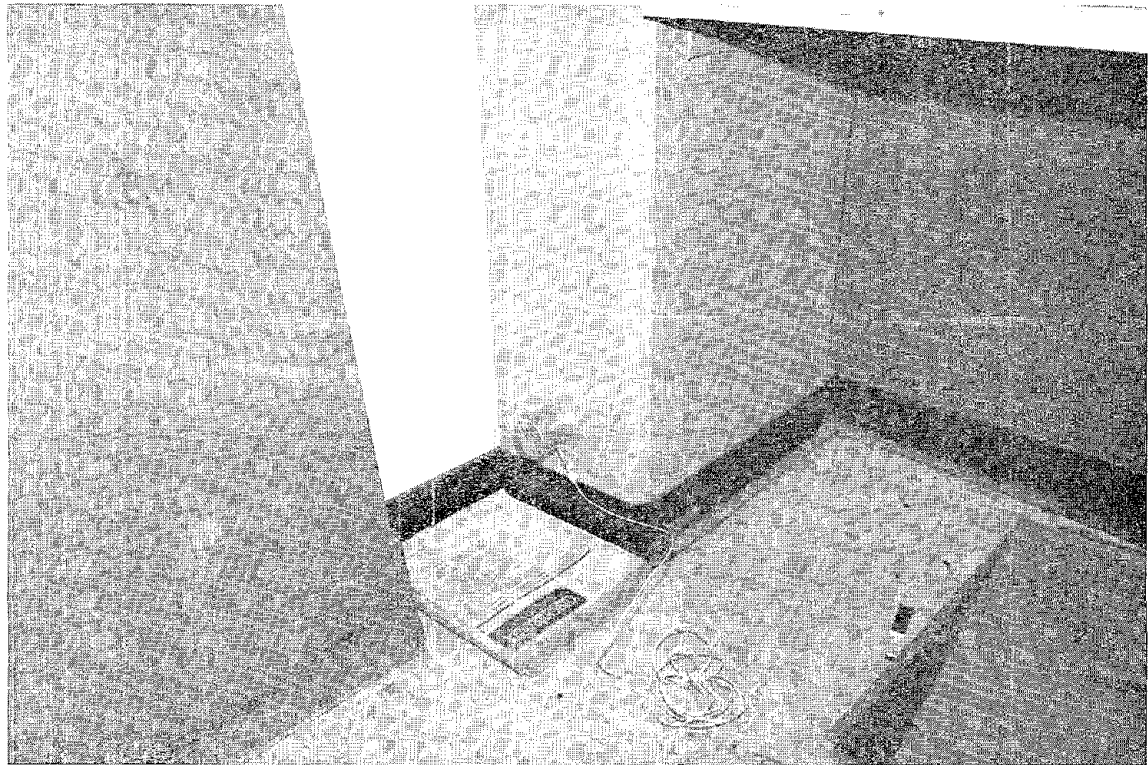


Figure 4-6 Location of the Exciter and Accelerometers at the Test Floor (Floor 25).

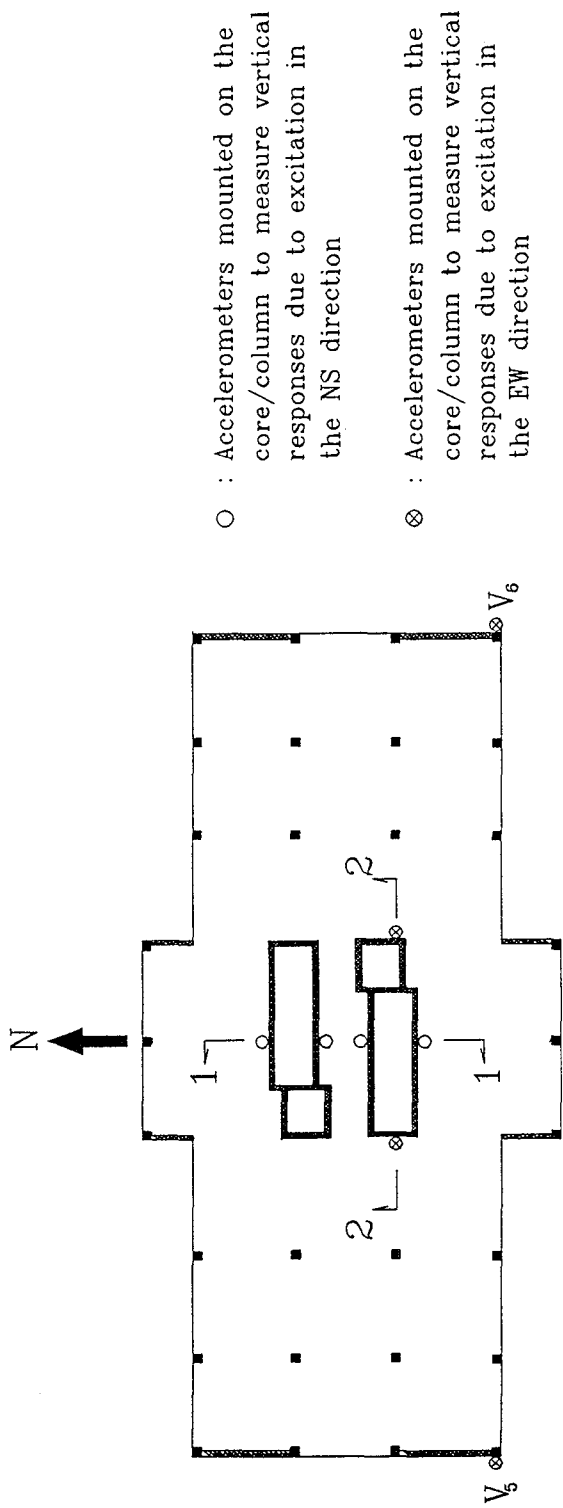


(a) At the Basement



(b) At the 26th Floor

Figure 4-7 Photographs of Accelerometers Mounted on the Core at the Basement and on the RC Column at the 26th Floor.



- : Accelerometers mounted on the core/column to measure vertical responses due to excitation in the NS direction
- ⊗ : Accelerometers mounted on the core/column to measure vertical responses due to excitation in the EW direction

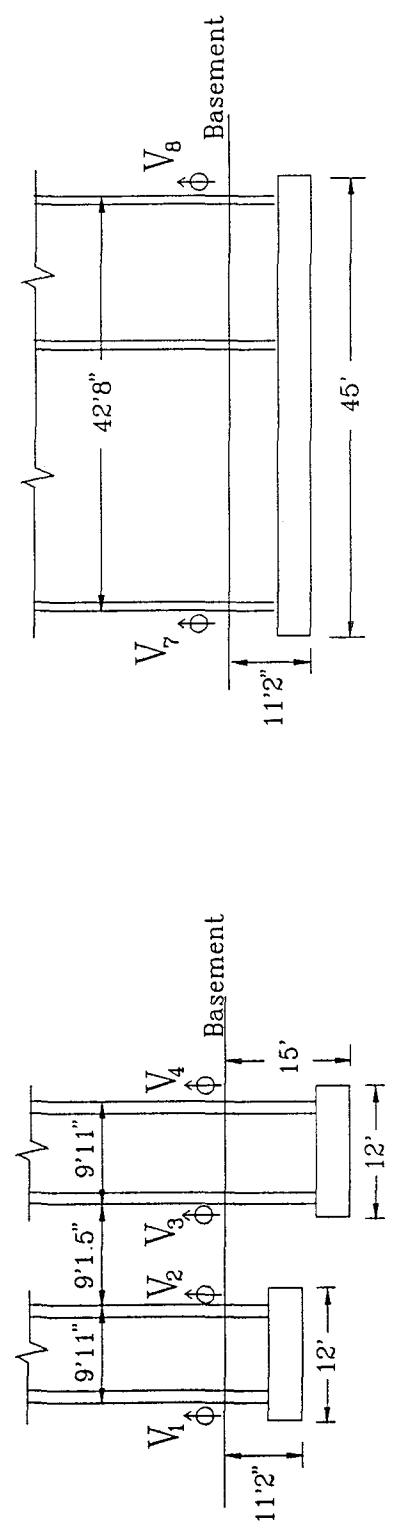


Figure 4-8 Location of Accelerometers at the Basement.

rocking and uplifting within the basement. Since the basement slab on grade was not monolithic with the RC core and RC columns, accelerometers were not located on this slab.

4.3 Significant Characteristics of the Test Setup

(1) **Excitation System:** The linear inertia-mass exciter developed for this test is judged to have many advantages over the rotating eccentric-mass exciters. The time needed for the exciter to ramp up from the initial stationary position to the specified force level is reduced. Less reaction time is required for frequency adjustments after ramping. It is possible to adjust the force level by stroke adjustment during response at a given frequency. This exciter is capable of generating random force in addition to harmonic force. For the same level of force, the size of this exciter is small and installation is easy.

(2) **Excitation Method:** Swept-sine excitation was used in the current modal test. The optimum excitation is dependent on building characteristics, hardware and software constraints, economic constraints, and test objectives. The swept-sine excitation better excites the building due to energy concentration and therefore, leads to a higher signal-to-noise ratio than random excitation. Considering the typical noise level in buildings due to ambient conditions, advantages of sine excitation over random excitation have become clear.

(3) **Closed-loop Test:** Closed-loop testing have many advantages over the manually controlled tests. The same system generates the excitation signal and data acquisition thereby eliminating synchronization errors. Generating the force signal by the same software that acquires the data, enables the software to control the force level automatically and maintain this within a specified interval. This is important for linearizing consistently. Decisions taken by the computer regarding settling time and signal averaging time during excitation and data acquisition, eliminates human errors once the software is calibrated for an individual test.

(4) **Accelerometers:** All 22 accelerometers used in the test remained stationary and simultaneously measured responses from all instrumented floors. The duration of the test

was reduced considerably. Data was measured at all the measurement points under identical wind and forced excitation. This eliminated experimental and linearization errors which normally result when the accelerometers are moved.

4.4 Description of the Equipment

4.4.1 Excitation System

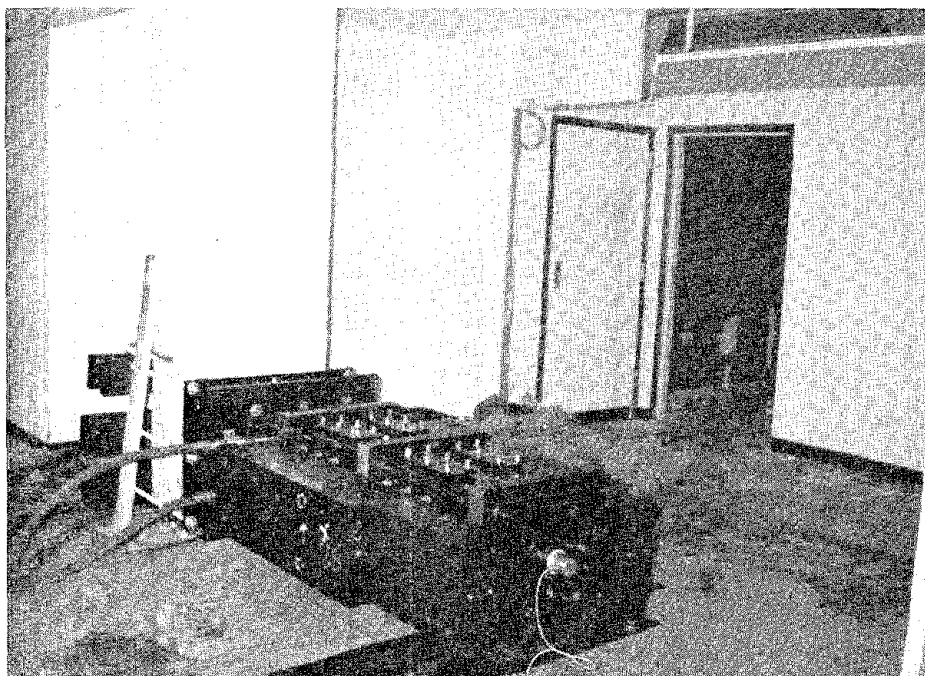
Photographs and the global block diagram of the excitation system (exciter, hydraulic pump, and servo-controller) are shown in Figs. 4-9, 4-10 and 4-11.

4.4.1.1 Exciter and Hydraulic Pump

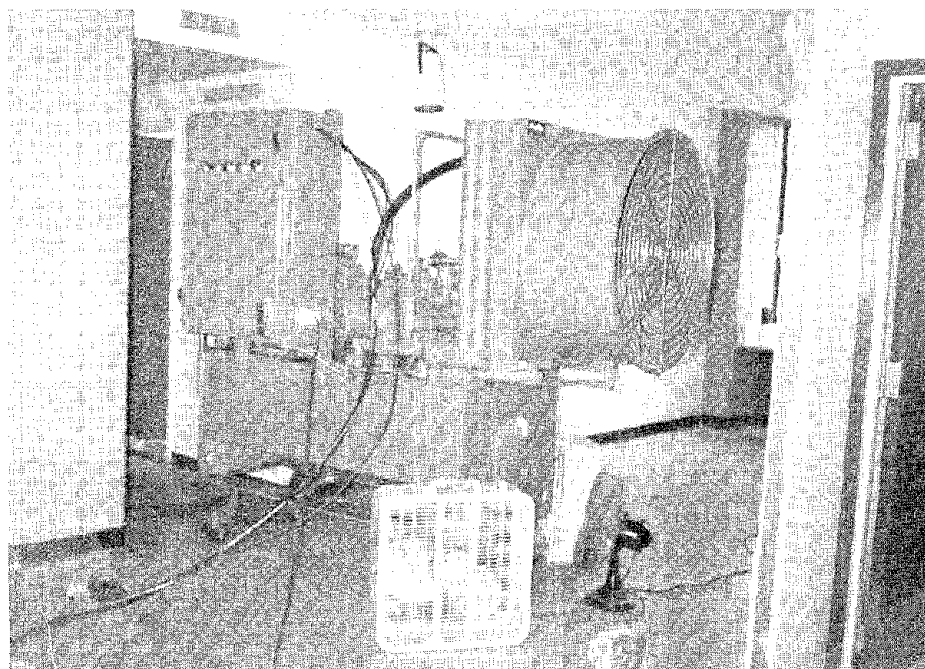
The linear inertia-mass exciter utilized in this test was developed by the Manta corporation. This local organization was established in 1989 by engineers who previously led the industrial systems testing activity at the Structural Dynamics Research Center (SDRC) in Cincinnati. They are also responsible for developing the linear 1500 lbf reactive mass exciter which was used in the previous modal test. Photographs of the exciter and pump are shown in Fig. 4-9.

The exciter consists of a movable outer shell which provides an active mass of 3550 lbf and ± 6 inches of stroke. This exciter was designed to provide an excitation force linearly increasing from 500 lbf to 5000 lbf between frequencies of 0.5 Hz and 1.6 Hz, followed by a peak force of 5000 lbf up to 20 Hz. The displacement responses are controlled by the servo-valve through the hydraulic pressure. The specifications and features of the hardware of this exciter are given in Appendix-A.

A portable hydraulic pump powers the exciter. The pump is driven by a 60 HP motor and provides a hydraulic flow of 30 GPM at 3000 PSI pressure. This pump has a 100 gallon oil reservoir.



Photograph of the Linear Inertia-Mass Exciter



Photograph of the Hydraulic Pump.

Figure 4-9 Photographs of the Linear Inertia-Mass Exciter and the Hydraulic Pump.

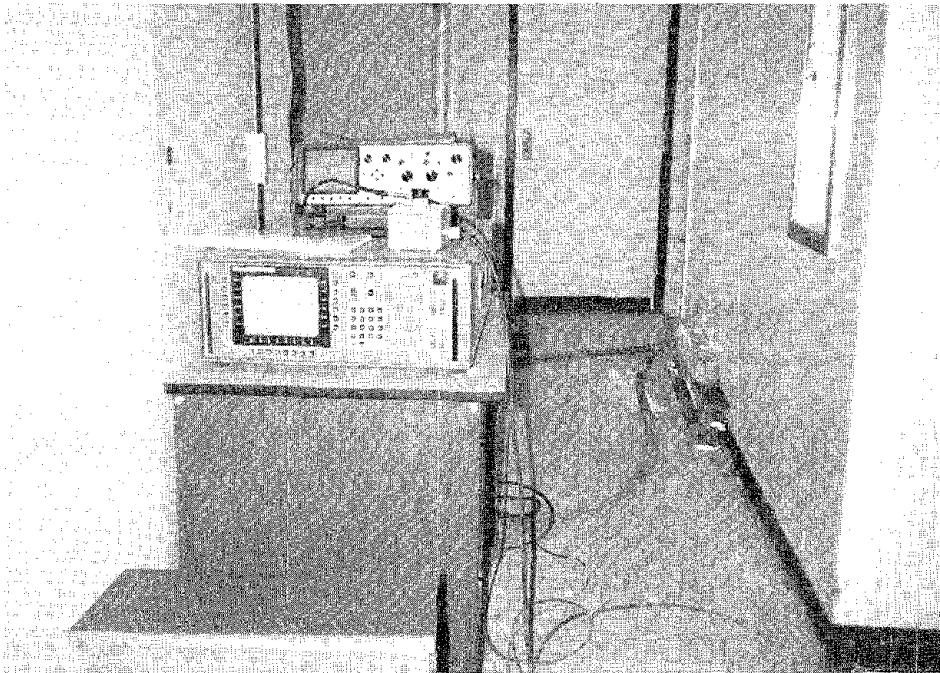


Figure 4-10 Photograph of the Digital Servo-Controller.

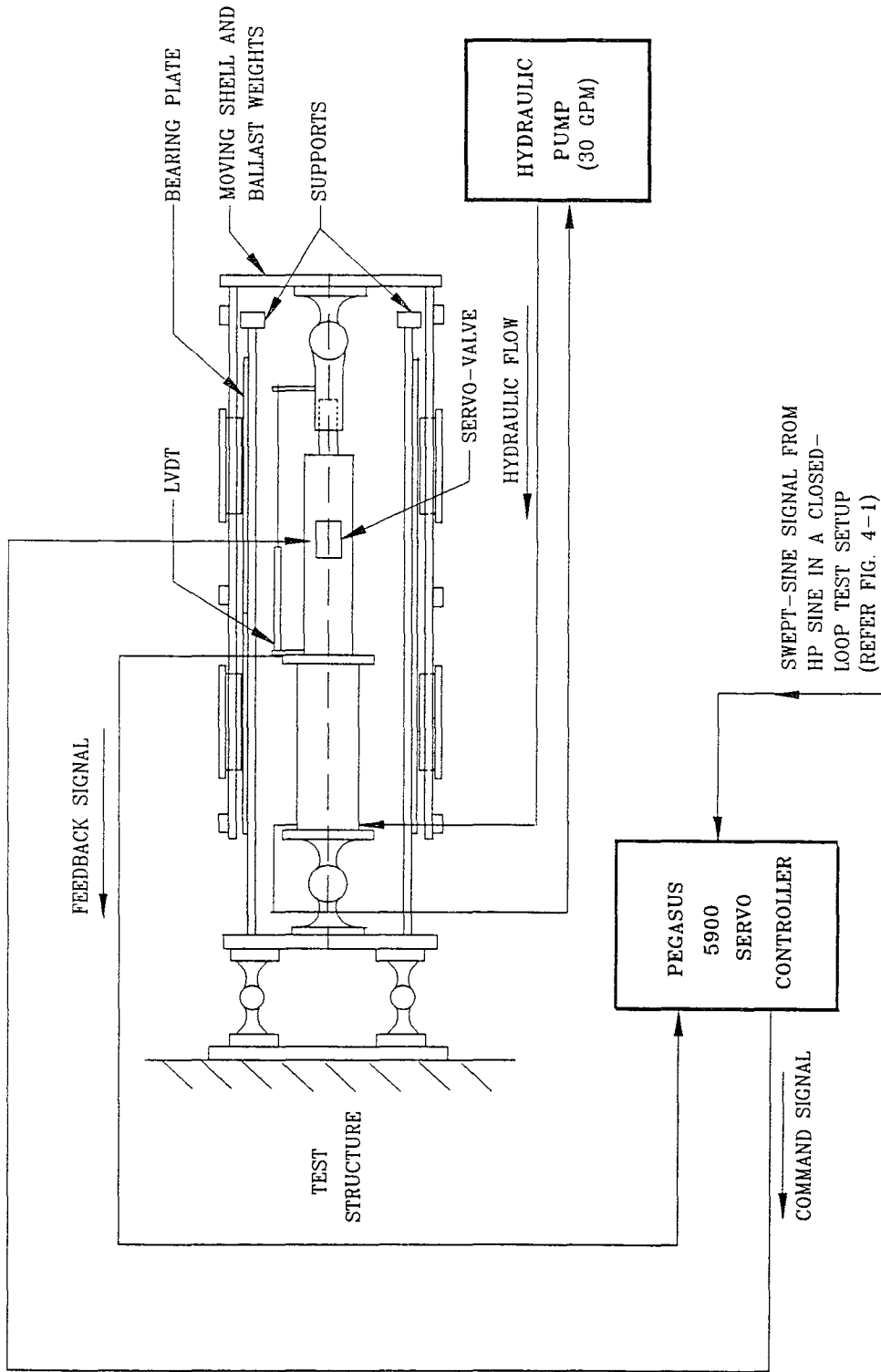


Figure 4-11 Block diagram of the Excitation System.

4.4.1.2 Servo-Controller

The SCHENCK PEGASUS 5900 Digital Servo-Controller is shown in Fig. 4-10. This unit is software-driven with a 72-bit processor, built-in-signal conditioners and function generators. This controller generates an excitation command signal to the servo-valve of the exciter and controls the exciter displacement to adjust force amplitude. This unit accepts a calibrated external analog signal also and generates a command signal of the same form and relative intensity. Therefore, this servo-controller can be integrated with the completely automated signal processing software and hardware, enabling the software to completely control the excitation. Finally, this unit minimizes deviation between the command and feedback signals continuously.

4.4.1.3 Verifying the Excitation System

After assembling the exciter, tests were conducted to check performance. An accelerometer was mounted on the moving shell to measure the actual force output. Swept-sine tests were conducted in a frequency range of 0-20 Hz using the same data acquisition system utilized for the closed-loop modal testing. The power spectrum of the force output was obtained.

The actual performance of the exciter is compared with the specified performance in Fig. 4-12. The exciter would safely deliver only 3200 lbf in the frequency range of 1.6-20 Hz during actual operation as against the designed force of 5000 lbf in the same frequency range. Attempts to drive the exciter for higher force output led to hydraulic cavitation or mechanical failures. While all the components of the exciter were individually rated for higher force, system interaction problems between the actuator, servo-valve, and other hardware and software led to a loss of performance. Exciter dynamics remain a complex problem because the hydraulic-mechanical components of the exciter retain their own complex response mechanisms and stress amplifications during operation.

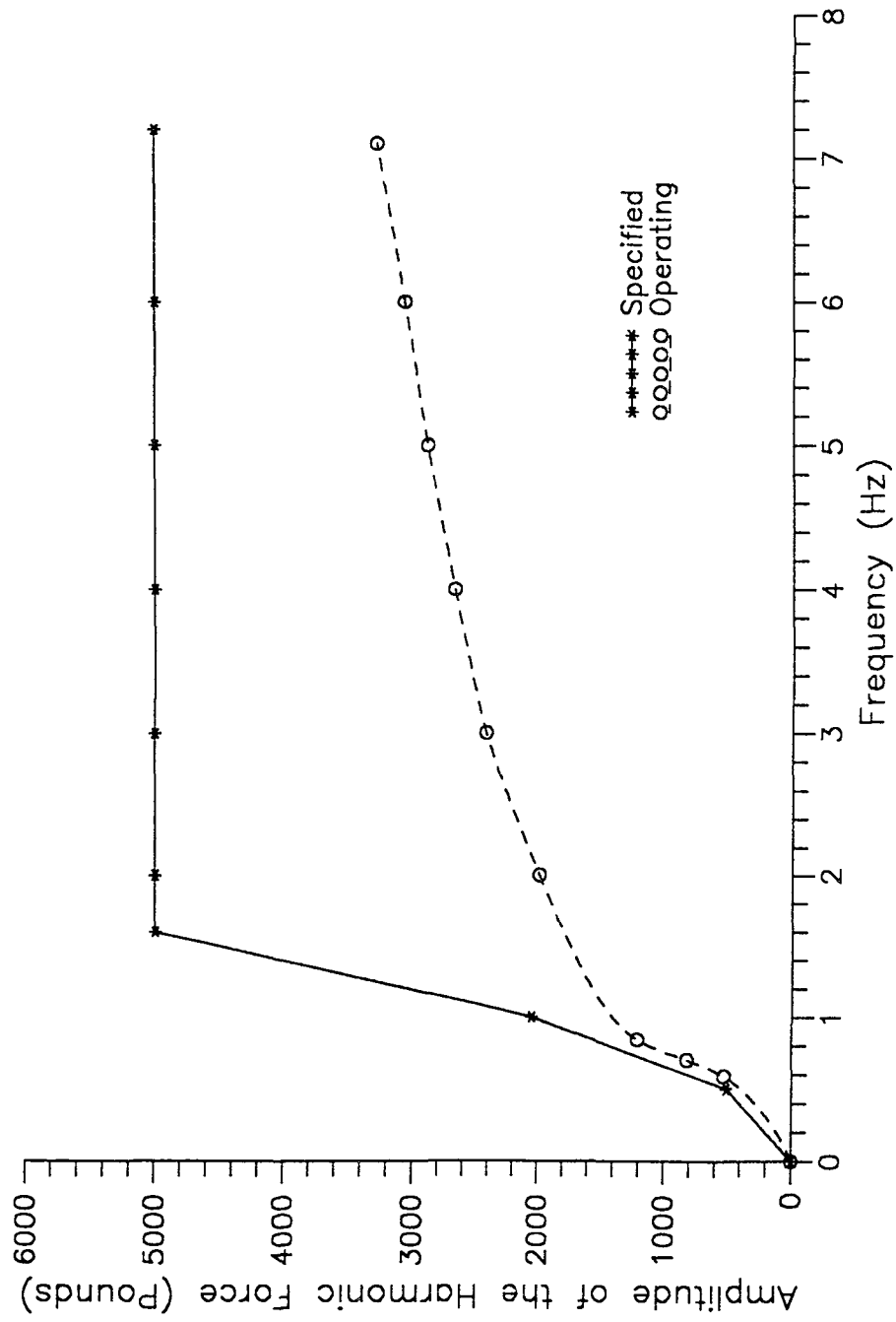


Figure 4-12 Comparison of Specified and Actual Dynamic Force Capacity Spectrum of the Exciter.

4.4.2 Data Acquisition System

The data acquisition system is comprised of a work station, signal processing hardware and signal processing software. The HP SINE signal processing software and HP 3565S measurement hardware are considered the state-of-the-art in modal testing and have been developed by HP for high performance modal test operations. Although they became available in 1986, the software was revised in 1989.

4.4.2.1 Work Station

The work station used for this test was an HP 9000 series 300 computer (model HP 370) with the HP-UX operating system. The computer has 16 megabytes of RAM to host the HP SINE signal processing software. A multi-window display permits mouse or keyboard interface to the measurement hardware and to the HP SINE's analysis tools.

4.4.2.2 Signal Processing Hardware

An HP 3565S measurement hardware system was employed. This consists of a mainframe, signal processing modules, source modules, and input modules. The mainframe acts as a chassis and powers, holds, and integrates the modules. The measurement hardware interfaces with the computer system. Controlled by the HP SINE signal processing software, the hardware-software assembly provides a multi-channel system for acquiring and processing data in both time and frequency domains. The multiplexer has the theoretical capacity to acquire and process data from 2048 channels simultaneously.

Functions and specifications of source modules, input modules, and signal processing modules are given in Appendix-A. The source module generates the swept-sine excitation signal and the input module measures the response signals. The signal processing operations take place at the signal processing module. Photographs of the hardware and a block diagram showing the role of each module within the test system, are shown in Figs. 4-13 and 4-14.

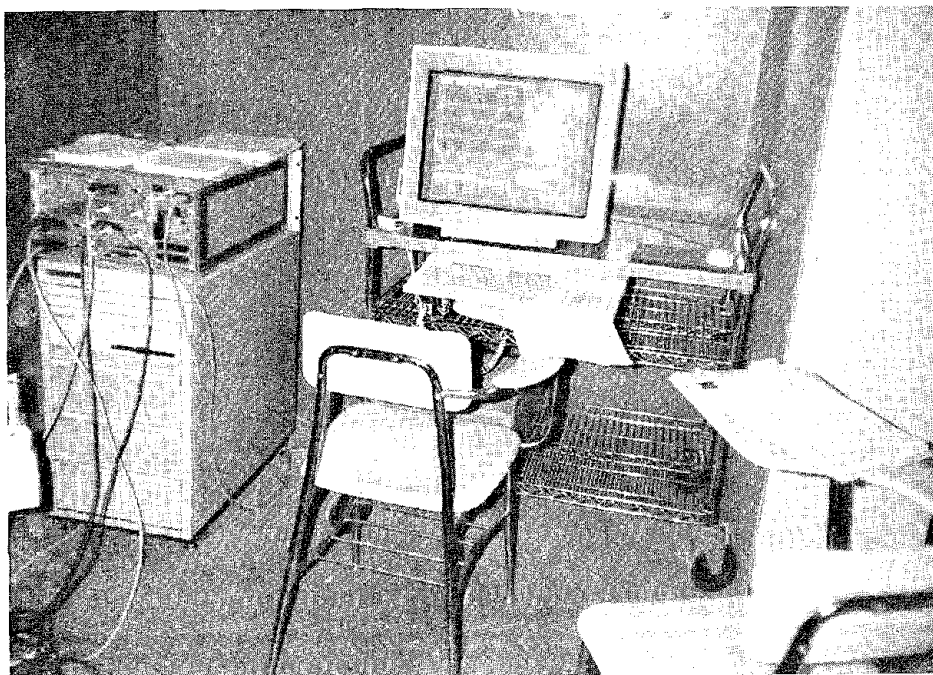


Figure 4-13 Photograph of the Data Acquisition Equipment Used for the Closed-Loop Modal Test.

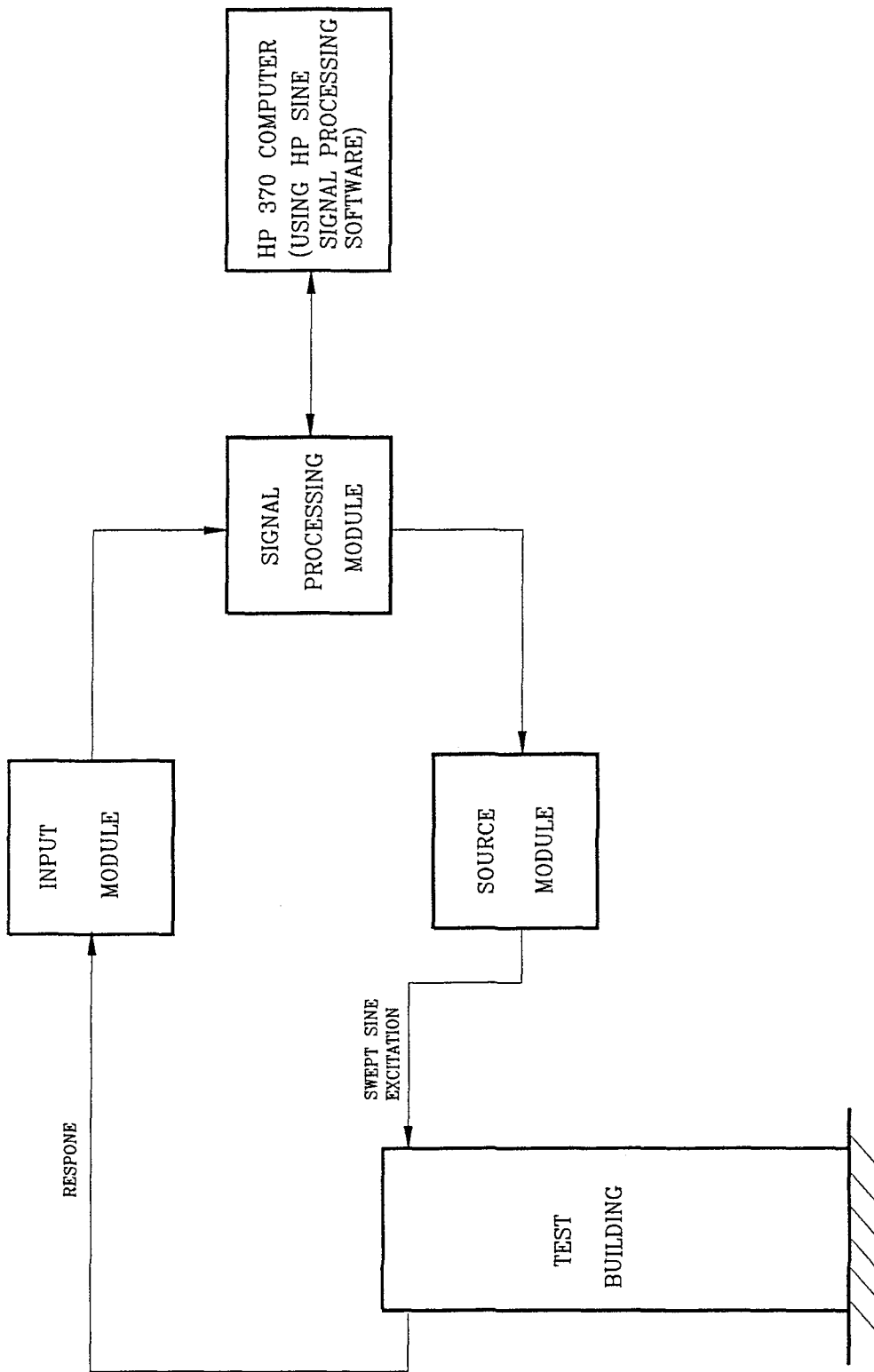


Figure 4-14 Block Diagram of Modules of the Measurement Hardware.

4.4.2.3 Signal Processing Software

The signal processing software HP SINE (1986, 1989) controlled the swept-sine excitation and performed signal processing operations. The software controls the measurement hardware system and uses the data transferred from the input module to the signal processor module. Other functions of this software include simultaneously processing data from up to 2048 channels and controlling multiple exciters which may be synchronized or operated at 180° out of phase. HP SINE uses a window system to control the information on the screen of the host computer. Interactive graphic window operations such as moving, creating, enlarging, or reducing windows are controlled by a pop-up menu. Some of the additional features of the HP SINE are given in Appendix-A.

4.4.2.4 Analog Filters

A DIFA filter (model SCADAS) providing low-pass, high-pass, band-pass, and by-pass analog filtering operations, was employed. The low-pass filter of this system was used at a cut off frequency of 15 Hz to condition two critical channels: forcing function and driving-point response.

4.4.2.5 Amplifiers

Two 12-channel amplifiers (model 483 B17 Piezotronics) were utilized in the modal test. Amplifiers are used to provide power to the accelerometers and to amplify their signals. These amplifiers provide an adjustable gain range from 0 to 100 and have a frequency band of 0.3 Hz to 150 kHz.

4.4.2.6 Accelerometers

The specifications of the Piezotronics model PCB 393C seismic accelerometers used in the test are given in Appendix-A. All twenty two accelerometers were calibrated by the gravimetric free-fall method to determine their sensitivity along with the signal conditioning

system. Accurate calibration is vital for determining the scaled modal vectors accurately.

4.4.2.7 Cables

BNC cables were used to connect the accelerometers to the measurement hardware system through amplifiers or filters. The longest cable used was 400 feet. The cables were cut in varied lengths of 50, 100, and 200 feet and were joined together by BNC coaxial connectors wherever necessary. Proper connection of cables and connectors was ensured by using the self-test meter of the amplifier boxes.

4.5 Execution of the Modal Test

4.5.1 General

The modal tests followed an extensive preparation and calibration effort and involved many personnel. Successful preparation was attributed to detailed time-scheduling and planning as illustrated in Fig. 4-15. The data acquisition system, amplifiers, and weather information display were set up, maintained, and monitored at a control room on the 25th floor.

4.5.2 Data Acquisition and Storage

Initially, the parameters for controlling the excitation and data acquisition were established. Important data acquisition settings are shown in Table 4-1. The swept sine measurement was initiated in a specified frequency range. The HP SINE software directed the source module of the measurement hardware (Fig. 4-14) to generate the swept sine excitation. The source module then sent an analog signal to the servo-controller that controlled the exciter.

After the source module began sending a signal to the servo-controller, a ramp up time of 10 seconds was needed for the exciter to ramp up to attain the specified force level at the starting frequency. After reaching this level, a settling time of 10 cycles was required

PRELIMINARY MODAL TEST OF THE SANDER HALL						
PROJECT SCHEDULE	EXCITER	SENSOR	CABLE	DATA ACQUISITION	WEATHER STATION	MISCELLANEOUS
MARCH 1990						
19 Mon	Ca Fixing	Cu Drop Calibration of Sensors	T		Purchase ?	Safety Lock ? Transportation ? Power line ? Elevator ?
20 Tue		everything prepared ? then installation		Cu Ambient Vibration Test	Install ?	Weather forecast check
21 Wed	Cu Proofing Test					preparing a schedule
22 Thu	Moving to the building					
23 Fri	Modal Test			Ca Modal Test		check up initial problems
A : Dr. Aktan B : Dr. Baseheart D : Dr. Brown R : Dr. Allemang Ca : Charles Cu : Chuan S : S. Hosahalli T : T. Toksoy Y : Yoshi						

Figure 4-15 Typical Plan-Time Schedule Used to prepare for the Test.

TABLE 4-1 Data Acquisition Settings Used in the Closed-Loop Modal Test.

Parameters	Value/ Settings	Remarks
<u>Sweep Control Parameters</u>		
Sweep Start (Hz)	0.5*	Initial frequency
Sweep Stop (Hz)	0.9*	Final frequency
Sweep Type	linear	Linear swept sine
Resolution (Hz)	0.015625	Finest resolution available
Autoresolution (off or on)	off	Not used
Integration Time (Sec)	80	Signal averaging time
Settle Time (Cycles)	10	Time for transients to die out
Input Span (Harmonics)	10	Span of input module's digital filter
<u>Source Module Setup</u>		
Output Level (Vp)	10	Excitation signal level
DC Offset	0	Controls ramp up time
Ramp Time (milli V/step)	100	Controls ramp up time
Output Type	Swept Sine	Type of excitation
Autolevel (off or on)	off	Not used
<u>Input Module Setup</u>		
Input Range	Adjusted manually	
Autorange (off or on)	off	Not used
Window	Hanning	Weighting function
Input Force	Voltage	Input signal
Coupling	DC	Coupling of input signals to input channels

* Values shown are the initial and final frequencies of the sweep in the range of 0.5-0.9 Hz

for the transients to diminish. At the steady-state, the response signals were averaged for 80 seconds to eliminate the noise in the signal. The source module maintains the signal at each successive frequency point until the steady state is reached and the signal has been averaged for 80 seconds before proceeding to the next frequency point.

The building's acceleration responses were monitored by the accelerometers. The building's typical response level during the test was in the order of milli g's. Measuring such low-level signals, particularly those from the lower floors and the basement, was a challenge. The signals were amplified 100 times except for the force reference channel and the driving-point response which were amplified only 10 times.

The input module measured the response signals and the data was transferred to the signal processing module. The signal processing module, controlled by HP SINE software, executed the signal processing operations. The processed data was stored in the hard disc for subsequent post processing.

The force reference and the driving-point response contained high frequency noise which not only caused autoranging problems, but also increased the input range for these channels and thereby decreasing the signal-to-noise ratio. Due to their importance, these signals were filtered before digitization using a low-pass filter set at a cut-off frequency of 15 Hz.

To optimize measurement time, swept sine measurements were carried out within small frequency ranges which were selected based on prior knowledge of building frequencies. In the absence of such information, ranges can be selected by conducting a preliminary sweep with a practical two-channel dynamic analyzer. The swept sine measurements in the NS direction were performed in three frequency ranges of 0.5-0.9 Hz, 1.81-2.6 Hz, and 3.5-5.2 Hz. These ranges covered the first three translational modes in the NS direction as well as the first three torsional modes. The tests were repeated by exciting the building in the EW direction to obtain the first three translational modes in this direction. The three frequency ranges during the swept sine measurements in the EW

direction were 0.56-0.84 Hz, 2.2-3.18 Hz, and 5.5-7.2 Hz.

The total time for conducting the sweeps in all the frequency ranges to obtain the first nine modes required only three hours. However, these three hours exclude any interruptions due to over heating of the excitation system and re-orienting the exciter and accelerometers.

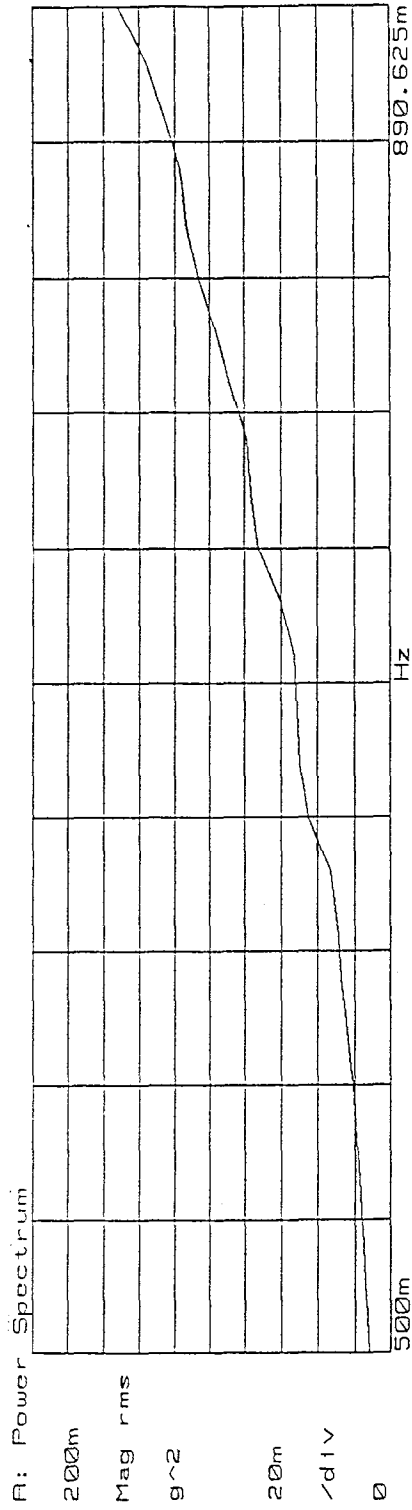
Ambient conditions were recorded every five minutes during measurements. The wind speed varied from 14-21 miles per hour while the interior and exterior temperature ranged between 90° F and 102° F.

4.5.3 Frequency Domain Measurements

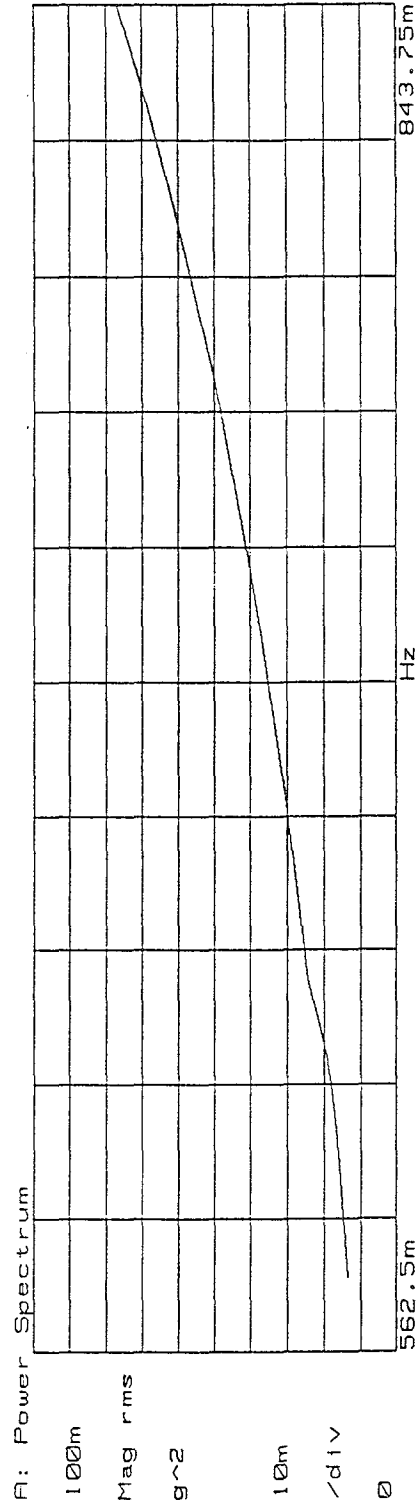
The accelerometer mounted on the moving part of the exciter acted as the reference channel for calculating the frequency response functions. The power spectra of the input force in the NS direction in the frequency range of 0.5 to 0.89 Hz and in the EW direction in the frequency range of 0.5625 to 0.84375 Hz, are shown in Fig. 4-16. These spectra indicate that the force is gradually increasing with the frequency. The FRFs were calculated for all the twenty accelerometer responses during excitation along both the NS and EW directions. Because the FRF is complex, it is stored in the form of magnitude and phase versus frequency. Typical FRF magnitudes obtained in NS and EW direction tests at the driving point are shown in Fig. 4-17. FRF magnitudes at different floors due to excitation along the EW direction in the frequency range of 0.5625 to 0.84375 Hz are shown in Fig. 4-18.

4.5.4 Response Time Histories

Time histories of excitation signal, driving-point response, and responses from various floors are exemplified in Figs. 4-19 and 4-20. Figs. 4-19 and 4-20 reveal the response attenuation from the 25th floor to the basement while the building is excited at its first bending mode along the EW direction. When a harmonic force of 1100 lbf amplitude

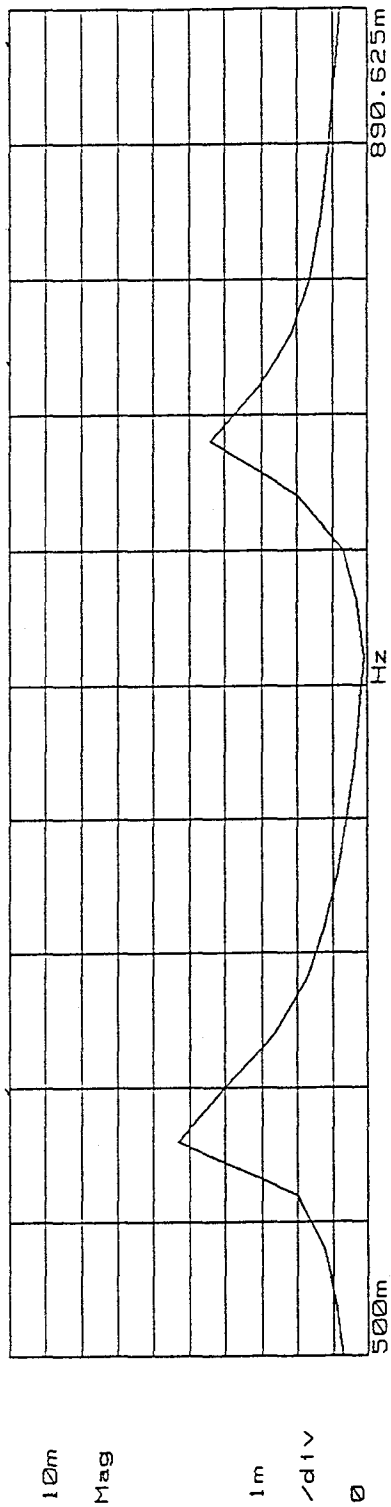


(a) NS Direction

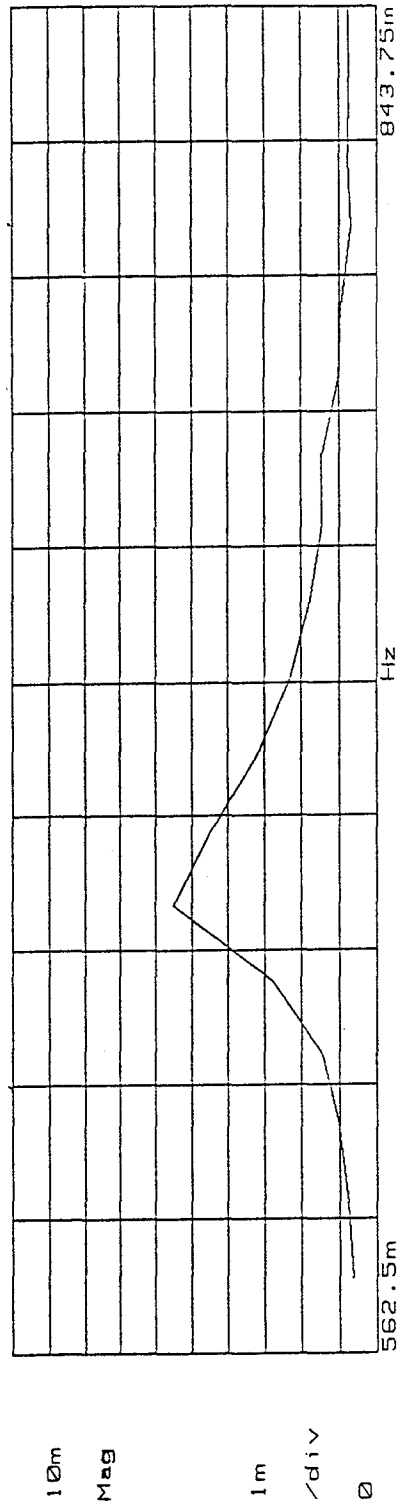


(b) EW Direction

Figure 4-16 Power Spectrum of the Input Force due to Excitation in NS and EW Directions.

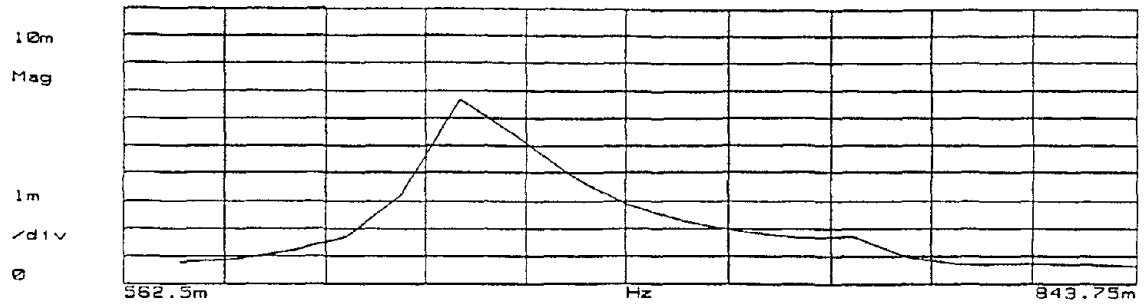


(a) Excitation Along NS Direction

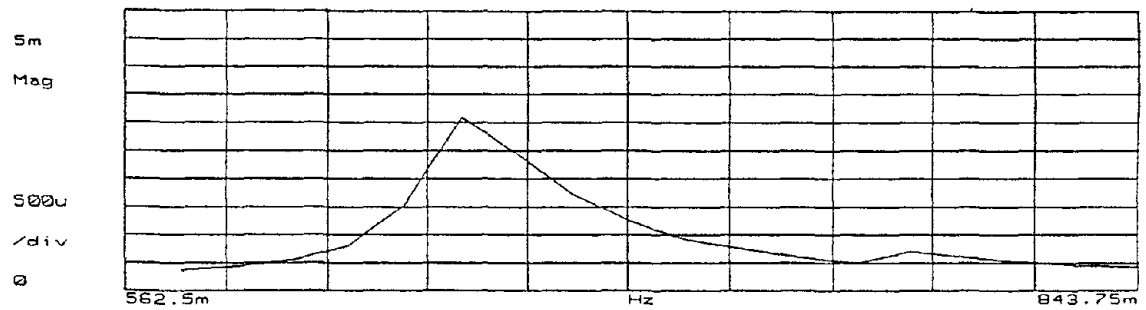


(b) Excitation Along EW Direction

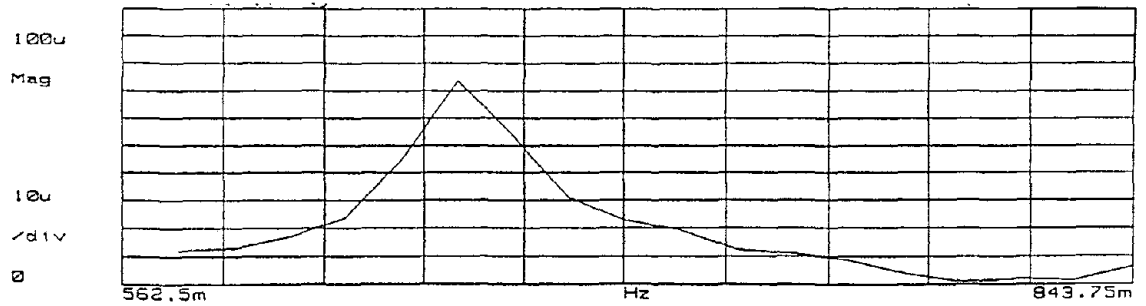
Figure 4-17 Frequency Response Function at the Driving-Point.



(a) Floor 26



(b) Floor 13



(c) Basement

Figure 4-18 Frequency Response Functions at Different Floors due to Excitation in the EW Direction.

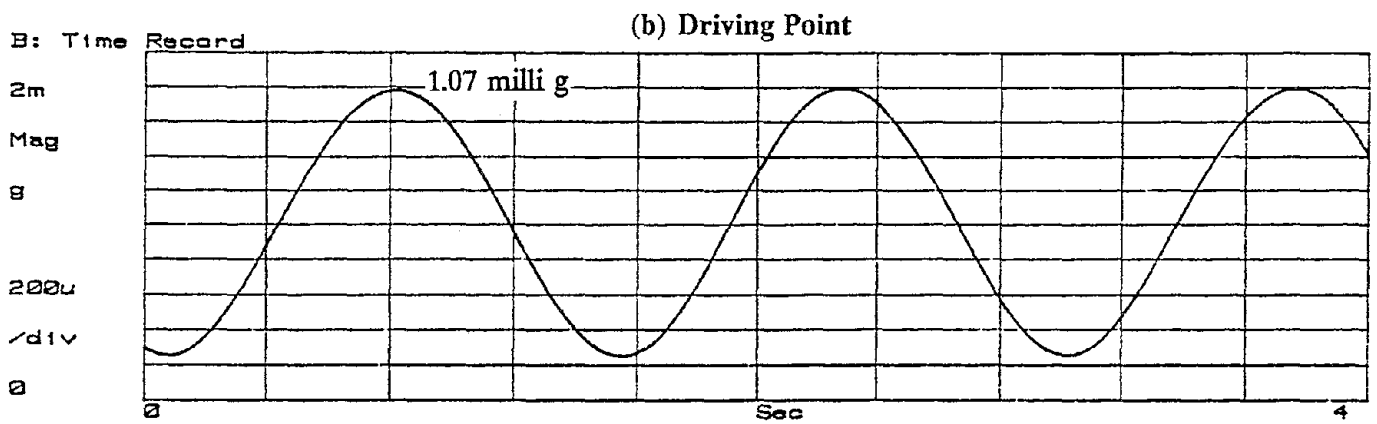
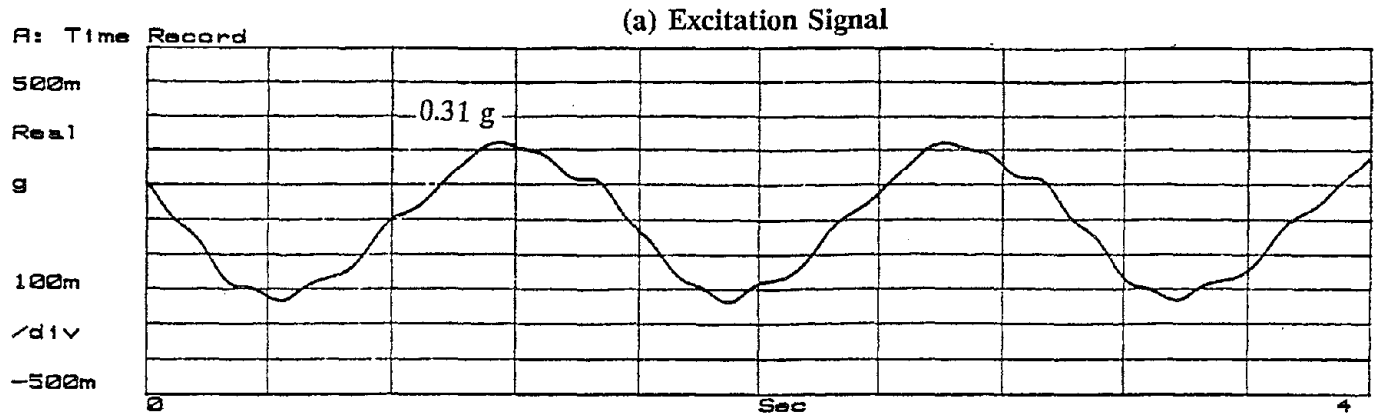
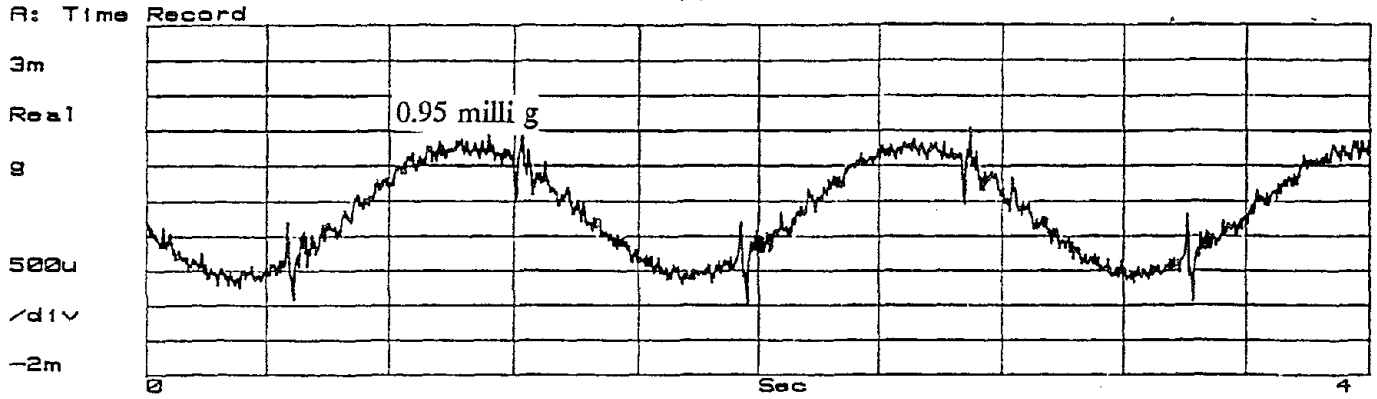
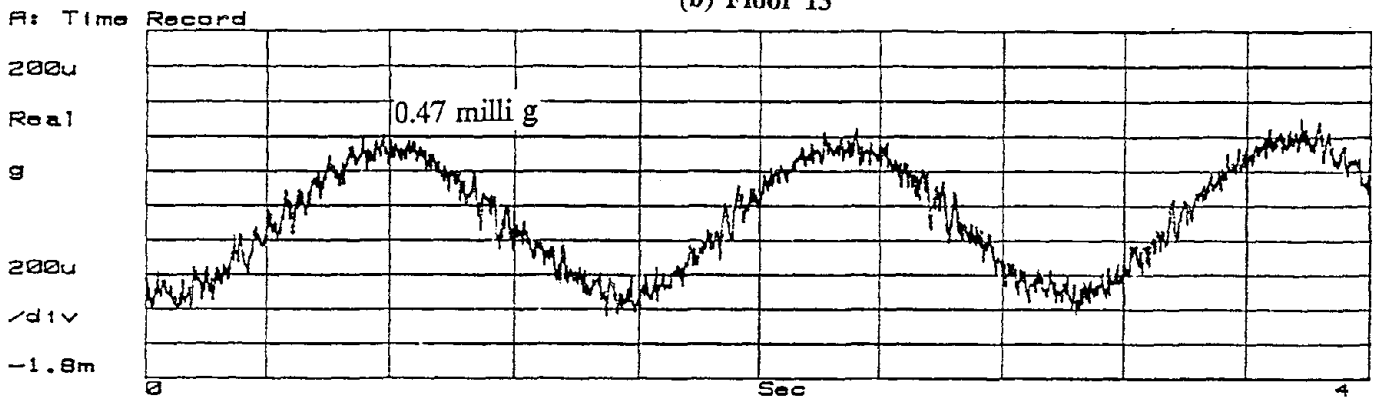


Figure 4-19 Time Histories (Filtered) of the Excitation Signal and Driving-Point at the First EW Mode.

(a) Floor 26



(b) Floor 13



(c) Basement

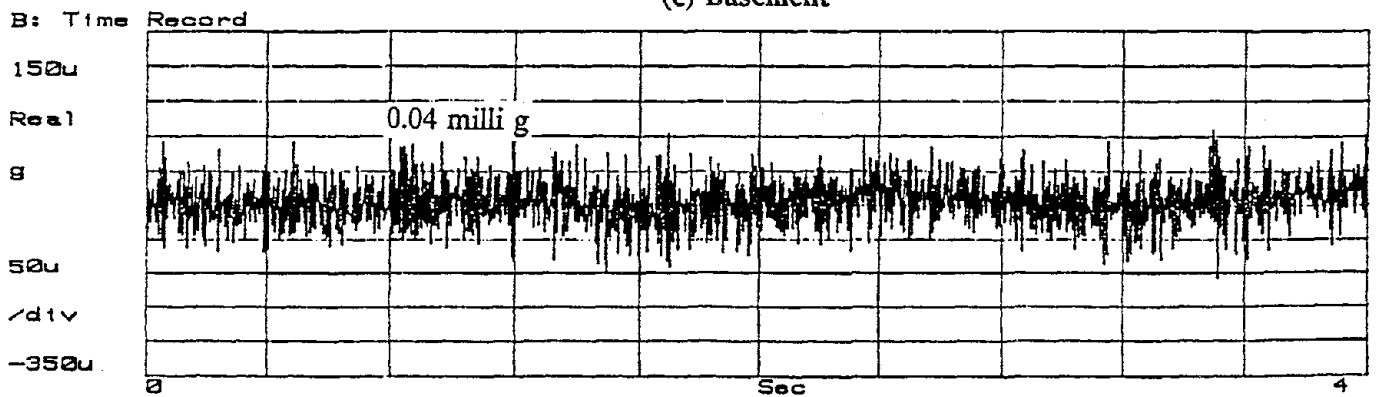


Figure 4-20 Time Histories of Responses (Unfiltered) at Different Floors at the First EW Mode.

(compared with 40000 kips of estimated building weight) was applied at the 25th floor, the driving-point response was found to be 1.07 milli g while response elsewhere on the 25th floor was 0.88 milli g. Response at the 26th and 13th floors were respectively 0.95 milli g and 0.47 milli g while the vertical response at the basement was 0.04 milli g. The attenuation characteristics would naturally change at different limit-states of the structure.

SECTION 5

POST PROCESSING

5.1 General

During each sweep, frequency domain data was obtained from 22 accelerometers located throughout the building. Twenty one of these channels were response while one was the force reference channel. The 21 frequency response functions (FRF) obtained in the form of acceleration (magnitude and phase) over force comprised the basis of parameter estimation.

5.2 Algorithm

Data processing included extracting the modes of vibration, natural frequencies, damping factors, and modal vectors (both unscaled and scaled) from the test results. For this purpose, the software "UC Modal" which incorporates the "Polyreference Frequency Domain Algorithm" was used. This software has been developed at the Structural Dynamics Research Laboratory of the MINE Department at the University of Cincinnati.

5.2.1 Significance of the Algorithm

Given a set of data, choosing the right algorithm is an important step for accurately and feasibly calculating the parameters. First, the time versus frequency domain should be decided. Time domain algorithms use impulse response functions as opposed to frequency response functions and have many advantages in the case of impact testing or burst random excitation. However, the most advantageous applications of time domain parameter estimation algorithms, such as the Ibrahim Time Domain or the Polyreference Time Domain, emerge in the case of decaying time domain data. In the case of sine testing, data is acquired at the frequency of excitation and the frequency response function is directly recorded by dividing the measured response with the force at that particular frequency. A

time domain parameter estimation method is not recommended since this would require an inverse Fast Fourier Transform (IFFT) which has disadvantages. First, in order to perform an inverse FFT, data should be acquired at a constant frequency spacing. Second, since most commercial FFT algorithms require the number of data points to be a power of two for speed and efficiency, the frequency bandwidth cannot be chosen arbitrarily when time-domain methods are used.

The HP SINE software applies an integration algorithm which involves determining the Fourier coefficients of the response and the force signal by Fourier transforming their sampled time histories. This process is repeated at every frequency with intervals dictated by the preset frequency resolution until the end of a window. The Polyreference Frequency Domain parameter estimation method was developed to directly process such data and fully exploit the sine testing method. In this particular test, the data was acquired over short frequency ranges. This removed any concerns related to numerical instability of frequency domain parameter estimation methods which is typical when large frequency bandwidth are considered.

5.2.2 Description of the Algorithm

The basis of the algorithm is decomposing the measured frequency response matrix. This matrix is represented by:

$$[H_{pq}(\omega)]_{N_i \times N_o}$$

where $H_{pq}(\omega)$ = response obtained at point p due to an excitation at point q.

N_i = number of input (reference) points

N_o = number of output (response) points

In the case of the current modal test, the number of reference points was one and the number of response points was twenty one. The measured frequency response matrix can be decomposed as follows:

where N = Number of modal frequencies

$$[H(\omega)]_{N_s \times N_s} = \sum_{r=1}^N \frac{[A_r]}{j\omega - \lambda_r} + \frac{[A_r^*]}{j\omega - \lambda_r^*} \quad (5-1)$$

$[A_r]$ = Residue matrix

$[A_r^*]$ = Complex conjugate of the residue matrix

λ_r = System pole = $\sigma + j\omega_r$

σ = Damping factor

ω_r = Frequency in radians/sec

Equation 5-1 is solved for the natural frequencies, damping factors, and residues. Since the number of equations, which depend on the number of sample points, are much higher than the number of unknowns, a least squares type of solution technique is utilized. The residues give the unscaled modal vectors. The procedure for obtaining scaled modal vectors is explained in Section 6. The residues obtained at the end of the least squares estimation process are in units of "g" since the measured FRF matrix is in an acceleration over force format. To convert these residues to length units, they were multiplied by the gravitational acceleration constant (32.2 feet/sec²) and divided by the square of the natural frequency.

5.2.3 Complex Modes vs Normal Modes

There is an ongoing dispute over whether complex modes better represent constructed facility dynamic response than normal modes. Assuming normal or complex modes becomes significant for appropriate curve fitting and obtaining accurate modal coefficients. Complex modes correspond to assuming non-proportional damping. With this assumption, every entry in the residue matrix is complex and therefore leads to complex modal vectors. In the case of normal modes, each entry in the residue matrix is a single imaginary number. Therefore, in the case of normal modes the number of parameters to be

solved is reduced to half. Fitting a curve to data with twice the number of degrees of freedom, naturally improves the correlation. However, this improvement may not be physically justified particularly if the damping of a system is below 10% of critical damping.

A comparison between complex vs normal curve fitting is shown in Fig. 5-1. This comparison shows that the difference was not significant for this test. In both cases the first peak is fairly well estimated with a slight variation in the damping whereas the second peak has a frequency error of only 0.016 Hz.

5.2.4 Residual Terms

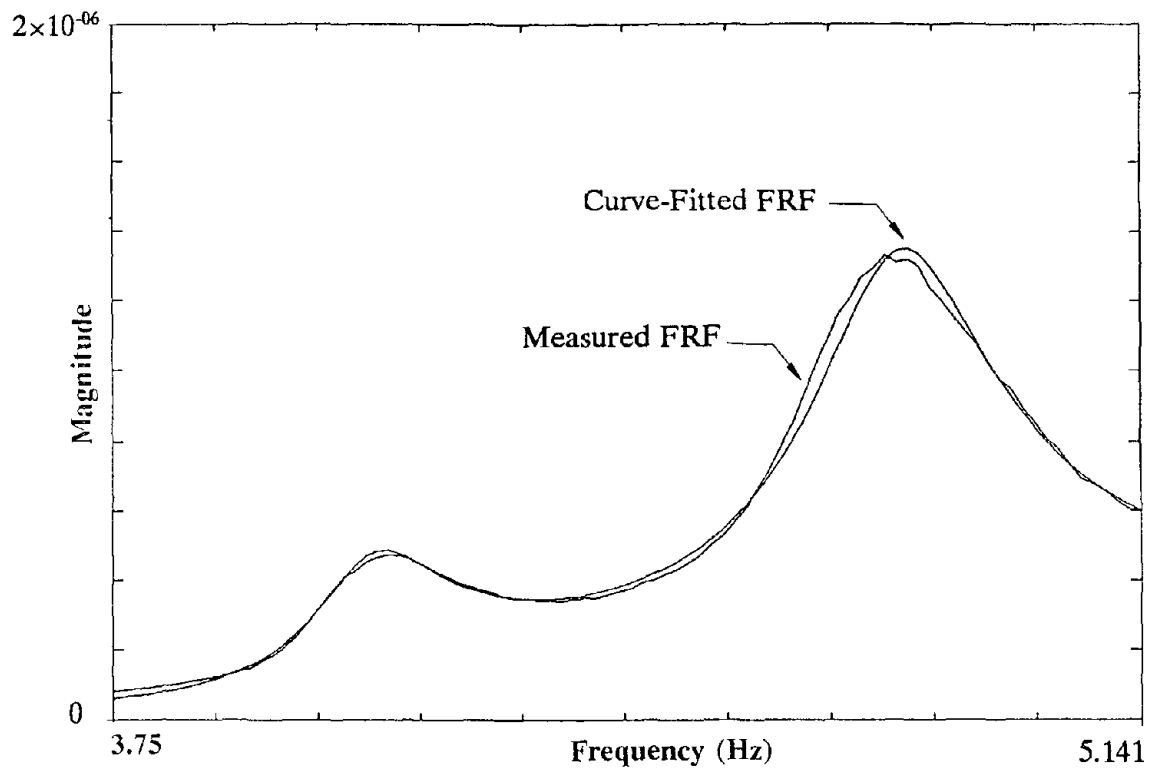
A feature of the selected frequency domain post-processing is the capability to account for the effect of any modes that are outside the frequency range of interest on the modes that are inside this range. When parameter estimation is performed on a zoomed section of a frequency spectrum, the modes that remain outside this window may affect the frequency and damping estimates. To account for this adverse effect, residual terms are included in the curve fitting procedure. Residuals are mathematical terms without any physical meaning. A frequency response function including the residual terms may be represented as:

$$H_{pq}(\omega) = R_{lpq} + \sum_{r=1}^N \frac{A_{pqr}}{j\omega - \lambda_r} + \frac{A_{pqr}^*}{j\omega - \lambda_r^*} + R_{fpq} \quad (5-2)$$

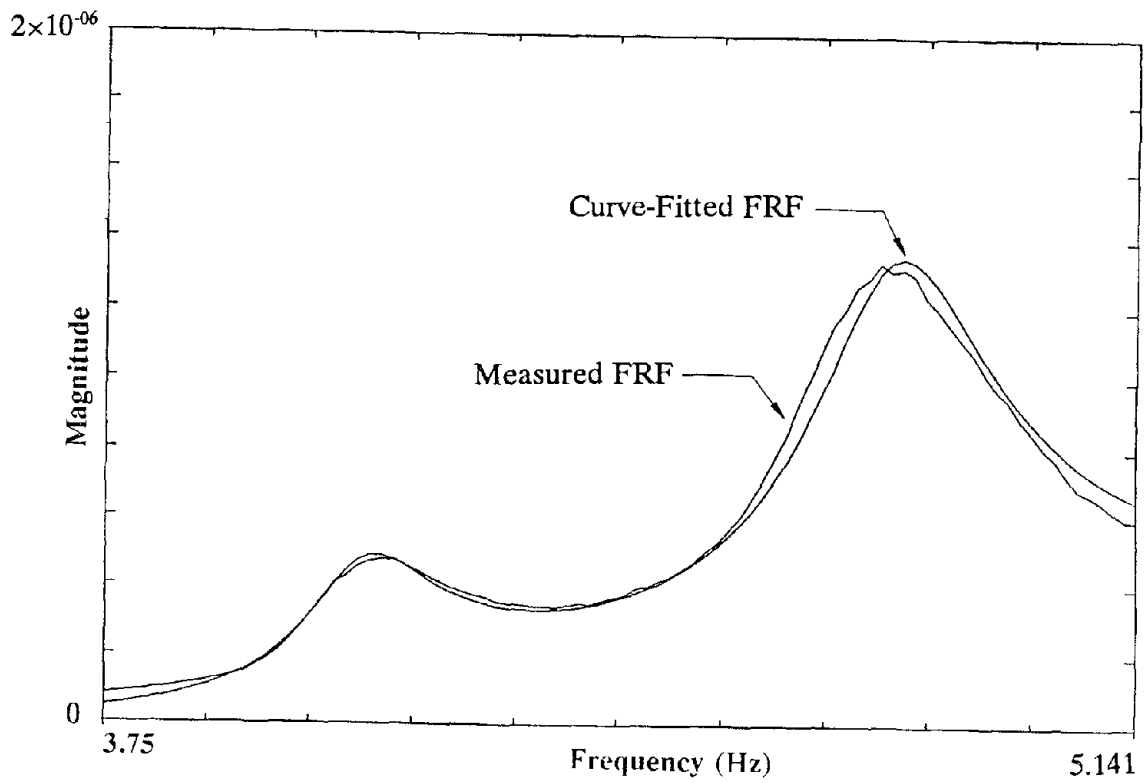
where $R_{lpq}(\omega)$ = Residual effect of lower frequency modes

$R_{fpq}(\omega)$ = Residual effect of higher frequency modes

A comparison of curve fitting with and without including the residuals is given in Fig. 5-2. In obtaining modal parameters from the current test data, residual terms were included.

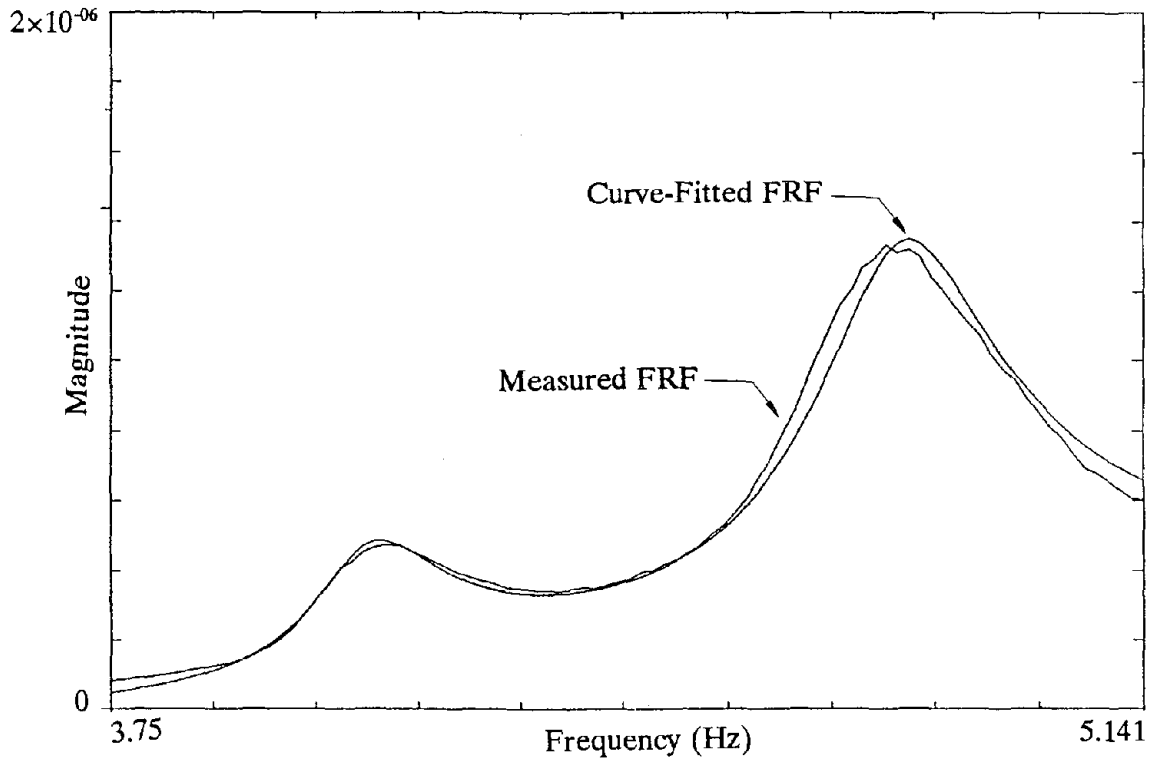


(a) Complex Curve Fitting

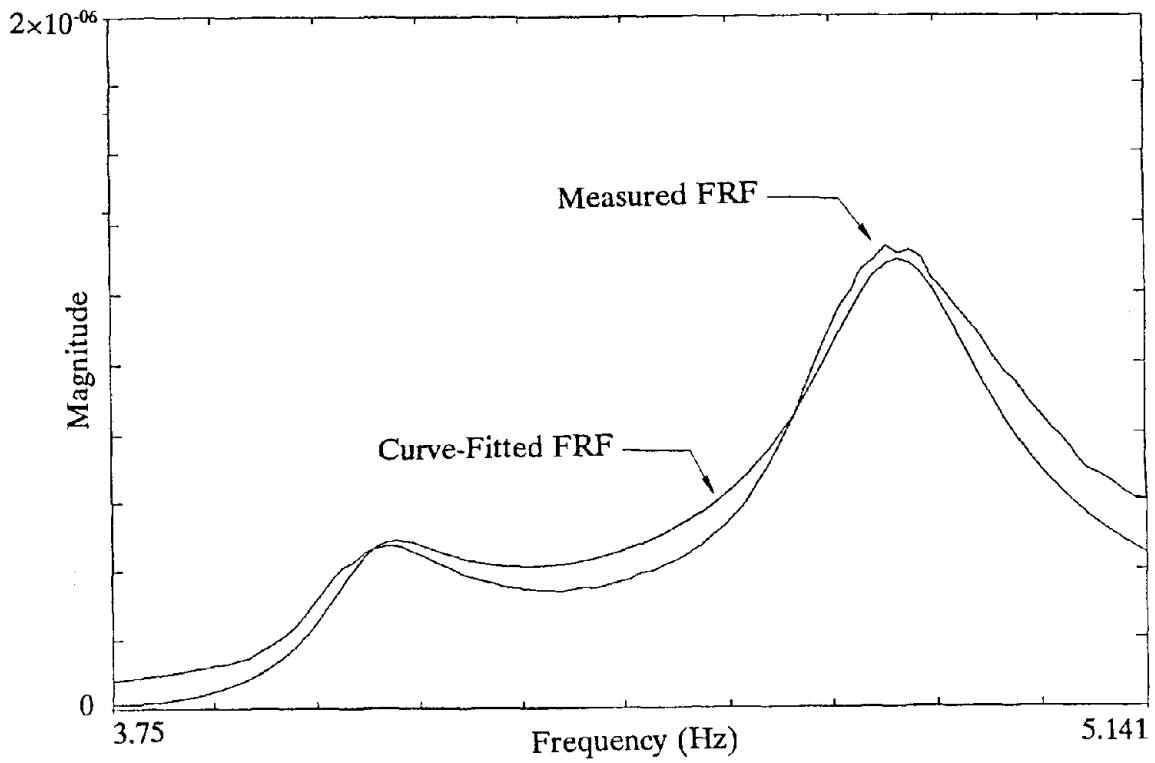


(b) Normal Curve Fitting

Figure 5-1 Comparison of Complex Curve Fitting with Normal Curve Fitting.



(a) With Residual Terms



(b) Without Residual Terms

Figure 5-2 Comparison of Curve fitting with and without including Residual Terms.

5.3 Filtering

5.3.1 Filter Characteristics

During the modal test, the signals from the two most critical channels, namely, the force (reference channel) and the driving-point response, were filtered using a low-pass analog filter set at a cut-off frequency of 15 Hz. It is known that low-pass filters introduce a phase lag effect. To determine this effect, the filter's characteristics were found in terms of a frequency response function of a filtered channel referenced to an unfiltered channel. This FRF, together with its phase information, is shown in Fig. 5-3. The phase plot indicated that the filter introduced a significant phase lag into the signal.

5.3.2 Correction for the Filter Effect

To correct the phase-lag, the frequency response function of the filter in the frequency intervals of the modal test was measured. This was accomplished using the HP Sine software and hardware with the same settings as in the modal test. For each sweep, a sinusoidal signal was provided by the source module and the response of the filter was measured. As a result, six FRFs were obtained for each frequency interval considered during sweeps. These were multiplied with the FRFs measured during the modal test. Hence the raw data was corrected for the filter effect prior to parameter estimation.

5.3.3 Effect of Filtering on the Modal Vectors and Flexibility

The mass normalized modal vectors obtained after correcting for the filter effect were 15% to 20% less than those obtained without correcting for this effect. It is observed that the flexibility coefficients obtained using the force channel records corrected for the filter effect are 31.5% less than those obtained without correcting for the filter effect. This is exemplified in Fig. 5-4. Filtering had little effect on the damping factors and no effect on the natural frequencies.

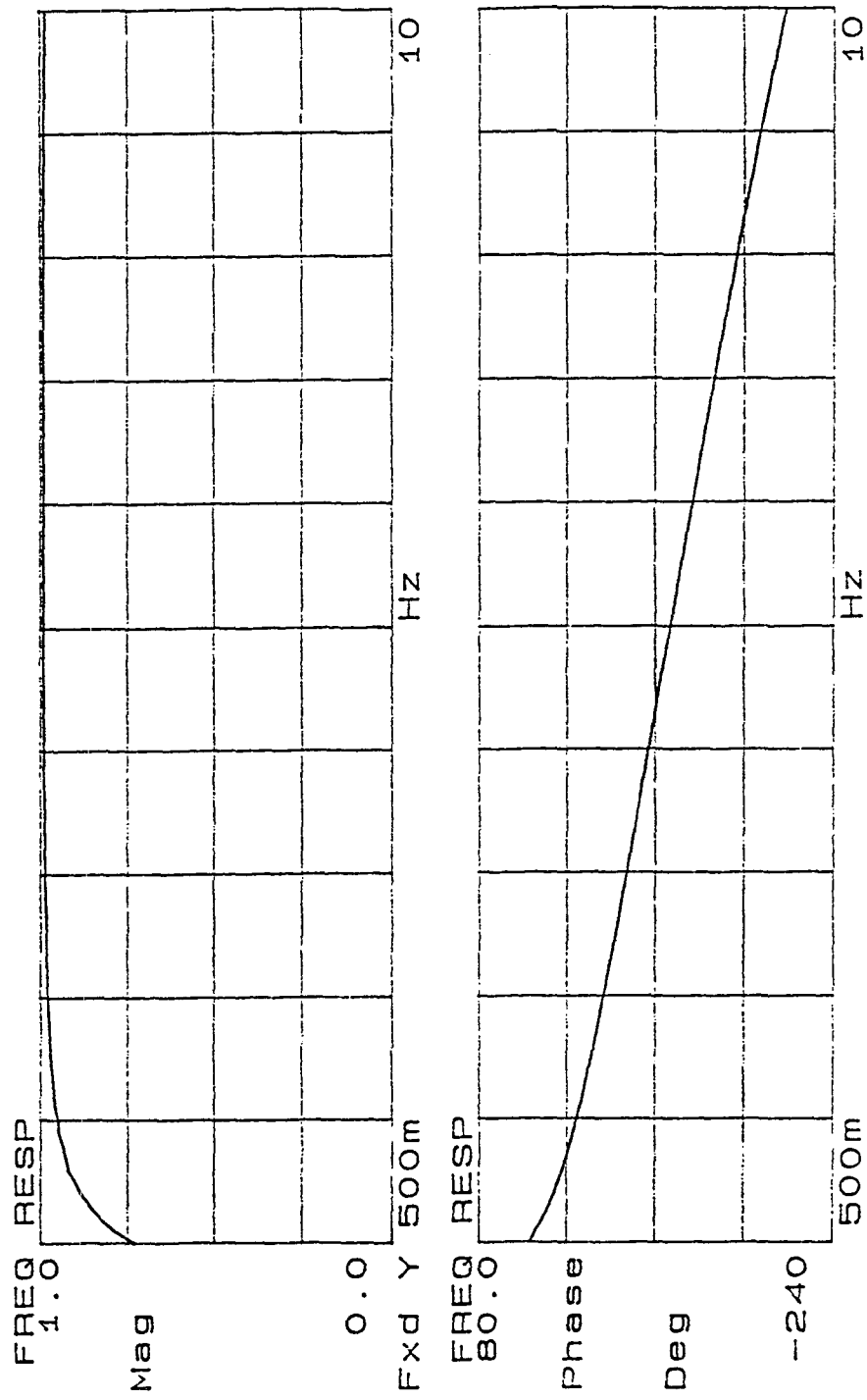


Figure 5-3 Frequency Response Function of Filtered Channel with Reference to Unfiltered Channel (Magnitude and Phase).

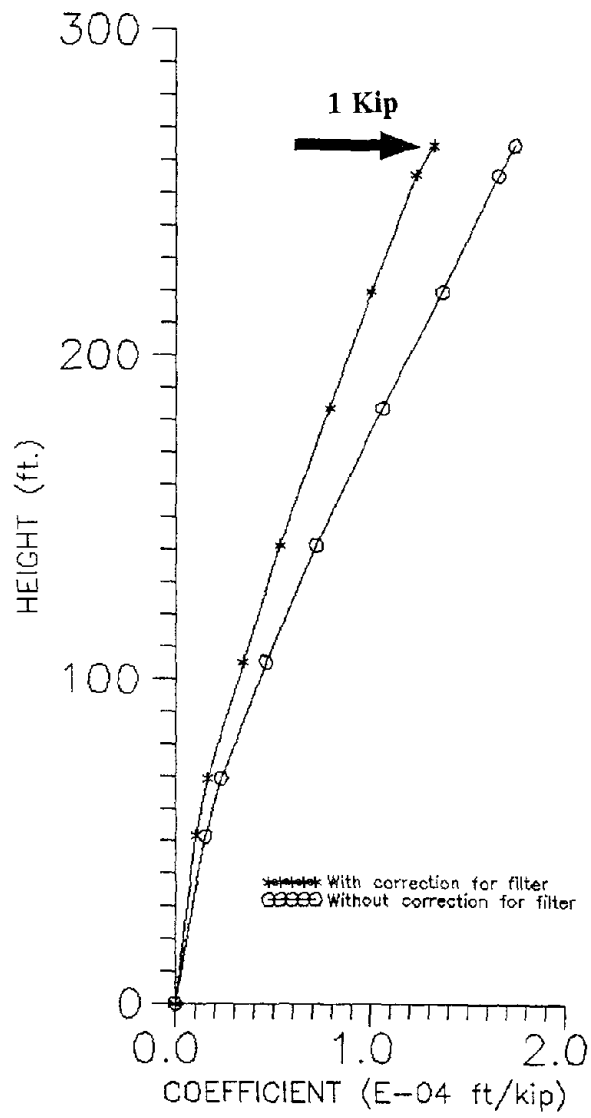


Figure 5-4 Comparison of Flexibility Obtained with and without Correction for Filter.

5.4 Discussion of Errors

Modal testing and theory were primarily developed for mechanical and aerospace structures. These structures, in general, satisfy the linearity, reciprocity, and time invariance requirements which are the basis of modal testing and parameter estimation algorithms. The application of modal testing to constructed facilities, however, is relatively new and challenging. The error sources, compared to mechanical or aerospace structures, are numerous. As discussed earlier, there are many mechanisms which render civil engineering structures highly nonlinear even at low stress levels. Hence, excitation used in the test should be such that mechanical characteristics of the structure are stabilized. The force level should also be kept as constant as possible through all the frequencies.

The presence of noise in the data is an important source of error. In the case of buildings, the sheer size of the building makes it very hard to obtain sufficiently high signal-to-noise ratios. The increase in the total impedance of the cable decreases the signal level and renders the data even noisier. The level of excitation, therefore, plays an important role. The constantly changing effect of ambient conditions on the data is a further source of error. Since wind is a random type of disturbance, its effect on the response can be reduced with sufficient averaging.

SECTION 6
RESULTS OF MODAL TEST

6.1 Natural Frequencies and Damping

The first nine mode characteristics in the frequency bandwidth of 0.5 Hz to 7.2 Hz were evaluated by post processing the measured data using the "Polyreference Frequency Domain Method". The natural frequencies and damping factors are summarized and compared with the corresponding quantities obtained from the previous modal test in Table 6-1.

The damping was obtained by using the following relation:

$$\lambda_r = \sigma_r + j\omega_r = \left(-\xi_r + j\sqrt{1-\xi_r^2}\right)\Omega_r \quad (6-1)$$

which leads to:

$$\xi_r = \frac{-\sigma_r}{\sqrt{\omega_r^2 + \sigma_r^2}} \quad (6-2)$$

where r = mode number

ξ_r = damping ratio

Ω_r = undamped natural frequency

σ_r = damping factor

ω_r = damped natural frequency

λ_r = system pole (eigenvalue)

Additional details are given by Allemang (1990).

6.2 Mode Shapes Including Foundation Displacements

The modal vectors were obtained by post processing the measured data. The first nine mode shapes of the building are shown in Fig. 6-1 and compared to their counterparts

TABLE 6-1 Comparison of Natural Frequencies and Damping Obtained from Previous and Current Tests.

Mode No.	NATURAL FREQUENCY (Hz)			DAMPING RATIO (Percent)		
	Previous Test	Current Test	% Difference	Previous Test	Current Test	% Difference
1 (First NS)	0.58	0.564	-2.76	1.542	2.055	+33.26
2 (First EW)	0.70	0.658	-6.0	1.527	2.091	+36.93
3 (First Torsional)	0.78	0.762	-2.31	1.426	1.594	+11.78
4 (Second NS)	2.06	2.034	-1.26	1.406	1.403	-0.210
5 (Second Torsional)	2.38	2.336	-1.85	1.183	1.206	+1.94
6 (Second EW)	2.92	2.874	-1.57	1.289	1.337	+3.72
7 (Third NS)	4.25	4.097	-3.60	2.977	2.053	-31.03
8 (Third Torsional)	4.84	4.814	-0.54	1.880	2.486	+32.23
9 (Third EW)	6.56	6.490	-1.07	2.953	2.436	-17.50

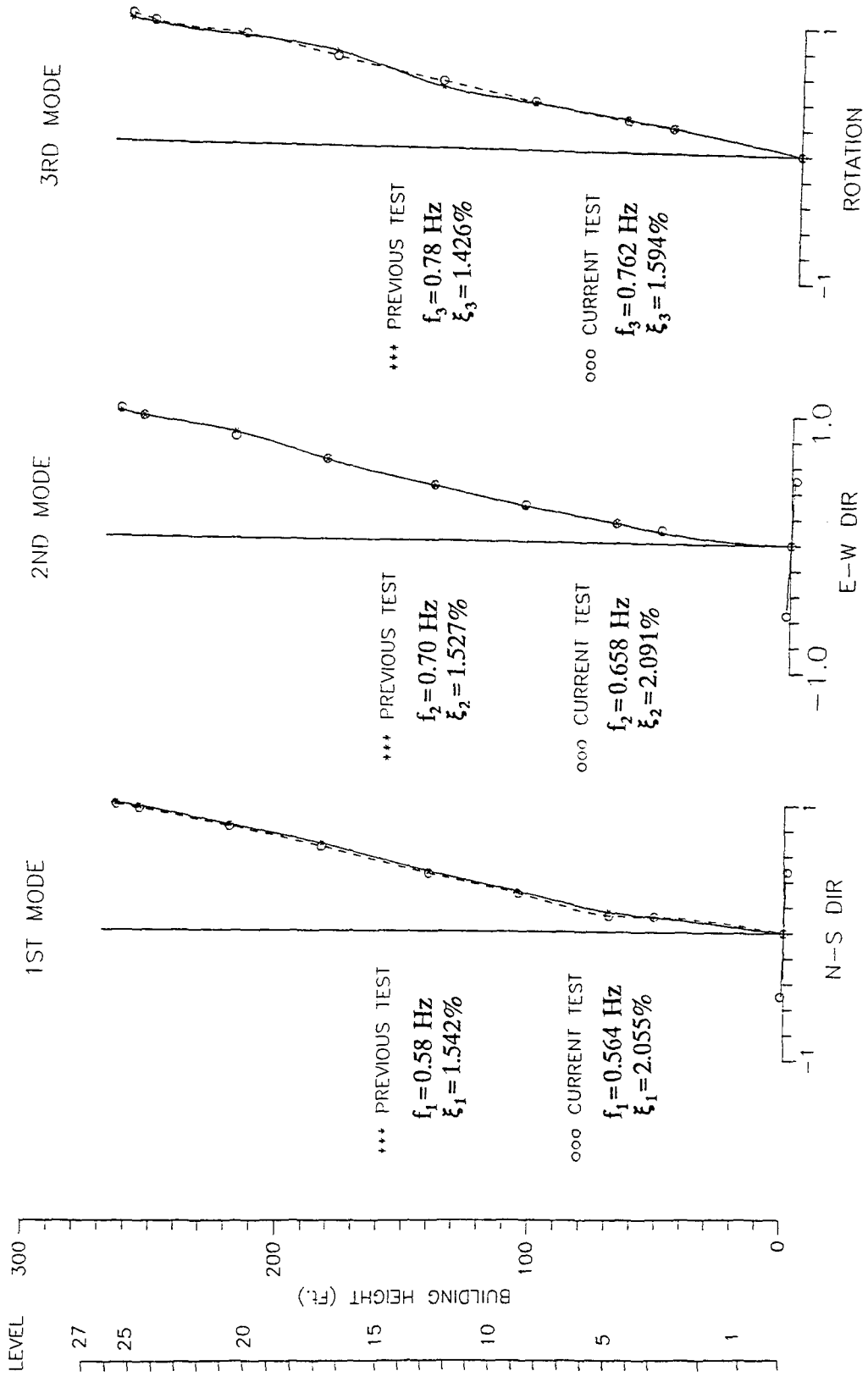


Figure 6-1 Comparison of the First Nine Mode Shapes obtained from the Previous and Current Modal Tests.

- Continued

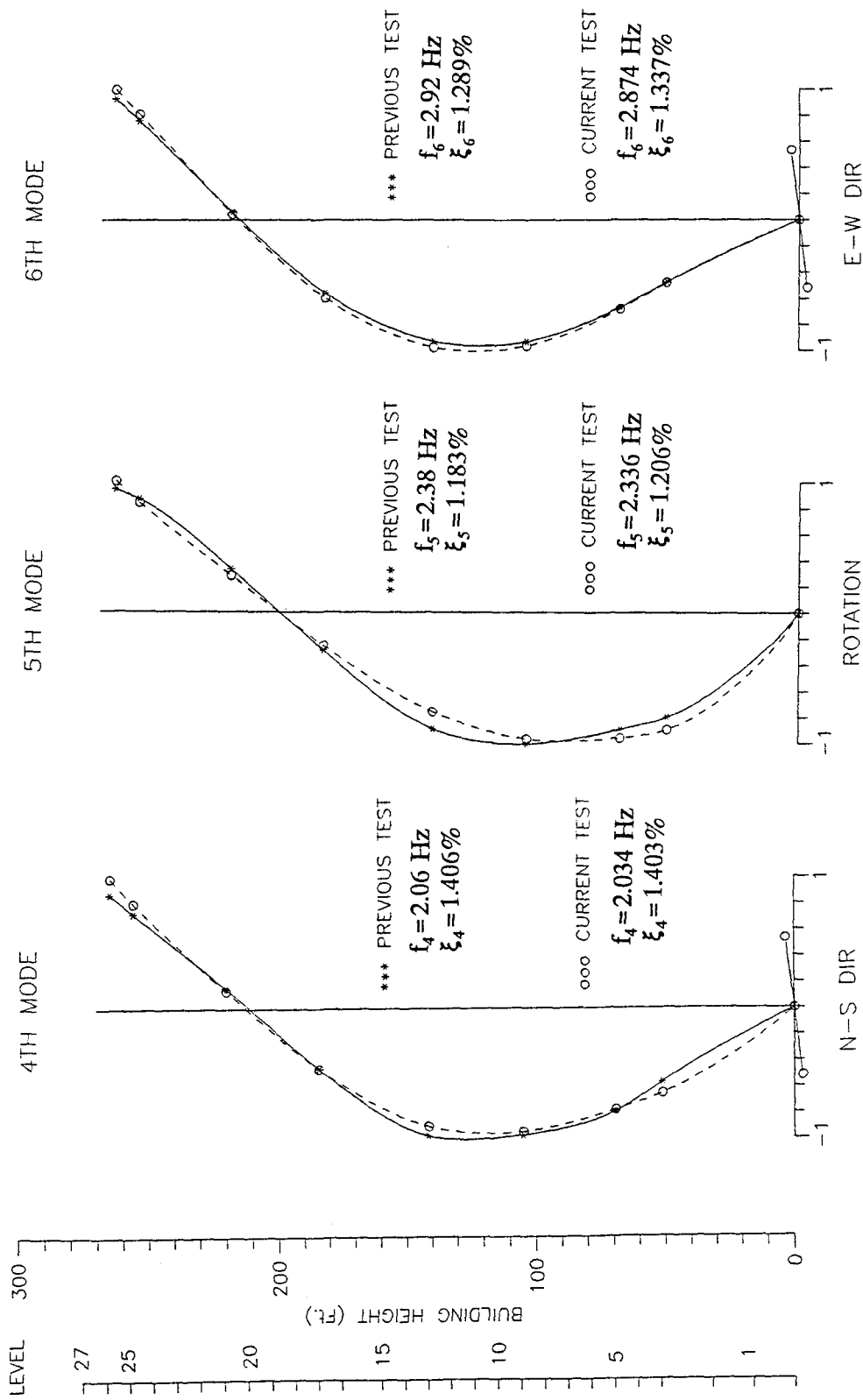


Figure 6-1 Comparison of the First Nine Mode Shapes obtained from the Previous and Current Modal Tests. - Continued

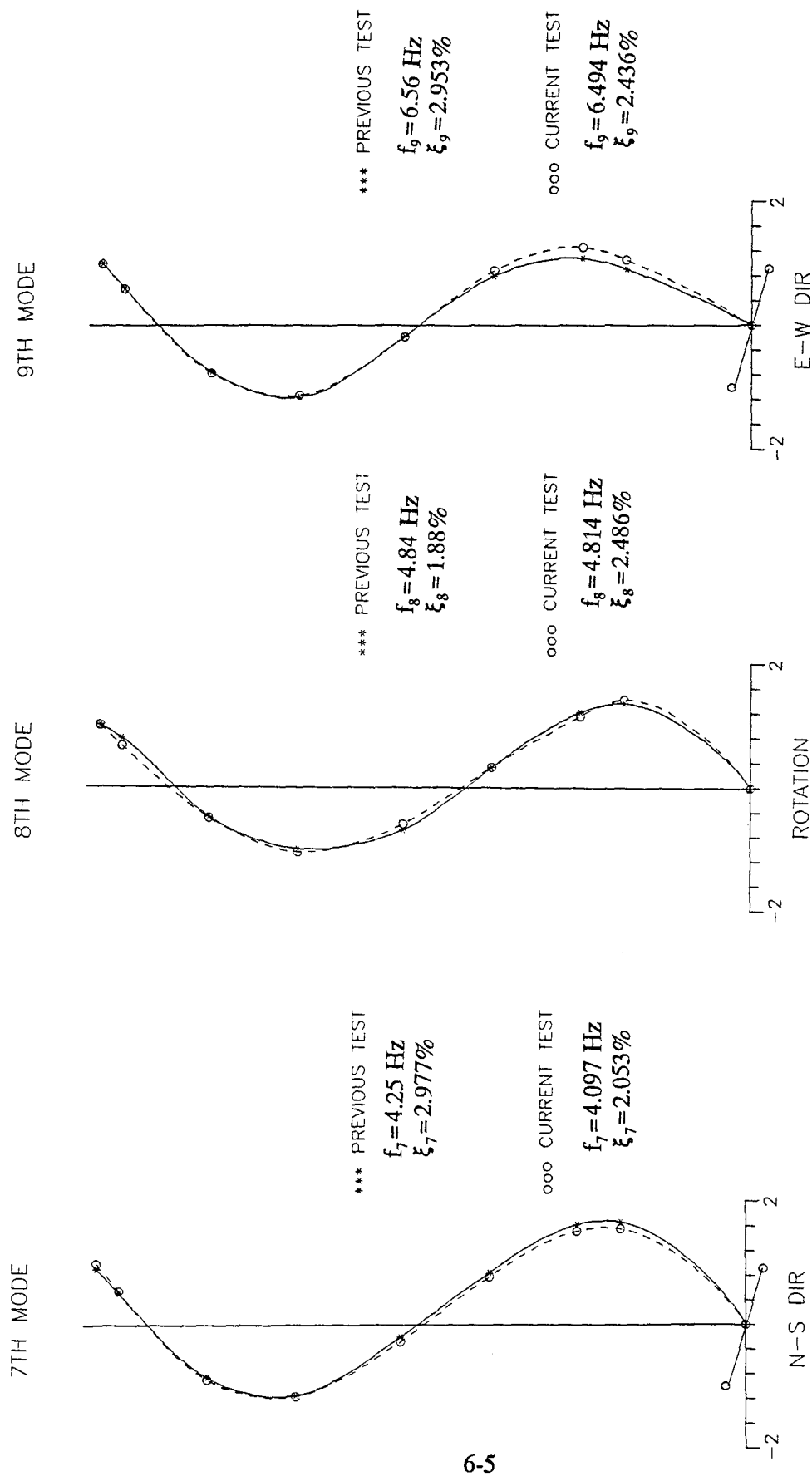


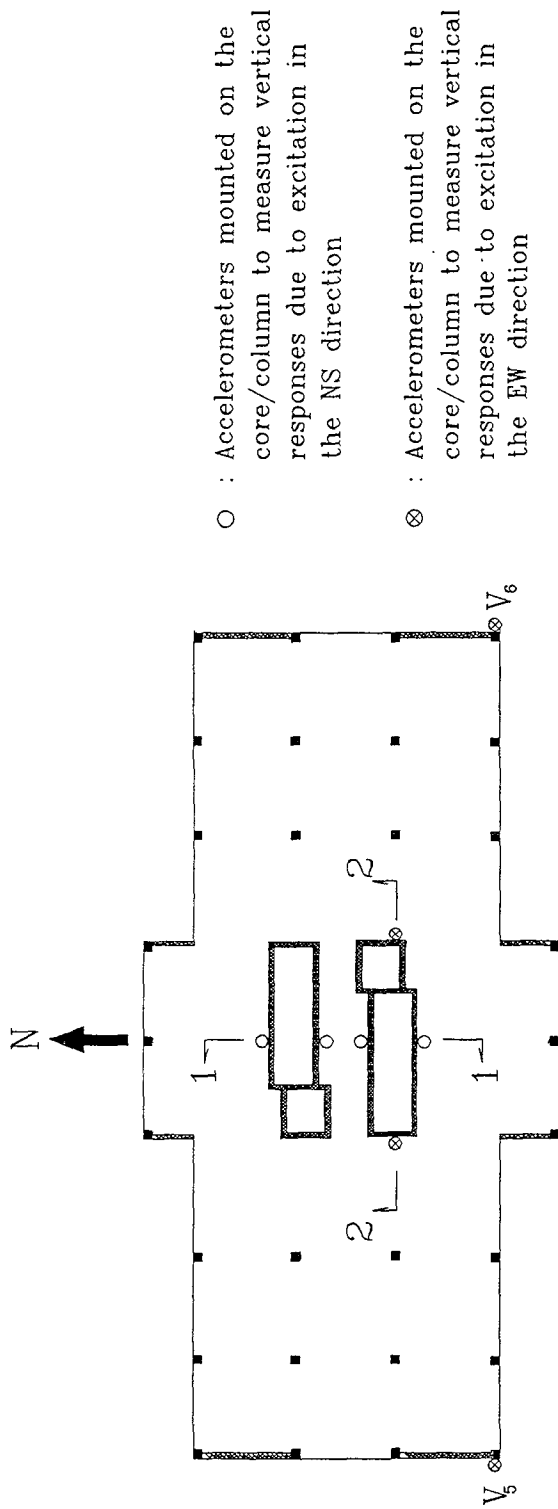
Figure 6-1 Comparison of the First Nine Mode Shapes obtained from the Previous and Current Modal Tests.

obtained from the previous modal test. The mode shapes obtained from the current test include the rocking of the core foundation. The rotations at the core bases due to rocking were magnified 50 times in the mode shapes (Fig. 6-1).

The vertical responses at the basement due to excitation in the NS direction were measured from accelerometers placed on either side of each core i.e at points V_1 - V_2 and V_3 - V_4 (Fig. 6-2). The phase differences between V_1 and V_2 and between V_3 and V_4 were studied to understand whether the core foundations were rocking or uplifting. The phase difference between responses on either side of each core was 180° which indicated that the core foundations were rocking in the NS direction as opposed to uplifting. The phase difference between vertical responses from V_1 and V_2 is shown in Fig. 6-3. The rotations of the cores were 0.027, 0.18, and 0.36 milli radians at the first, second, and third NS translational modes respectively. These were the relative rotations when the response amplitude was one inch at the 26th floor.

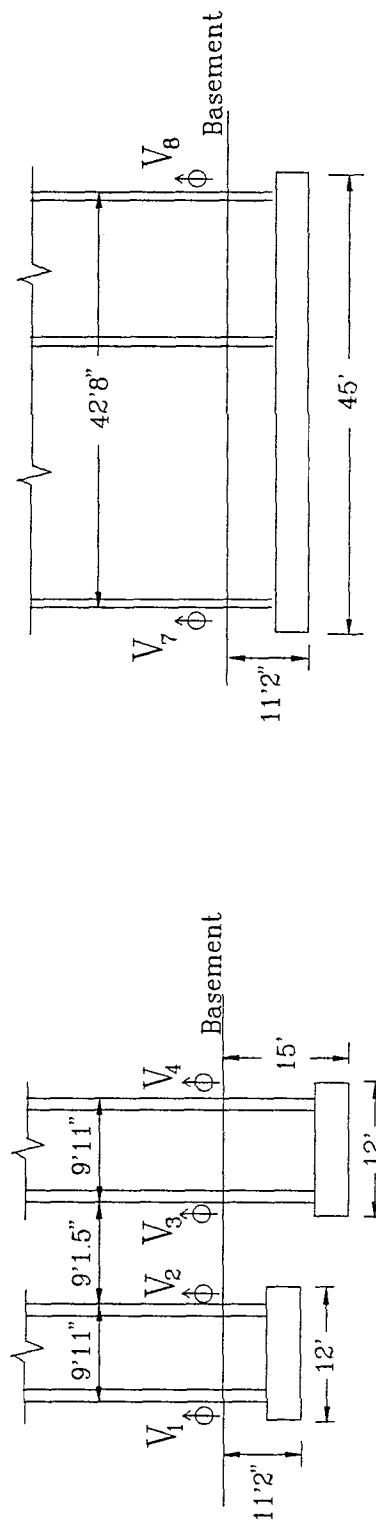
The vertical responses of the basement, due to excitation in the EW direction, further indicated that the core foundations were rocking in the EW direction. Shown in Fig. 6-4, the imaginary parts of the frequency response function measured at V_7 and V_8 i.e on either side of the core (Fig. 6-2) are opposite in sign. The rotations of the cores were 0.041, 0.205, and 0.433 milli radians at the first, second, and third EW translational modes respectively. These were the relative rotations when the response amplitude was one inch at the 26th floor.

The vertical accelerometer responses of the RC columns on either side of the building were very low (labelled as V_5 and V_6 in Fig. 6-2). The vertical responses of V_5 and V_6 were -0.19 micro g and +0.15 micro g, respectively, at the first EW translational mode. The vertical responses at the second and third EW translational modes were in the range of 5-7 micro g's. The measurements indicated that the vertical responses of the two columns were contradicting each other. While one column was moving up, the opposite column was moving down. The vertical responses of the columns due to excitation in the NS direction



- : Accelerometers mounted on the core/column to measure vertical responses due to excitation in the NS direction
- ⊗ : Accelerometers mounted on the core/column to measure vertical responses due to excitation in the EW direction

PLAN AT THE BASEMENT



SECTION 1-1

SECTION 2-2

Figure 6-2 Location of Accelerometers at the Basement for Measuring Foundation Displacements.

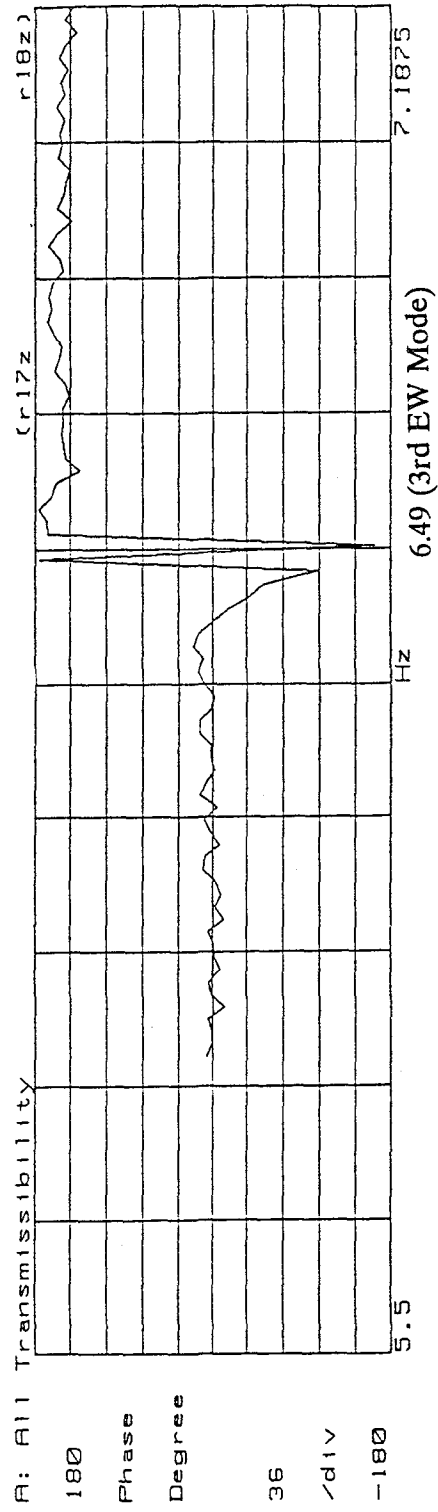
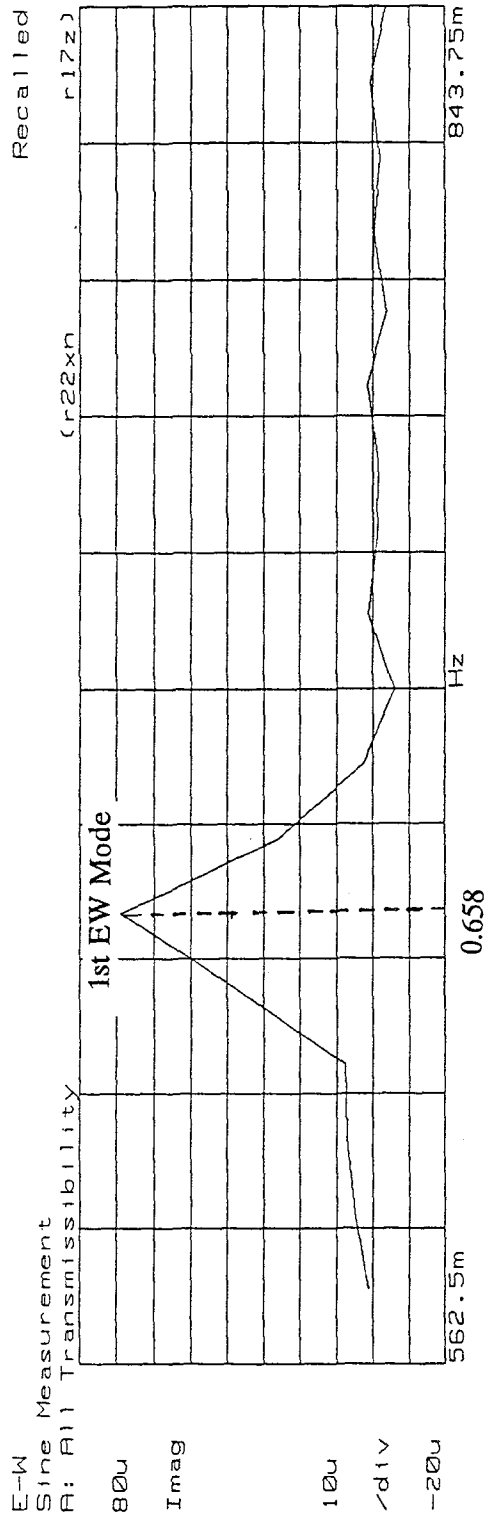


Figure 6-3 Phase Difference Between Responses on Either Side of the Core (Between V_1 and V_2 in Fig. 6-2) at the Third EW Mode.



F=843.75m

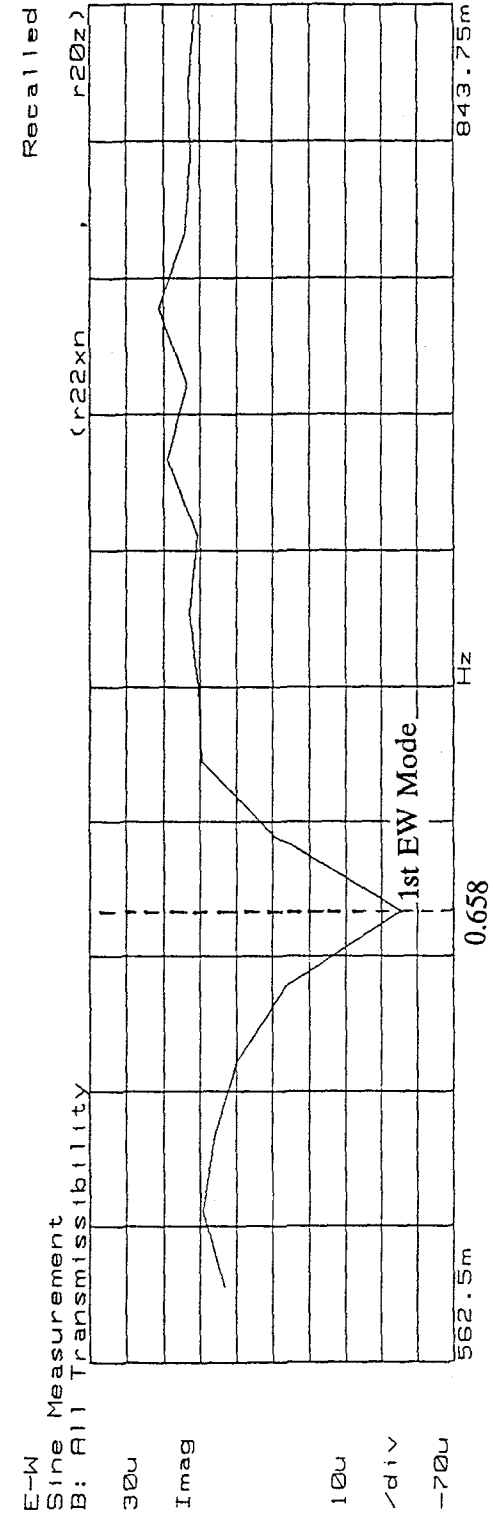


Figure 6-4 Imaginary Part of Frequency Response Functions Measured on Either Side of the Core in the EW Direction in the Frequency Range of 0.5625 Hz to 0.84375 Hz.

were lower than those due to excitation in the EW direction.

6.3 Mass-Orthonormal Modal Vectors and Flexibility

The modal vectors obtained from the polyreference method were further normalized to obtain mass-orthonormal modal vectors. The procedure for obtaining the mass-orthonormal modal vectors is explained in Appendix-B. Mass-orthonormal modal vectors transfer to lateral flexibility of the building without assuming a mass matrix.

The flexibility coefficients serve as a conceptual basis for identifying an element-level analytical model in the geometric coordinates. There are many assumptions and idealizations made in constructing an analytical model. The selection of flexibility space for parameter identification leads to a better conceptualization of their influence. The key in transforming mass-orthonormal modal vectors to flexibility is in a sufficiently complete definition of the modal vectors in discretization and number so that a convergence of the flexibility is accomplished. It was verified from analytical sensitivity studies by ETABS analyses that more than 92% of the flexibility was obtained by considering the first nine modes.

The flexibility matrix, [f] can be expressed as:

$$[f] = [\psi] [\omega^2]^{-1} [\psi]^T \quad (6-3)$$

where $[\psi]$ = experimentally determined mass-orthonormal modal vectors arranged from left to right in the order from lower to higher frequencies.

$[\omega]$ = Diagonal matrix of natural frequencies (radian/sec) from lower to higher frequencies.

The lateral flexibility of the building when loaded at the 26th floor is shown in Fig. 6-5. It was also possible to quantify the rotational flexibility of the core foundations. The relative rotation of the core foundation is 0.03 micro radians when unit load (one Kip) is applied at the 26th floor in the NS direction. Similarly, the rotation is 0.75 micro radians in

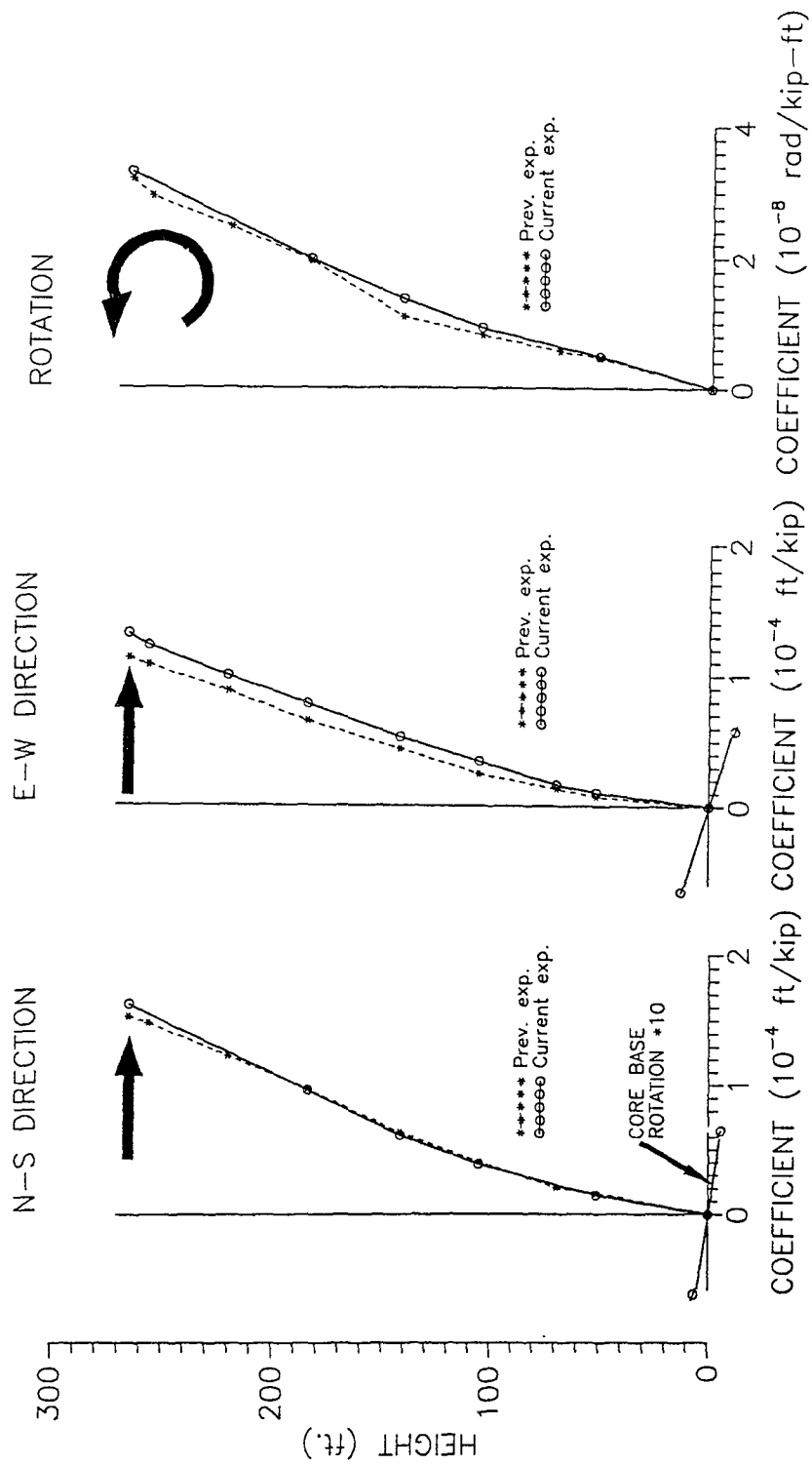


Figure 6-5 Comparison of the Lateral Flexibility Coefficients of the Building Obtained When Loaded at the 26th Floor from the Previous and Current Modal Tests.

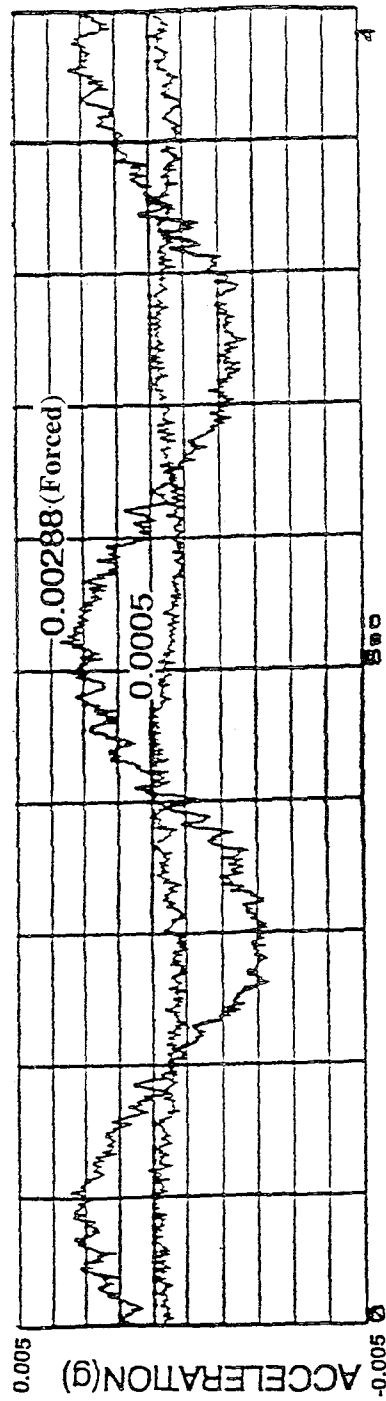
the EW direction. In Fig. 6-5, the core foundation rotations are magnified by ten times.

6.4 Assessment of Differences Between the Results of Current Test, Previous Test, and Ambient Test

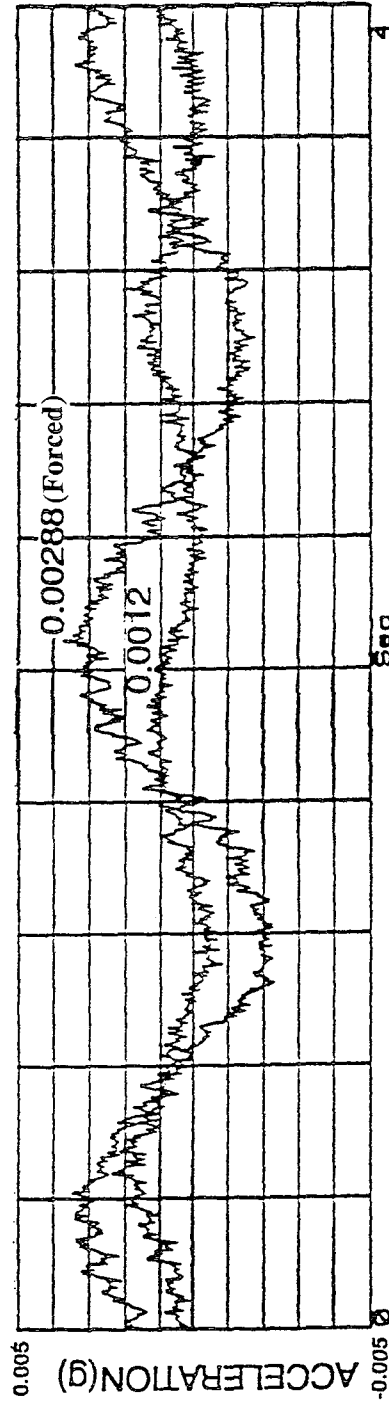
The frequencies, damping, and mode shapes obtained from current and previous modal tests have been compared in Fig. 6-1. The natural frequencies obtained from the current test are 1.26% to 3.6% less than the corresponding values obtained from the previous test. Variation of the damping ratios at different modes was as much as 37%. The mode shapes obtained from both the tests are quite similar. The lateral flexibility coefficients have been compared in Fig. 6-5. They have increased from 6% to 13% during the second test. The decreases in natural frequencies and increases in flexibility in the current test are attributed to the change in the type of input force (from random to harmonic excitation) and increase in the level of force (75 lbf to 450 lbf in the first mode). It was possible to understand the kinematics at the foundation level and quantify the core foundation rotational flexibility in the current test.

In order to better understand the level of input excitation relative to the ambient excitation, the time responses of the 26th floor were obtained. This was accomplished as the building was excited in its first natural frequency in the NS direction. In Fig. 6-6, these results are compared to responses due to ambient excitation caused by low and high wind.

Variations in natural frequencies were observed to be caused by fluctuations in the level of wind excitation. The relation between fundamental frequency versus base shear is given in Fig. 6-7. This relation is based on such factors as combined ambient and forced excitation and different wind speeds. To construct this figure, the equivalent base shear due to wind was calculated at different wind speeds based on ANSI (1982). The base shear due to harmonic loading was estimated from linear viscous damped system dynamics. The base shear due to high wind at the fundamental frequency was 53 kips. Since the wind force is random in nature and is distributed over the building surface area, this estimate is



LOWER WIND (0-8 MPH)



HIGHER WIND (16-21 MPH)

Figure 6-6 Time Histories of Response at the 26th Floor due to Different Wind Levels and Forced Excitation at the First NS Mode.

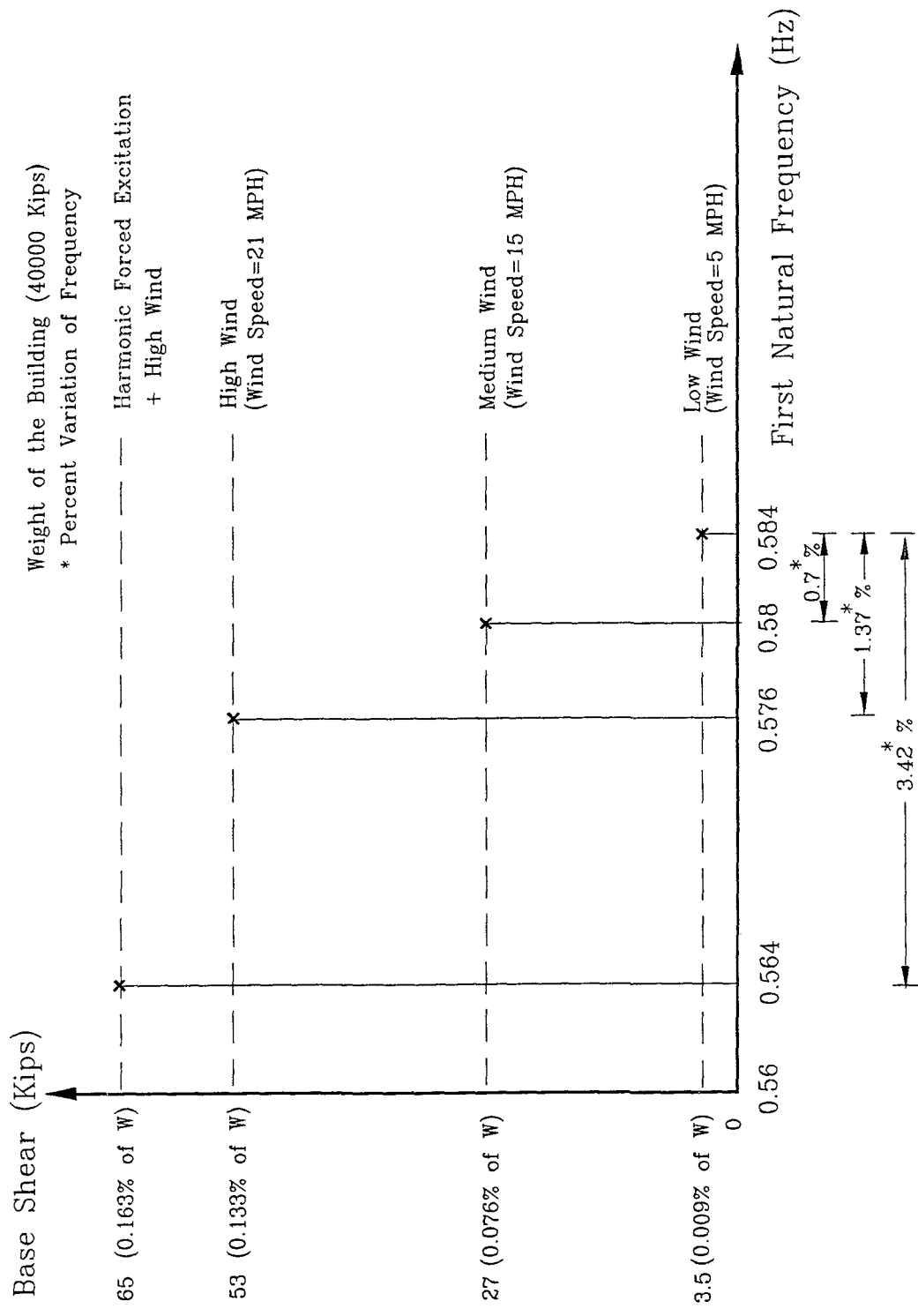


Figure 6-7 Effect of Type and Level of Force on the First Natural Frequency of the Building.

approximate. The total base shear due to high wind and forced excitation at the same frequency was estimated at 65 kips. The dynamic amplification of the harmonic response was estimated as 24. The frequency decreased from 0.584 Hz to 0.576 Hz (1.37% decrease) due to the increase in wind levels. A harmonic force of 0.5 kips provided by linear inertia-mass exciter further decreased the frequency from 0.576 Hz to 0.564 Hz (2.08 % decrease).

According to modal theory, parameters such as frequency, damping, and modal vectors do not vary with any changes in input force levels if the structure is linear and time invariant. The average stress level of the current modal tests is not judged to correspond to the nonlinear range of the material. The changes observed are mainly attributed to changes in the boundary conditions and in particular, the soil-foundation responses. The changes (shown in Fig. 6-7) shed light on the possible extent of variations in critical response mechanisms at the serviceability limit states.

The core foundation was rocking even under a base shear of 0.16% of the building weight. This tendency has important implications regarding response under moderate ground shaking which may have a frequency content in the range of 0.50 Hz-1.5 Hz. Since the foundations are not anchored to rock, increased shears should be expected to lead to further changes in building frequency.

SECTION 7

TEST FOLLOWING PARTIAL REMOVAL OF EXTERIOR CLADDING

7.1 General

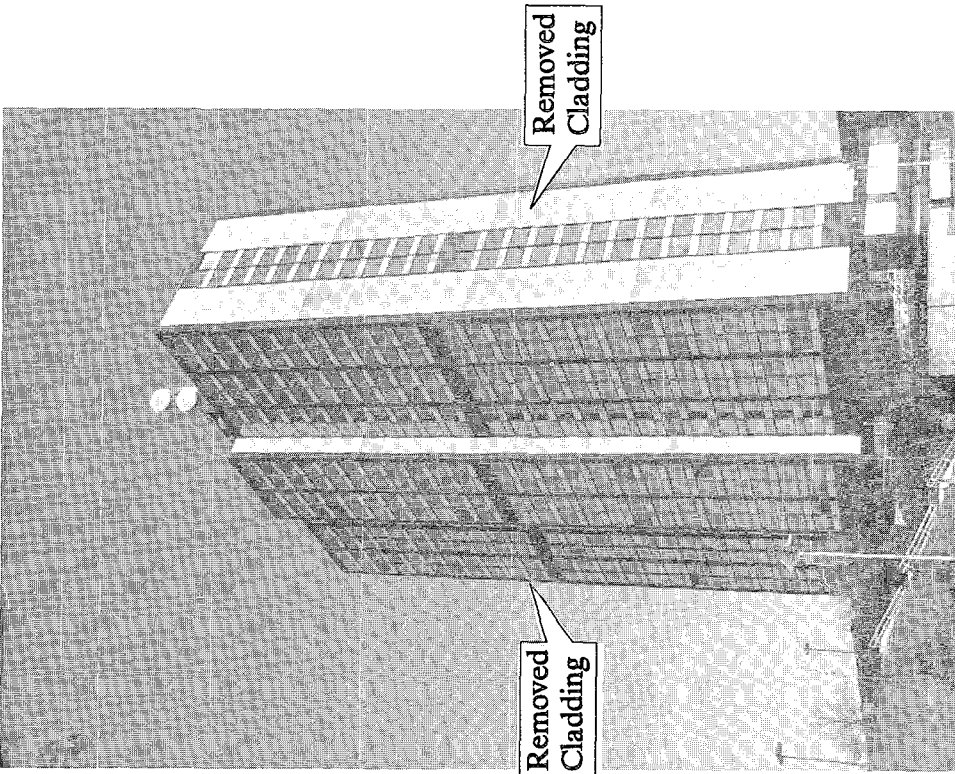
In June and July 1991, rigorous closed-loop modal tests were performed on the test building with all the nonstructural elements. Subsequently, portions of the exterior cladding were removed to eliminate asbestos before imploding the building. This included exterior concrete panel cladding on the north and south faces of the building and exterior prefabricated concrete panels which decorated the structural walls on the east and west facades of the building. Photographs of the test building before and after removal of these elements are shown in Fig. 7-1.

Since it is not practical to include all the nonstructural elements in an analytical model, these are generally omitted. On the other hand, some of the nonstructural elements may contribute significantly to the stiffness of the building. It is important to identify these elements to formulate an accurate analytical model.

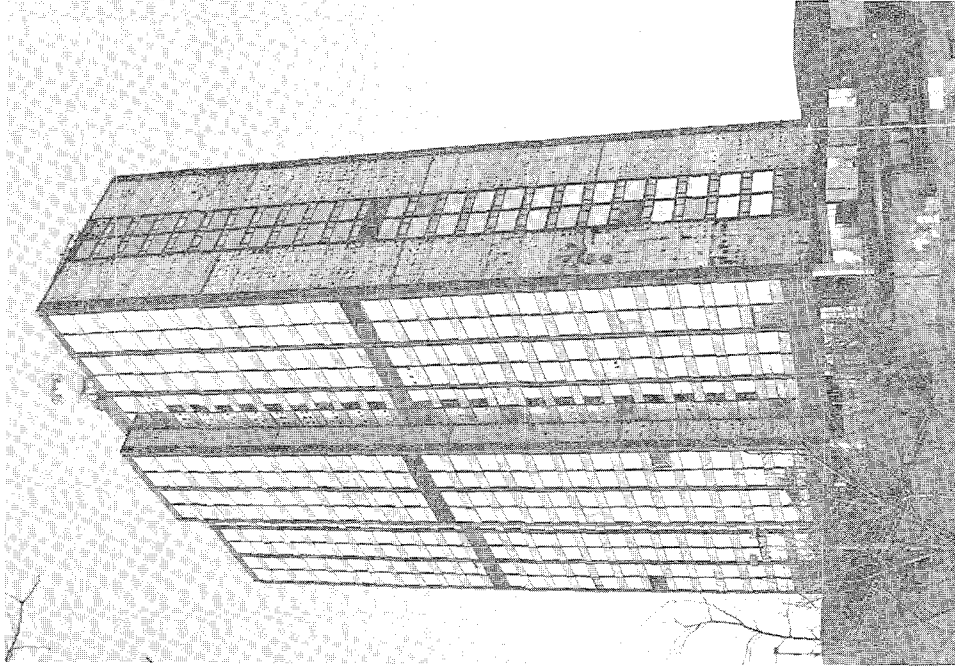
Various architectural elements such as exterior glass cladding, interior light-weight partitions, false ceilings etc., comprised the nonstructural elements in the building. However, only some of these exterior architectural elements were removed. Tests were repeated to verify whether the panels, which were removed on the north and south faces of the building, contributed to the stiffness, particularly the torsional stiffness of the building. Variations in the natural frequencies were also checked.

7.2 Test Setup and Data Acquisition

The block diagram of the test setup is shown in Fig. 7-2. The hardware and software used for this test were a 2-channel HP 3562A Dynamic Signal Analyzer, a linear Inertia-mass Exciter and its Hydraulic Pump, a Pegasus 5900 Servo-controller, two Seismic Accelerometers, and a 12-channel Amplifier (model Piezotronics 483 B17).



(a) Before Removal



(b) After Removal

Figure 7-1 Photographs of the Building Before and After Removal of Some of the Exterior Cladding.

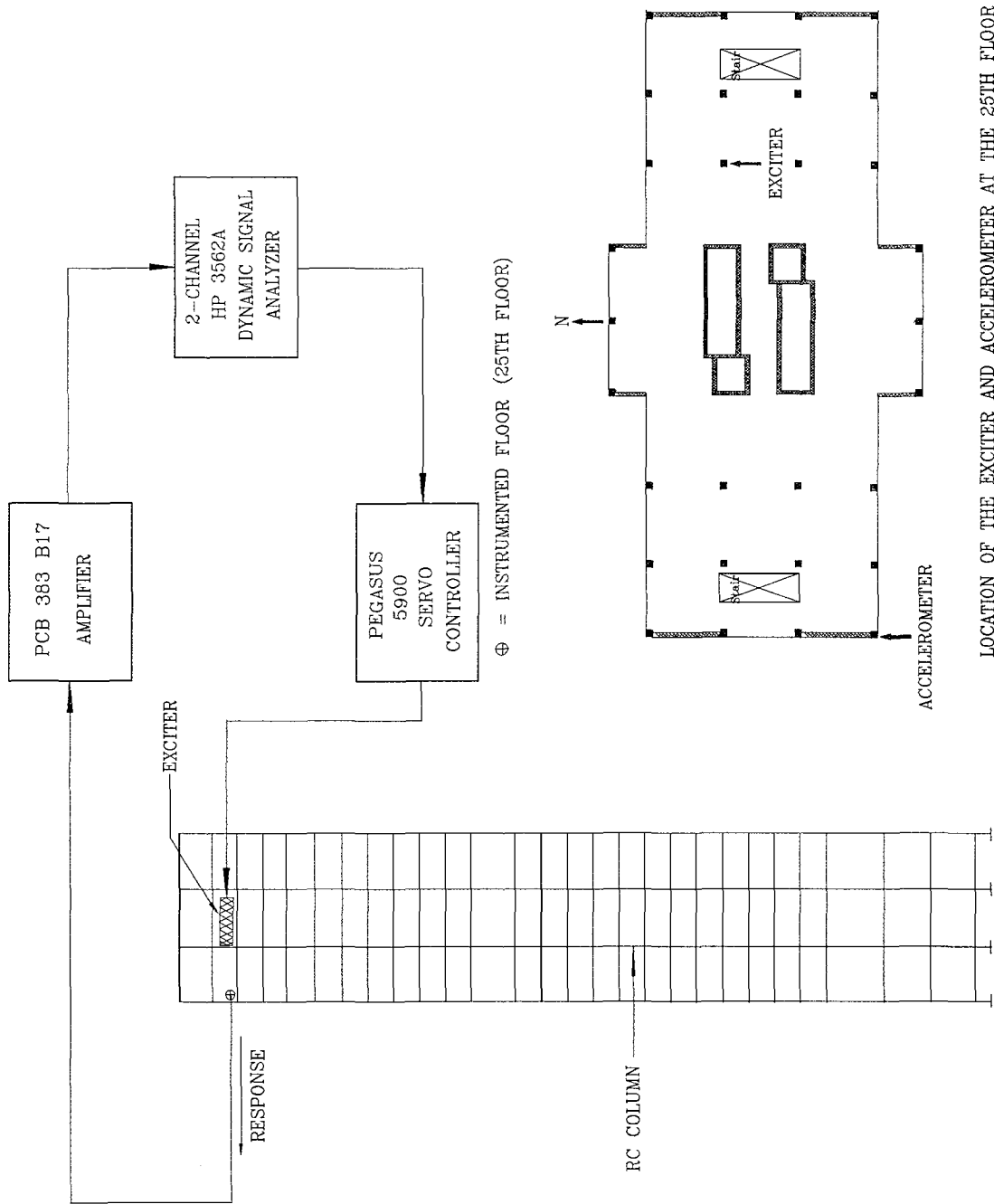


Figure 7-2 Block Diagram of the Test Setup for Tests Following Asbestos Removal.

The natural frequencies of the building can be obtained by measuring acceleration responses from only one floor. Therefore, a 2-channel HP 3562A Dynamic Signal Analyzer that can direct swept-sine excitation signal to the servo-controller as well as measure acceleration responses, was employed. The exciter was mounted against an RC column on the 25th floor in the NS direction. One accelerometer, located at the south west corner on the 25th floor, measured the NS translational response as well as the torsional response. The locations of the exciter and accelerometer are shown in

Fig. 7-2. In addition, another accelerometer was mounted on the moving shell of the exciter to use as a reference channel for calculating the frequency response functions. The signals were amplified by 100 times.

The swept sine measurements were performed in three frequency ranges of 0.5-0.9 Hz, 1.8-2.6 Hz, 3.5-5.2 Hz. In this manner, the natural frequencies at the first three NS translational modes as well as the first three torsional modes could be measured. The maintained frequency resolution and excitation force levels were similar to those adopted in the modal tests conducted in June 1990. The natural frequencies were obtained from frequency response functions.

7.3 Test Results

The first three NS translational frequencies and torsional frequencies obtained from this test are compared to the 1990 modal test results in Table 7-1.

The natural frequencies obtained from the 1991 tests were higher than those obtained from the 1990 tests for the same level of excitation force. The explanation that can be offered is that the increase in frequencies was due to the reduction in the mass of the structure after the removal of the materials. Increase in torsional frequencies was slightly higher than the increase in the NS translational frequencies. This may be due to the reduction of the mass moment of inertia in addition to the reduction of the mass.

The increase of frequencies in this test clearly reflected that the stiffness of the

TABLE 7-1 Comparison of Natural Frequencies Measured by Different Tests.

Mode	NATURAL FREQUENCY (Hz.)		
	July 1990 Test	April 1991 Test	Increase
First NS Translational	0.564	0.5704	0.0064
First Torsional	0.762	0.7717	0.0097
Second NS Translational	2.034	2.0535	0.0195
Second Torsional	2.336	2.361	0.025
Third NS Translational	4.097	4.178	0.081
Third Torsional	4.814	4.912	0.098

building was not reduced. Therefore, additional modal tests to determine the unit mass normal modal vectors and the flexibility of the building were not performed. Since the exterior architectural elements did not influence the stiffness of the building, special modeling techniques need not be adopted to model these elements.

SECTION 8

DIAPHRAGM DISTORTION TEST

8.1 General

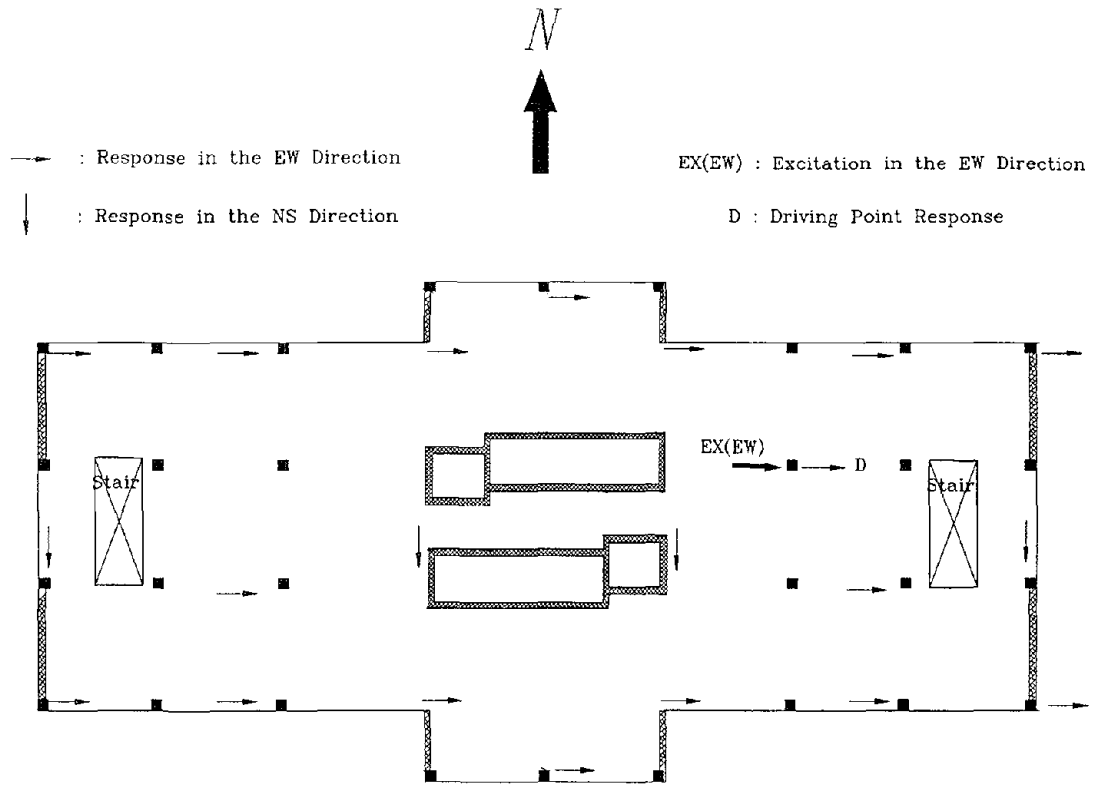
Many computer programs consider floor diaphragms to be infinitely rigid in-plane and infinitely flexible out-of-plane. If the diaphragm is sufficiently stiff in-plane, a building can be represented as a lumped-mass stick system for defining its mode shapes and lateral flexibility. In earlier forced vibration tests of buildings, in-plane diaphragm deformations were observed at higher modes (Stephen et al, 1985). Since the diaphragm of the test building has openings and the plan aspect ratio is 2.7, it is desired to verify the in-plane stiffness of the diaphragm. Hence, a test was conducted to investigate the in-plane diaphragm deformations as the building was excited at different modes. This was performed by applying the excitation force in both the EW and NS directions. These tests focussed on in-plane diaphragm distortions at the 25th floor.

8.2 Test Setup

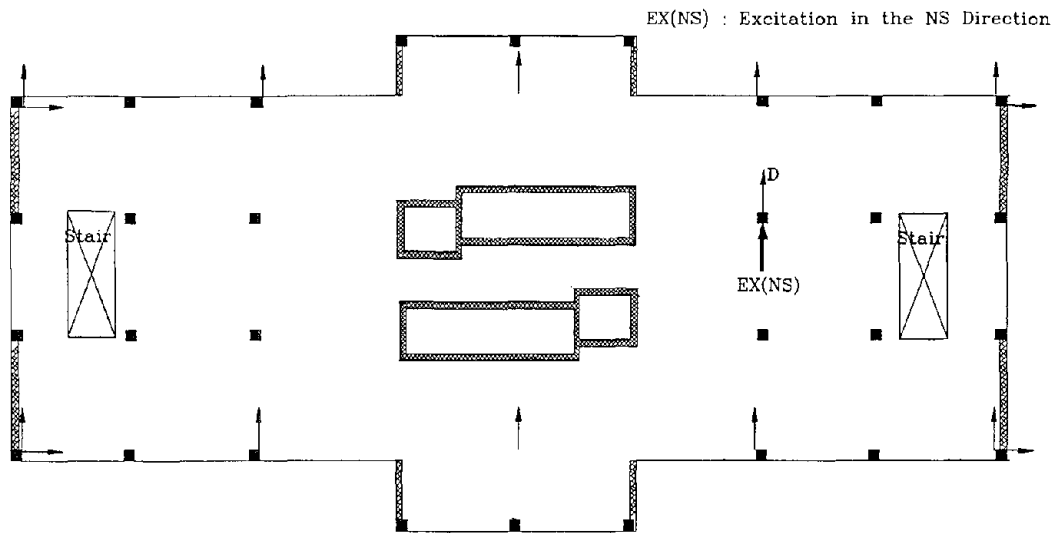
Except for the location of the accelerometers, the test setup for this test and the closed-loop setup were identical. The diaphragm test was conducted by applying the excitation force in the EW direction and the accelerometers were distributed over the diaphragm of the 25th floor as shown in Fig. 8-1. Sixteen of these accelerometers were aligned to measure lateral responses in the EW direction and the remaining four accelerometers were aligned in the NS direction to measure responses due to torsion.

The settings for the excitation, data acquisition, and procedure are the same as those adapted for the forced excitation test. The data was acquired for the excitation in two frequency ranges of 0.5-0.90 Hz and 2.2-3.18 Hz.

After performing tests by applying the force in the EW direction, the exciter was rotated towards the NS direction. The locations of the 14 accelerometers distributed over



(a) Exciter in the EW Direction



(b) Exciter in the NS Direction

Figure 8-1 Location of the Exciter and Accelerometers for the Diaphragm Distortion Test.

the diaphragm on the 25th floor are shown in Fig. 8-1. Ten of the fourteen accelerometers were aligned in the NS direction and the remaining accelerometers were aligned in the EW direction to measure responses due to torsion. A maximum excitation force of 3200 lbf was applied at the third torsional frequency.

8.3 Test Results and Conclusions

8.3.1 Excitation in the EW Direction

The responses at the first two bending modes in the EW direction and the first two torsional modes obtained throughout the diaphragm indicated no diaphragm distortion at the 25th floor. Fig. 8-2 illustrates the positions of the measurement points at the peak force and indicates that the diaphragm was essentially displaced as a rigid body. The following reasons are assessed: (a) The in-plane stiffness of the diaphragm along the EW direction is significantly more than that along the NS direction; and (b) the point of application of the excitation force was close to the mass center of the building. Hence, torsional modes were not strongly excited.

8.3.2 Excitation in the NS Direction

The responses at the third torsional mode also indicated no diaphragm deformation at the 25th floor (Fig. 8-2). Maximum excitation force was applied in the flexible NS direction at a sufficient eccentricity in order to strongly excite the torsional mode. In spite of this, no diaphragm distortion was detected.

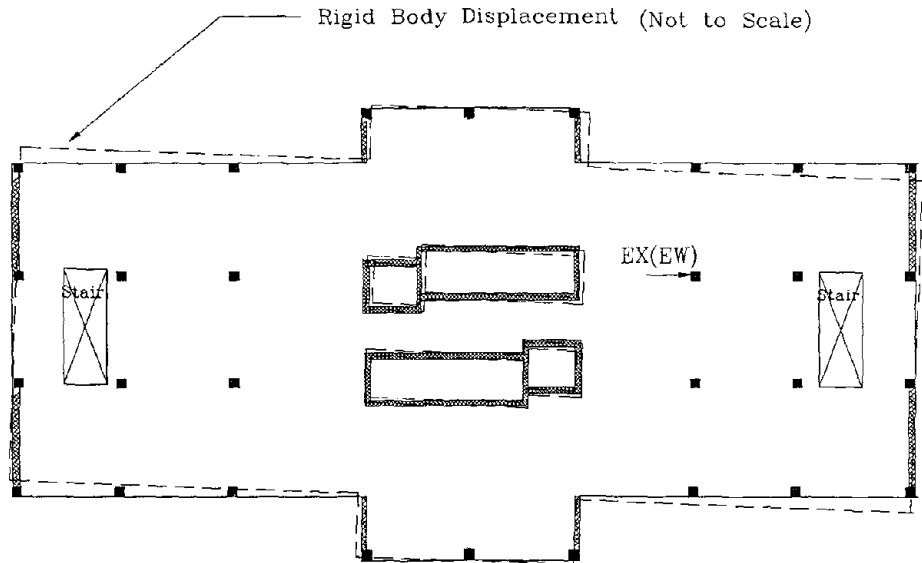
8.3.3 Conclusions

The test results indicated no in-plane diaphragm deformation at the first nine modes. Therefore, the building can be idealized as a stick system in defining its mode shapes and lateral flexibility.

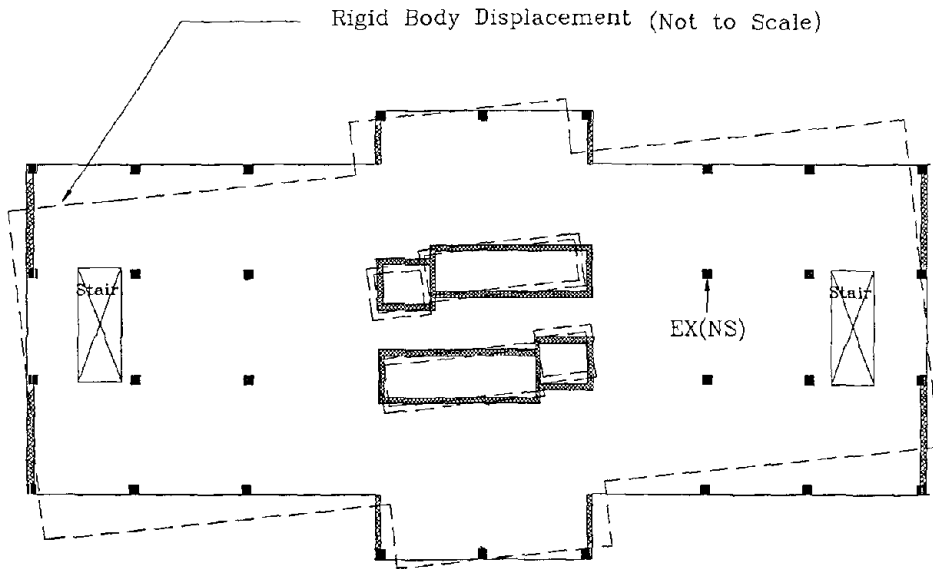
The diaphragm distortion at higher force levels and higher frequencies corresponding

——— Original Position of the Diaphragm
 - - - Displaced Position of the Diaphragm at the Maximum Force Amplitude

EX(EW) : Exciter in the EW Direction
 EX(NS) : Exciter in the NS Direction



(a) Exciter in the EW Direction (At the Second Torsional Mode)



(a) Exciter in the NS Direction (At the Third Torsional Mode)

Figure 8-2 Diaphragm Displacement at Torsional Modes due to the Excitation Force in EW and NS Directions.

to local diaphragm modes, is not ruled out. The excitation force level was sufficient enough to measure the global characteristics of the building, but was insignificant for observing the local response characteristics of the diaphragm.

SECTION 9

SYSTEM PERFORMANCE AND CONTROL IMPLICATIONS

9.1 General

The performance of the closed-loop test arrangement was successful. The test was administered in a systematic manner and the quality of the data was reliable. High signal to noise ratio was maintained by using the sine excitation and the input force could distinctly overcome the effects of wind excitation.

The performance, problems, and feasibility for structural control implications are discussed below.

(a) Excitation System: The performance of the excitation system varied from the design specifications. If an electro-hydraulic linear exciter is to be custom designed for a specific application, the design specifications may not be achieved during the actual implementation. This would be due to system interaction between the actuator, servo valve, and bearings and needs to be taken into account in designing structural control applications.

Another important factor is the ramp time. Ramp time is the time needed for the exciter to ramp up from the stationary position to the specified force level at a specified frequency. For a linear exciter, a ramp up time of 5-10 seconds should be expected before the full performance of the exciter may be attained. This may be quite critical in structural control implementations.

The inside room temperature remained in the range of 90°-100° F during the tests because the building was not air conditioned. The pump stopped automatically when the hydraulic temperature reached 51.7° C (125° F) and installation of fans around the heat exchanger proved insufficient for air circulation. In order to solve this problem, the pump temperature was closely monitored during each swept sine measurement in the frequency range of interest. The test was paused whenever the temperature reached 50° C. After allowing 30-45 minutes for the pump to cool down to a temperature of 40° C, the excitation

continued to complete the sweep in the frequency range. This apparently trivial problem reveals that the realities of operation may not be fully predicted unless experimentation is performed.

Hardware Problems: The break-down of excitation system components posed problems during the test. Bolts that held the cylinder to the inner shell of the exciter loosened and then broke, the gaskets in the cylinder broke due to excessive cavitation, and contamination clogged the servo valve due to improper filtration.

(b) Test Control and Data Acquisition System:

Autorangeing problem: The autorangeing option for 22 channels was attempted to eliminate the manual adjustment of the input range and to prevent underloads and overloads. Naturally, not all the channels will contain the same level of response at the same time. Some channels may overload or underload whereas others may not. Since the multiplexer system acquired the data simultaneously, whenever a channel was autoranged, the data from every channel had to be taken again. This process was time consuming and hence the HP SINE signal processing software estimated a sweep time of approximately 15 hours with all channels autoranged for a sweep between 0.5 Hz to 0.9 Hz. To overcome this problem, the input ranges of all but two channels (i.e. input force reference and driving point channels) were manually adjusted and fixed during the tests.

Autoleveling problem: An attempt was made to utilize the "autolevel" feature of the HP SINE software to control the level of the input force without exceeding the specified level of the exciter. Due to a lack of proper protocol between the HP SINE software and the servo controller controlling the exciter, this feature did not work. However, the level of the force could be adjusted through the servo controller, and therefore, the "autolevel" feature was not essential. The desired amplitude of the excitation signal was attained by manually adjusting at the beginning of a sweep. The importance of a proper and complete protocol between all the "smart" components is indicated.

Time Considerations: The performance and problems faced during this modal test

regarding the ramp up time, time required to reach steady state, time for averaging signals and time required for autoranging, have significant implications in the design of structural control with an electro-hydraulic inertia-mass exciter system. The total time estimate for the control system to respond to an external excitation is necessary in assessing the feasibility of constructed facility control. Below is a possible control scenario in its simplest form:

External excitation inputs energy into the building. Sensors located in the building pick up the response. The response level exceeds a certain pre-set value and the data acquisition system starts recording the signals. The time required for the software to act upon recording responses is entirely dependent on the type of control strategy employed. If data acquisition block sizes of 1 to 10 are used, the time required for action may be very small (if sampling frequency is 8 Hz and 4 data blocks are used, the time to acquire these 4 blocks is only $4 \times \frac{1}{8} = 0.5$ seconds). After deciding on the mode to suppress, the software commands the source module to start sending input signals to the exciter. The exciter ramps up in 5-10 seconds and starts exciting input in accordance with the control method being utilized. It takes approximately 10 cycles (20 seconds in the case of first bending mode) for the building to reach a steady state. Vibrations die out and the software responds accordingly. The interaction between the exciter and the software may require the exciter input force to vary while maintaining a constant frequency. For this reason, employing a servo-controlled linear-inertia-mass exciter as opposed to a rotating-mass exciter, would be advantageous. As a result, the total time required for the control measures to become effective could be 25 - 30 seconds. This time estimate is naturally dependent on the type of hardware and control algorithm utilized.

9.2 Conclusions Regarding System Performance

The level of response at the 26th floor due to forced excitation measured approximately 0.003 g (as compared with 0.001 g due to the high wind excitation in the wind speed range of 16-21 mph). The exciter (driven by a 60 HP pump providing a hydraulic flow

of 30 GPM) with an active mass of 3.5 kips could generate responses of a building of 40000 kips weight to overcome the wind excitation. If an exciter with an active mass of approximately 0.01 % of the building mass can overcome the wind effects, there is obviously a feasible manner of controlling earthquake responses by increasing the active mass of the exciter. The mass can be increased by either adding weights to an exciter or by synchronizing multiple exciters. The possible costs of the hardware and software for a two-exciter closed-loop active tuned-mass control system are estimated to be within a million dollars. This may certainly be feasible for a facility valued at 30 million dollars as was in the case of the test building.

SECTION 10

CONCLUSIONS AND RECOMMENDATIONS

10.1 Conclusions

Regarding Modal Testing

Modal testing is the most efficient tool used for structural identification in the mechanical and aerospace engineering disciplines. The natural frequencies, mass-orthonormal modal vectors, and damping factors identified from this type of test become a basis for improving and calibrating linear analytical models of structures. Most importantly, the modal data may be transformed into the flexibility of a structure if a sufficient number of modes have been excited and measured. Therefore, regarding the amount and reliability of information revealed about a test structure, modal testing is far more superior than the older generation forced-vibration testing of constructed facilities.

Modal testing can be successfully applied to constructed facilities provided the following requirements are satisfied:

- (1) A complete understanding of the experimental modal analysis theory, modal data acquisition, and modal parameter estimation is necessary.
- (2) Prior to conducting modal testing, it is necessary to conceptualize the complete constructed facility (soil-foundation-superstructure) and develop a preliminary 3D linearized analytical model. This will serve as a basis for exciter location and accelerometer locations.
- (3) A preliminary modal test should be conducted as a basis for performing the rigorous modal test.
- (4) To acquire reliable data, the excitation force should be high enough to overcome the influence of wind and other ambient excitation. More importantly, to reliably identify the flexibility coefficients, the level of excitation force should be high enough to activate and stabilize the service-level soil-foundation displacements due to

foundation rocking/uplift. In addition, the level of excitation force should be capable of stabilizing any structural-nonstructural element interactions or soil-foundation-structure interactions at the service limit state.

- (5) Appropriate signal processing software and hardware that can be appropriately integrated with the excitation system should be utilized. Employing these in a closed-loop test setup is preferred since the same software controls the excitation and acquires the data.
- (6) In order to measure all the modes of interest, the accelerometers should be located at various levels to discretize the building into a sufficient number of lateral displacement coordinates. These measured modes should account for over 90% of the lateral flexibility of the building.
- (7) Noise in the measured response signal affects the accuracy of the data. Minimizing this noise can be accomplished by selecting a sufficient number of response signal averages. The swept-sine excitation is preferred since it leads to high signal-to-noise ratio. Moreover, by adopting this type of excitation, it is possible to perform tests in a selected frequency band and concentrate the data acquisition around the modes. These modes can be approximately determined from the preliminary modal test.

Regarding the Test Specimen Characteristics

Modal testing of a 27-story building was performed in two phases by providing different levels of forced excitation. The natural frequencies, damping factors, and mass-orthonormal modal vectors were obtained from these modal tests. It was possible to determine the lateral flexibility of the building from the mass-orthonormal modal vectors without assuming a mass matrix.

In the earlier test, the level of excitation force was insufficient to completely overcome the effects of wind excitation and also did not activate the foundation rocking. The dynamic characteristics and flexibility, without inclusion of the effect of foundation

displacements, could not constitute a basis for a complete and accurate model. In the currently reported test, a higher level of excitation force completely overwhelmed the ambient wind effects and activated the foundation rocking. This led to changes in the measured response characteristics of the building. It was possible to understand the kinematics at the soil-foundation level and quantify the core foundation rotational flexibility.

An increase in the level of excitation force resulted in variations in the dynamic characteristics and flexibility of the building. The decrease in the natural frequencies was 1.26% to 6% and the increase in the damping ratios was as much as 37%. The increase in the lateral flexibility coefficients was 6% to 13%. However, the mode shapes obtained from both tests were quite similar.

Additional tests of the building following partial removal of the exterior cladding indicated that these elements do not affect the flexibility of the building. Therefore, special modeling techniques were not adopted in the analytical model.

The diaphragm distortion tests indicated no diaphragm deformation at the first nine modes. Therefore, the building can be idealized as a stick system in defining its mode shapes and lateral flexibility.

The results of the current modal test, which include the effect of foundation displacements, are more reliable. By correlating these current test results, a more complete and accurate linearized analytical model can be constructed. This test-verified analytical model will be used for accomplishing the global objective of the research which is to reliably evaluate the seismic vulnerability of constructed facilities which have not experienced earthquakes and have not revealed their weak links.

Because the test building was designed and constructed without considering earthquake forces, it contained many undesirable seismic attributes including significant irregularities. This building, constructed with flat slabs and cores, is representative of many mid-rise buildings in the Midwestern and Eastern United States. The research and findings on seismic vulnerability evaluation of this building will be applicable to a large population

of constructed facilities. The findings will be published in future papers and reports.

Regarding Structural Control Implications

The hardware and software administered in the modal test are expected to be applicable to structural control implementations. Therefore, experience gained from the errors and difficulties encountered during testing may be relevant to future structural control implementations. Certain parameters governing the data acquisition, signal processing, and excitation signal generation may have bearing on the mathematical approach to structural control techniques since seldom does a theoretical approach cover all aspects of real life applications.

A reliable analytical model is needed for the design of structural control. The modal test-verified analytical model is more complete and accurate and therefore, can be utilized for structural control applications.

In the current modal test, the exciter with an active mass of 0.01% of the building mass generated responses overcoming the wind excitation. This mass can be increased by synchronizing multiple exciters, and therefore, feasible means of controlling earthquake responses by increasing the mass is possible.

10.2 Recommendations

The frequencies varied due to changes in the level of forced excitation. The nonlinearity exhibited by the building was mainly attributed to the reduction of stiffness due to soil and foundation flexibility. For constructing a reliable linearized analytical model, the test stress level should be well above the service stress level. Further research is needed to verify whether increases in the force level will lead to further changes in the dynamic characteristics.

Although modal tests have been performed by many researchers for identification of global characteristics of structures, little research has been conducted for identification

of local response characteristics. Further research is necessary to identify the local response characteristics of constructed facilities.

The performance of the hardware and software utilized in the current closed-loop modal test has important bearing on a number of the parameters governing active structural control applications. Further research is necessary to investigate the possible application of the hardware and software employed in this test for structural control.

SECTION 11 REFERENCES

- Aktan, A.E., "Building Identification: Needs and Means," Dynamic Response of Structures, G.C. Hart and R.B. Nelson, Editors, ASCE, 1986.
- Aktan, A.E., "Present and Future in RC Buildings Analysis," Proceedings of the 9th World Conference on Earthquake Engineering, Tokyo-Kyoto, Japan, August 1988.
- Aktan, A.E., Baseheart, T.M., Shelley, S., and Ho, I.-K., "Forced-Excitation Testing and Identification of a Mid-Rise RC Building To Evaluate Vulnerability," Proceedings, Fourth U.S. National Conference on Earthquake Engineering, EERI, 1990.
- Aktan, A.E., Bertero, V.V., Chowdhury, A.A., and Nagashima, T., "Experimental and Analytical Predictions of the Mechanical Characteristics of a 1/5-Scale Model of a 7-Story R/C Frame- Wall Building Structure," Report No. UCB/EERC-83/13, Earthquake Engineering Research Center, University of California, Berkeley, CA, August 1983.
- Aktan, A.E., and Bertero, V.V., "Evaluation of Seismic Response of RC Buildings Loaded to Failure," Journal of Structural Engineering, ASCE, Vol. 113, No. 5, May 1987.
- Aktan, A.E., and Ho, I.-K., "Seismic Vulnerability Evaluation of Existing buildings," Earthquake Spectra, Vol. 6, No. 3, 1990.
- Aktan, A.E., and Nelson, G.E., "Problems in predicting Seismic Responses of RC Buildings," Journal of Structural Engineering, ASCE, 1988.
- Aktan, A.E., Toksoy, T., and Hosahalli, S., "Implications of Modal Test and Structural Identification on Active Control," Proceedings of U.S. National workshop on Structural Control Research, USC, LA, October 1990.
- Allemang, R.J., "Vibrations: Experimental Modal Analysis," Course Notes No. UC-SDRL-CN-20-263-662. Structural Dynamics Research Laboratory, University of Cincinnati, 1990
- Allemang, R.J., and Brown, D.J., "Experimental Modal Analysis And Dynamic Components Synthesis," Report No. AFWAL-TR-87-3069, Structural Dynamics Research Laboratory, University of Cincinnati, Cincinnati, 1987.
- American National Standard Building Minimum Design Loads For Buildings And Other Structures, ANSI A58.1-1982, American National Standards Institution, New York, 1982.
- Beliveau, J-G., "System Identification of Civil Engineering Structures," Canadian Journal of Civil Engineering, Vol. 14, No. 1, pp. 7-18, 1987.
- Beliveau, J-G., "Structural System Identification from Modal Information," Structural Safety Evaluation Based on System Identification Approaches, H.G. Natke and J.T.P. Yao, Editors, Published by Friedr. Vieweg and Sohn, Germany, 1988.

Brown, D.J., "System Dynamics Analysis", Course Notes, Structural Dynamics Research Laboratory, University of Cincinnati, 1990.

Clough, R.W., and Penzien, J., "Dynamics of Structures," McGraw Hill Publishers, 1985.

Craig, J.I., and Lewis, F.D., "A Rectilinear Force Generator For Full Scale Vibration Testing," Dynamic Response of Structures: Experimentation, Observation, Prediction and Control, G. Hart, Editor, ASCE, 1981.

Eykhoff, P., "Trends and Progress in System Identification," Pergamon Press, 1981.

Hart, G.C., and Yao, J.T.P., "System identification in Structural Dynamics," Journal of the Engineering Mechanics Division, ASCE, vol. 103, No. EM6, pp. 1089-1104, Dec., 1977.

Hewlett-Packard, "HP SINE User's Manual," Software Version B.02.10, Manual No. 35631-90002, 1989.

Hewlett-Packard, "System reference for HP 35650 Series Hardware," Manual No. 35651-90000, March 1987.

Ho, I.-K., and Aktan, A.E., "Linearized Identification of Buildings with Cores for Seismic Vulnerability Assessment," National Center for Earthquake Engineering Research, Technical Report No. NCEER-89-0041, 1989.

Hogue, T., Aktan, A.E., and Hoyos, A., "Localized Identification of Constructed Facilities," Journal of Structural Engineering, ASCE, January 1991.

Hudson, D.E., "Resonance Testing of Full-Scale Structures," Journal of Engineering Mechanics Division, ASCE, EM3, June 1964.

Hudson, D.E., "Dynamic Tests of Full-Scale Structures," Journal of Engineering Mechanics Division, ASCE, Vol. 103, EM6, pp. 1141-1157, Dec. 1977.

Ibrahim, R.S., "Computation of Normal Modes from Identified Complex Modes," AIAA Journal, Vol. 21, No. 3, pp. 446-451, March 1983.

Ibrahim, R.S., "Dynamic Modeling of Structures from Measured Complex Modes," AIAA Journal, Vol. 21, No. 3, pp. 898-901, March 1983.

Ibrahim, R.S., "Correlation of Analysis and Test in Modeling of Structures: Assessment and Review," Structural Safety Evaluation Based on System Identification Approaches, H.G. Natke and J.T.P. Yao, Editors, Published by Friedr. Vieweg and Sohn, Germany, 1988.

Jeary, A.P., and Ellis, B.R., "Vibration Tests of Structures at Varied Amplitudes," Dynamic Response of Structures: Experimentation, Observation, Prediction and Control, G. Hart, Editor, ASCE, 1981.

Leipholtz, H.H.E., Abdel-Rohman, M., "Control of Structures," Martinus Nijhoff Publishers, 1986.

Liu, S.-C., and Yao, J.T.P., "Structural Identification Concept.," Journal of the Structural Division, ASCE, Vol. 104, No. ST12, pp. 1845-1858, Dec., 1978.

Natke, H.g., and Yao, J.T.P.(Editors), "Structural Safety Evaluation Based on System Identification Approaches," Friedr. Vieweg and Sohn, Germany, 1988.

Neuss, C.F., Maison, B.F., and Bouwkamp, J.G., " A Study of Computer Modeling Formulation and Special Analytical Procedures for Earthquake Response of Multistory Building," A Report to the National Science Foundation, J.G. Bouwkamp, Inc., Berkeley, CA, 1983.

Nielsen, N.N., "Vibration Tests of a Nine-Story Steel Frame Building," Journal of the Engineering Mechanics Division, ASCE, Vol. 92, No. EM1, pp. 81-110, Feb.,1966.

Schenck, "5900 Digital Servo Controller Operator's manual," No. P/N 590000 rev.c.

Schiff, A.J., "Identification of Large Structures Using Data from Ambient and Low Level Excitation," System Identification of Vibrating Structures, W.D. Pilkey and R. Cohen, Editors, ASME, 1972.

Simiu, E. and Scanlan, R.H., "Wind Effects on Structures," Wiley, New York, 1978.

Soong, T.T., "Active Structural Control in Civil Engineering," National Center for Earthquake Engineering Research, Technical Report No. NCEER-87-0023, 1987.

Stephen, R.M., Wilson, E.L., and Stander, N., "Dynamic Properties of a Thirty Story Condominium Tower Building," Report No. UCB/EERC-85/03, Earthquake Engineering Research Center, University of California, Berkeley, 1985.

Ward, H.S., and Crawford, R., "Wind-Induced Vibrations and Building Modes," Bulletin of the Seismological Society of America, Vol. 56, No. 4, pp. 793-813, August 1966.

Yao, J.T.P., "Safety and Reliability of Existing Structures," Pitman Advanced Publishing program, 1985.

APPENDIX - A

SPECIFICATIONS OF THE HARDWARE AND SOFTWARE USED FOR THE MODAL TEST

A.1 General

The specifications and/or features of the exciter, signal processing hardware and software, and accelerometers employed for the closed-loop modal test are presented.

A.2 Linear Inertia-mass Exciter

The hardware of the linear inertia-mass exciter consists of: (a) An inner shell weighing 1500 lbs that is designed for attachment to the test structure; (b) a movable outer shell which provides up to 3550 lbs weight for an active mass. The outer shell glides on linear dry-friction bearings; (c) a cylinder with 12 inches of stroke and 2.5 square inch cross sectional area connects the movable outer shell to the inner shell; (d) a servo-valve that controls the displacement response through the hydraulic pressure; and, (e) an LVDT (linear variable differential transformer) within the moving piston for displacement feedback.

A.3 HP 3565S Signal Processing Hardware

The HP 3565S signal processing hardware consists of a main frame, signal processing modules, input modules, and source modules. The specifications and/or functions of these modules are given in the following.

A.3.1 HP 35651A Signal Processing Module

The functions of the signal processing module are:

- (i) Transfers the acquired data from the input channel to the host computer;
- (ii) High speed signal processing operations such as Fast Fourier Transformation (FFT),

weighting functions (windowing), and other operations such as forward or inverse of a complex FFT, addition, subtraction, and multiplication of any two complex blocks, and a conjugate of a complex block; and,

- (iii) Stores the filtered and digitized time data directly onto a throughput disc for later processing and display.

A.3.2 HP 35655A 8-Channel Input Module:

The input module measures the eight channels within a 7.6 micro Hz to 12.8 Hz frequency band and with a dynamic range of 72 db. This module consists of an analog to digital converter (ADC), an anti-aliasing filter, a digital to analog convertor (DAC), and a digital hardware filter. Three signal input modes are possible: (i) voltage: pseudo differential input with full scale ranges of 1.26 milli V to 39 V; (ii) charge mode: eliminates the need for external charge amplifiers for accelerometer operation; (iii) 4 milli Amp constant current source to provide power to accelerometers.

The built-in anti-aliasing filter (low-pass analog filter) practically eliminates aliasing error. The digital filter adjusts the filter bandwidth depending on the frequency and eliminates any undesired harmonics that do not correspond to the excitation. After filtering the signal, the data is transferred to the signal processing module.

A.3.3 HP 35653A Source Module:

The source module generates the swept-sine excitation signal at each frequency point and waits for the input module to measure the response signals. After the data is transferred to the signal processing module, the source module generates the excitation signal for the next frequency point.

A.4 HP SINE Signal Processing Software

Some of the features of HP SINE signal processing software are:

- (a) Autolevel feature (optional): This controls the level of exciter force output by adjusting the signal level from the source module.
- (b) Autorange feature (optional): This feature automatically increases the input range when an overload occurs or decreases the range when underload occurs;
- (c) Autoresolution feature (optional). This feature automatically adjusts the frequency resolution to make it either finer or courser depending on the changes in response amplitude.
- (d) Log-sweep or linear-sweep feature: This feature allows frequency domain measurements at logarithmically or linearly spaced frequency intervals.
- (e) Sweep direction feature: This feature allows the measurement to sweep up, sweep down, or take continuous readings at a frequency until this frequency is changed by the user.
- (f) Allows multiple display of data such as linear spectrum, power spectrum, and frequency response function. Time histories of responses from up to 16 channels can be displayed simultaneously in order to monitor and verify meaningful accelerometer signals. This is helpful in ascertaining whether the key accelerometers are recording properly.

A.5 PCB 483 B17 Accelerometers

The specifications of PCB B17 accelerometers are: (a) Amplitude range of ± 2.5 g with a resolution of 0.0001 g; (b) nominal sensitivity of 1 Volt/g; (c) frequency range of 0.025 to 800 Hz ($\pm 5\%$ error) and 0.01 to 1200 Hz ($\pm 10\%$ error).

APPENDIX - B

NORMALIZED MODAL VECTORS AND FLEXIBILITY

B.1 Mass-orthonormal Modal Vectors

The mass-normalized modal vectors can be obtained from the modal test (Allemang, 1990) by the following method.

If the modal tests are conducted with m measurement degrees of freedom (measurement points times measurement directions) and with force reference points at m points, the frequency response function matrix $[H(\omega)]$ consists of m^2 frequency response functions. The frequency response function matrix is represented as:

$$[H(\omega)] = \begin{bmatrix} H_{11}(\omega) & \dots & H_{1m}(\omega) \\ \vdots & \ddots & \vdots \\ H_{m1}(\omega) & \dots & H_{mm}(\omega) \end{bmatrix} \quad (\text{B-1})$$

where $H_{ik}(\omega)$ = frequency Response function at i -th degree of freedom due to input force at k

The k -th column of $[H(\omega)]$ measured by modal test is represented as follows:

$$\begin{bmatrix} H_{1k}(\omega) \\ \vdots \\ H_{ik}(\omega) \\ \vdots \\ H_{mk}(\omega) \end{bmatrix} = \sum_{r=1}^N \frac{(A_r)_k}{j\omega - \lambda_r} + \frac{(A_r^*)_k}{j\omega - \lambda_r^*} \quad (\text{B-2})$$

where N = number of modal frequencies

r = mode number

A_r = residue

λ_r = system pole = $\sigma_r + j\omega_r$

For any particular mode, m modal frequencies and m residues can be obtained by

post processing algorithm. The residue matrix, directly related to the modal vector, is shown below:

$$[A_r] = Q_r \{\psi\}_r \{\psi\}_r^T \quad (B-3)$$

where $[A_r]$ = residue matrix

Q_r = scaling constant

ψ_r = modal vector at r th mode

The equation is rewritten for only k th column at r th mode as follows:

$$\begin{bmatrix} A_{1k} \\ \vdots \\ A_{ik} \\ \vdots \\ A_{mk} \end{bmatrix} = Q_r \begin{bmatrix} \psi_1 \psi_k \\ \vdots \\ \psi_i \psi_k \\ \vdots \\ \psi_m \psi_k \end{bmatrix} = Q_r \psi_{kr} \begin{bmatrix} \psi_1 \\ \vdots \\ \psi_i \\ \vdots \\ \psi_m \end{bmatrix} \quad (B-4)$$

$$A_{qqr} = Q_r \psi_{qr} \psi_{qr} \quad (B-5)$$

where A_r = driving point residue

ψ_r = driving point modal coefficient

From this relation, the modal coefficients at any mode r can be obtained from the residue matrix at mode r. The modal vector scaling to calculate the mass-normalized modal vectors is as follows:

$$Q_r = \frac{1}{j 2M_r \omega_r} \quad (B-6)$$

The modal mass is unity and hence,

$$Q_r = \frac{1}{j 2\omega_r} \quad (B-7)$$

The scaled modal coefficient at the driving point can be obtained from the following relation:

$$\Psi_{qr} = \sqrt{\frac{A_{qgr}}{Q_r}} \quad (\text{B-8})$$

The mass-normalized modal vectors at any mode r can be determined from the following relation:

$$[\Psi]_r = \frac{1}{Q_r \Psi_{qr}} [A]_r \quad (\text{B-9})$$

B.2 Flexibility

After obtaining the unit mass normalized modal vectors, the flexibility can be determined from the following relation:

$$[\Psi]^T [M] [\Psi] = [I] \quad (\text{B-10})$$

$$[\Psi]^T [K] [\Psi] = [\omega^2] \quad (\text{B-11})$$

where [M] = mass matrix

[K] = stiffness matrix

ω = natural frequency (radian/sec)

[Ψ] = unit mass normalized modal vectors

The flexibility matrix [f] can now be expressed as:

$$[f] = [\Psi] [\omega^2]^{-1} [\Psi]^T \quad (\text{B-12})$$

where [Ψ] = experimentally determined unit mass normalized modal vectors arranged from left to right in order from lower to higher frequencies.

[ω^2] = diagonal matrix of the square of natural frequencies (radian/sec) from lower to higher frequencies.

**NATIONAL CENTER FOR EARTHQUAKE ENGINEERING RESEARCH
LIST OF TECHNICAL REPORTS**

The National Center for Earthquake Engineering Research (NCEER) publishes technical reports on a variety of subjects related to earthquake engineering written by authors funded through NCEER. These reports are available from both NCEER's Publications Department and the National Technical Information Service (NTIS). Requests for reports should be directed to the Publications Department, National Center for Earthquake Engineering Research, State University of New York at Buffalo, Red Jacket Quadrangle, Buffalo, New York 14261. Reports can also be requested through NTIS, 5285 Port Royal Road, Springfield, Virginia 22161. NTIS accession numbers are shown in parenthesis, if available.

- NCEER-87-0001 "First-Year Program in Research, Education and Technology Transfer," 3/5/87, (PB88-134275/AS).
- NCEER-87-0002 "Experimental Evaluation of Instantaneous Optimal Algorithms for Structural Control," by R.C. Lin, T.T. Soong and A.M. Reinhorn, 4/20/87, (PB88-134341/AS).
- NCEER-87-0003 "Experimentation Using the Earthquake Simulation Facilities at University at Buffalo," by A.M. Reinhorn and R.L. Ketter, to be published.
- NCEER-87-0004 "The System Characteristics and Performance of a Shaking Table," by J.S. Hwang, K.C. Chang and G.C. Lee, 6/1/87, (PB88-134259/AS). This report is available only through NTIS (see address given above).
- NCEER-87-0005 "A Finite Element Formulation for Nonlinear Viscoplastic Material Using a Q Model," by O. Gyebe and G. Dasgupta, 11/2/87, (PB88-213764/AS).
- NCEER-87-0006 "Symbolic Manipulation Program (SMP) - Algebraic Codes for Two and Three Dimensional Finite Element Formulations," by X. Lee and G. Dasgupta, 11/9/87, (PB88-219522/AS).
- NCEER-87-0007 "Instantaneous Optimal Control Laws for Tall Buildings Under Seismic Excitations," by J.N. Yang, A. Akbarpour and P. Ghaemmaghami, 6/10/87, (PB88-134333/AS).
- NCEER-87-0008 "IDARC: Inelastic Damage Analysis of Reinforced Concrete Frame - Shear-Wall Structures," by Y.J. Park, A.M. Reinhorn and S.K. Kunnath, 7/20/87, (PB88-134325/AS).
- NCEER-87-0009 "Liquefaction Potential for New York State: A Preliminary Report on Sites in Manhattan and Buffalo," by M. Budhu, V. Vijayakumar, R.F. Giese and L. Baumgras, 8/31/87, (PB88-163704/AS). This report is available only through NTIS (see address given above).
- NCEER-87-0010 "Vertical and Torsional Vibration of Foundations in Inhomogeneous Media," by A.S. Veletsos and K.W. Dotson, 6/1/87, (PB88-134291/AS).
- NCEER-87-0011 "Seismic Probabilistic Risk Assessment and Seismic Margins Studies for Nuclear Power Plants," by Howard H.M. Hwang, 6/15/87, (PB88-134267/AS).
- NCEER-87-0012 "Parametric Studies of Frequency Response of Secondary Systems Under Ground-Acceleration Excitations," by Y. Yong and Y.K. Lin, 6/10/87, (PB88-134309/AS).
- NCEER-87-0013 "Frequency Response of Secondary Systems Under Seismic Excitation," by J.A. HoLung, J. Cai and Y.K. Lin, 7/31/87, (PB88-134317/AS).
- NCEER-87-0014 "Modelling Earthquake Ground Motions in Seismically Active Regions Using Parametric Time Series Methods," by G.W. Ellis and A.S. Cakmak, 8/25/87, (PB88-134283/AS).
- NCEER-87-0015 "Detection and Assessment of Seismic Structural Damage," by E. DiPasquale and A.S. Cakmak, 8/25/87, (PB88-163712/AS).
- NCEER-87-0016 "Pipeline Experiment at Parkfield, California," by J. Isenberg and E. Richardson, 9/15/87, (PB88-163720/AS). This report is available only through NTIS (see address given above).

- NCEER-87-0017 "Digital Simulation of Seismic Ground Motion," by M. Shinozuka, G. Deodatis and T. Harada, 8/31/87, (PB88-155197/AS). This report is available only through NTIS (see address given above).
- NCEER-87-0018 "Practical Considerations for Structural Control: System Uncertainty, System Time Delay and Truncation of Small Control Forces," J.N. Yang and A. Akbarpour, 8/10/87, (PB88-163738/AS).
- NCEER-87-0019 "Modal Analysis of Nonclassically Damped Structural Systems Using Canonical Transformation," by J.N. Yang, S. Sarkani and F.X. Long, 9/27/87, (PB88-187851/AS).
- NCEER-87-0020 "A Nonstationary Solution in Random Vibration Theory," by J.R. Red-Horse and P.D. Spanos, 11/3/87, (PB88-163746/AS).
- NCEER-87-0021 "Horizontal Impedances for Radially Inhomogeneous Viscoelastic Soil Layers," by A.S. Veletsos and K.W. Dotson, 10/15/87, (PB88-150859/AS).
- NCEER-87-0022 "Seismic Damage Assessment of Reinforced Concrete Members," by Y.S. Chung, C. Meyer and M. Shinozuka, 10/9/87, (PB88-150867/AS). This report is available only through NTIS (see address given above).
- NCEER-87-0023 "Active Structural Control in Civil Engineering," by T.T. Soong, 11/11/87, (PB88-187778/AS).
- NCEER-87-0024 Vertical and Torsional Impedances for Radially Inhomogeneous Viscoelastic Soil Layers," by K.W. Dotson and A.S. Veletsos, 12/87, (PB88-187786/AS).
- NCEER-87-0025 "Proceedings from the Symposium on Seismic Hazards, Ground Motions, Soil-Liquefaction and Engineering Practice in Eastern North America," October 20-22, 1987, edited by K.H. Jacob, 12/87, (PB88-188115/AS).
- NCEER-87-0026 "Report on the Whittier-Narrows, California, Earthquake of October 1, 1987," by J. Pantelic and A. Reinhorn, 11/87, (PB88-187752/AS). This report is available only through NTIS (see address given above).
- NCEER-87-0027 "Design of a Modular Program for Transient Nonlinear Analysis of Large 3-D Building Structures," by S. Srivastav and J.F. Abel, 12/30/87, (PB88-187950/AS).
- NCEER-87-0028 "Second-Year Program in Research, Education and Technology Transfer," 3/8/88, (PB88-219480/AS).
- NCEER-88-0001 "Workshop on Seismic Computer Analysis and Design of Buildings With Interactive Graphics," by W. McGuire, J.F. Abel and C.H. Conley, 1/18/88, (PB88-187760/AS).
- NCEER-88-0002 "Optimal Control of Nonlinear Flexible Structures," by J.N. Yang, F.X. Long and D. Wong, 1/22/88, (PB88-213772/AS).
- NCEER-88-0003 "Substructuring Techniques in the Time Domain for Primary-Secondary Structural Systems," by G.D. Manolis and G. Juhn, 2/10/88, (PB88-213780/AS).
- NCEER-88-0004 "Iterative Seismic Analysis of Primary-Secondary Systems," by A. Singhal, L.D. Lutes and P.D. Spanos, 2/23/88, (PB88-213798/AS).
- NCEER-88-0005 "Stochastic Finite Element Expansion for Random Media," by P.D. Spanos and R. Ghanem, 3/14/88, (PB88-213806/AS).
- NCEER-88-0006 "Combining Structural Optimization and Structural Control," by F.Y. Cheng and C.P. Pantelides, 1/10/88, (PB88-213814/AS).
- NCEER-88-0007 "Seismic Performance Assessment of Code-Designed Structures," by H.H.-M. Hwang, J.-W. Jaw and H.-J. Shau, 3/20/88, (PB88-219423/AS).

- NCEER-88-0008 "Reliability Analysis of Code-Designed Structures Under Natural Hazards," by H.H-M. Hwang, H. Ushiba and M. Shinozuka, 2/29/88, (PB88-229471/AS).
- NCEER-88-0009 "Seismic Fragility Analysis of Shear Wall Structures," by J-W Jaw and H.H-M. Hwang, 4/30/88, (PB89-102867/AS).
- NCEER-88-0010 "Base Isolation of a Multi-Story Building Under a Harmonic Ground Motion - A Comparison of Performances of Various Systems," by F-G Fan, G. Ahmadi and I.G. Tadjbakhsh, 5/18/88, (PB89-122238/AS).
- NCEER-88-0011 "Seismic Floor Response Spectra for a Combined System by Green's Functions," by F.M. Lavelle, L.A. Bergman and P.D. Spanos, 5/1/88, (PB89-102875/AS).
- NCEER-88-0012 "A New Solution Technique for Randomly Excited Hysteretic Structures," by G.Q. Cai and Y.K. Lin, 5/16/88, (PB89-102883/AS).
- NCEER-88-0013 "A Study of Radiation Damping and Soil-Structure Interaction Effects in the Centrifuge," by K. Weissman, supervised by J.H. Prevost, 5/24/88, (PB89-144703/AS).
- NCEER-88-0014 "Parameter Identification and Implementation of a Kinematic Plasticity Model for Frictional Soils," by J.H. Prevost and D.V. Griffiths, to be published.
- NCEER-88-0015 "Two- and Three- Dimensional Dynamic Finite Element Analyses of the Long Valley Dam," by D.V. Griffiths and J.H. Prevost, 6/17/88, (PB89-144711/AS).
- NCEER-88-0016 "Damage Assessment of Reinforced Concrete Structures in Eastern United States," by A.M. Reinhorn, M.J. Seidel, S.K. Kunnath and Y.J. Park, 6/15/88, (PB89-122220/AS).
- NCEER-88-0017 "Dynamic Compliance of Vertically Loaded Strip Foundations in Multilayered Viscoelastic Soils," by S. Ahmad and A.S.M. Israil, 6/17/88, (PB89-102891/AS).
- NCEER-88-0018 "An Experimental Study of Seismic Structural Response With Added Viscoelastic Dampers," by R.C. Lin, Z. Liang, T.T. Soong and R.H. Zhang, 6/30/88, (PB89-122212/AS).
- NCEER-88-0019 "Experimental Investigation of Primary - Secondary System Interaction," by G.D. Manolis, G. Juhn and A.M. Reinhorn, 5/27/88, (PB89-122204/AS).
- NCEER-88-0020 "A Response Spectrum Approach For Analysis of Nonclassically Damped Structures," by J.N. Yang, S. Sarkani and F.X. Long, 4/22/88, (PB89-102909/AS).
- NCEER-88-0021 "Seismic Interaction of Structures and Soils: Stochastic Approach," by A.S. Veletsos and A.M. Prasad, 7/21/88, (PB89-122196/AS).
- NCEER-88-0022 "Identification of the Serviceability Limit State and Detection of Seismic Structural Damage," by E. DiPasquale and A.S. Cakmak, 6/15/88, (PB89-122188/AS).
- NCEER-88-0023 "Multi-Hazard Risk Analysis: Case of a Simple Offshore Structure," by B.K. Bhartia and E.H. Vanmarcke, 7/21/88, (PB89-145213/AS).
- NCEER-88-0024 "Automated Seismic Design of Reinforced Concrete Buildings," by Y.S. Chung, C. Meyer and M. Shinozuka, 7/5/88, (PB89-122170/AS).
- NCEER-88-0025 "Experimental Study of Active Control of MDOF Structures Under Seismic Excitations," by L.L. Chung, R.C. Lin, T.T. Soong and A.M. Reinhorn, 7/10/88, (PB89-122600/AS).
- NCEER-88-0026 "Earthquake Simulation Tests of a Low-Rise Metal Structure," by J.S. Hwang, K.C. Chang, G.C. Lee and R.L. Ketter, 8/1/88, (PB89-102917/AS).
- NCEER-88-0027 "Systems Study of Urban Response and Reconstruction Due to Catastrophic Earthquakes," by F. Kozin and H.K. Zhou, 9/22/88, (PB90-162348/AS).

- NCEER-88-0028 "Seismic Fragility Analysis of Plane Frame Structures," by H.H-M. Hwang and Y.K. Low, 7/31/88, (PB89-131445/AS).
- NCEER-88-0029 "Response Analysis of Stochastic Structures," by A. Kardara, C. Bucher and M. Shinozuka, 9/22/88, (PB89-174429/AS).
- NCEER-88-0030 "Nonnormal Accelerations Due to Yielding in a Primary Structure," by D.C.K. Chen and L.D. Lutes, 9/19/88, (PB89-131437/AS).
- NCEER-88-0031 "Design Approaches for Soil-Structure Interaction," by A.S. Veletsos, A.M. Prasad and Y. Tang, 12/30/88, (PB89-174437/AS).
- NCEER-88-0032 "A Re-evaluation of Design Spectra for Seismic Damage Control," by C.J. Turkstra and A.G. Tallin, 11/7/88, (PB89-145221/AS).
- NCEER-88-0033 "The Behavior and Design of Noncontact Lap Splices Subjected to Repeated Inelastic Tensile Loading," by V.E. Sagan, P. Gergely and R.N. White, 12/8/88, (PB89-163737/AS).
- NCEER-88-0034 "Seismic Response of Pile Foundations," by S.M. Mamoon, P.K. Banerjee and S. Ahmad, 11/1/88, (PB89-145239/AS).
- NCEER-88-0035 "Modeling of R/C Building Structures With Flexible Floor Diaphragms (IDARC2)," by A.M. Reinhorn, S.K. Kunnath and N. Panahshahi, 9/7/88, (PB89-207153/AS).
- NCEER-88-0036 "Solution of the Dam-Reservoir Interaction Problem Using a Combination of FEM, BEM with Particular Integrals, Modal Analysis, and Substructuring," by C-S. Tsai, G.C. Lee and R.L. Ketter, 12/31/88, (PB89-207146/AS).
- NCEER-88-0037 "Optimal Placement of Actuators for Structural Control," by F.Y. Cheng and C.P. Pantelides, 8/15/88, (PB89-162846/AS).
- NCEER-88-0038 "Teflon Bearings in Aseismic Base Isolation: Experimental Studies and Mathematical Modeling," by A. Mokha, M.C. Constantinou and A.M. Reinhorn, 12/5/88, (PB89-218457/AS).
- NCEER-88-0039 "Seismic Behavior of Flat Slab High-Rise Buildings in the New York City Area," by P. Weidlinger and M. Ettouney, 10/15/88, (PB90-145681/AS).
- NCEER-88-0040 "Evaluation of the Earthquake Resistance of Existing Buildings in New York City," by P. Weidlinger and M. Ettouney, 10/15/88, to be published.
- NCEER-88-0041 "Small-Scale Modeling Techniques for Reinforced Concrete Structures Subjected to Seismic Loads," by W. Kim, A. El-Attar and R.N. White, 11/22/88, (PB89-189625/AS).
- NCEER-88-0042 "Modeling Strong Ground Motion from Multiple Event Earthquakes," by G.W. Ellis and A.S. Cakmak, 10/15/88, (PB89-174445/AS).
- NCEER-88-0043 "Nonstationary Models of Seismic Ground Acceleration," by M. Grigoriu, S.E. Ruiz and E. Rosenblueth, 7/15/88, (PB89-189617/AS).
- NCEER-88-0044 "SARCF User's Guide: Seismic Analysis of Reinforced Concrete Frames," by Y.S. Chung, C. Meyer and M. Shinozuka, 11/9/88, (PB89-174452/AS).
- NCEER-88-0045 "First Expert Panel Meeting on Disaster Research and Planning," edited by J. Pantelic and J. Stoye, 9/15/88, (PB89-174460/AS).
- NCEER-88-0046 "Preliminary Studies of the Effect of Degrading Infill Walls on the Nonlinear Seismic Response of Steel Frames," by C.Z. Chrysostomou, P. Gergely and J.F. Abel, 12/19/88, (PB89-208383/AS).

- NCEER-88-0047 "Reinforced Concrete Frame Component Testing Facility - Design, Construction, Instrumentation and Operation," by S.P. Pessiki, C. Conley, T. Bond, P. Gergely and R.N. White, 12/16/88, (PB89-174478/AS).
- NCEER-89-0001 "Effects of Protective Cushion and Soil Compliancy on the Response of Equipment Within a Seismically Excited Building," by J.A. HoLung, 2/16/89, (PB89-207179/AS).
- NCEER-89-0002 "Statistical Evaluation of Response Modification Factors for Reinforced Concrete Structures," by H.H.-M. Hwang and J.-W. Jaw, 2/17/89, (PB89-207187/AS).
- NCEER-89-0003 "Hysteretic Columns Under Random Excitation," by G.-Q. Cai and Y.K. Lin, 1/9/89, (PB89-196513/AS).
- NCEER-89-0004 "Experimental Study of 'Elephant Foot Bulge' Instability of Thin-Walled Metal Tanks," by Z.-H. Jia and R.L. Ketter, 2/22/89, (PB89-207195/AS).
- NCEER-89-0005 "Experiment on Performance of Buried Pipelines Across San Andreas Fault," by J. Isenberg, E. Richardson and T.D. O'Rourke, 3/10/89, (PB89-218440/AS).
- NCEER-89-0006 "A Knowledge-Based Approach to Structural Design of Earthquake-Resistant Buildings," by M. Subramani, P. Gergely, C.H. Conley, J.F. Abel and A.H. Zaghw, 1/15/89, (PB89-218465/AS).
- NCEER-89-0007 "Liquefaction Hazards and Their Effects on Buried Pipelines," by T.D. O'Rourke and P.A. Lane, 2/1/89, (PB89-218481).
- NCEER-89-0008 "Fundamentals of System Identification in Structural Dynamics," by H. Imai, C.-B. Yun, O. Maruyama and M. Shinozuka, 1/26/89, (PB89-207211/AS).
- NCEER-89-0009 "Effects of the 1985 Michoacan Earthquake on Water Systems and Other Buried Lifelines in Mexico," by A.G. Ayala and M.J. O'Rourke, 3/8/89, (PB89-207229/AS).
- NCEER-89-R010 "NCEER Bibliography of Earthquake Education Materials," by K.E.K. Ross, Second Revision, 9/1/89, (PB90-125352/AS).
- NCEER-89-0011 "Inelastic Three-Dimensional Response Analysis of Reinforced Concrete Building Structures (IDARC-3D), Part I - Modeling," by S.K. Kunnath and A.M. Reinhorn, 4/17/89, (PB90-114612/AS).
- NCEER-89-0012 "Recommended Modifications to ATC-14," by C.D. Poland and J.O. Malley, 4/12/89, (PB90-108648/AS).
- NCEER-89-0013 "Repair and Strengthening of Beam-to-Column Connections Subjected to Earthquake Loading," by M. Corazao and A.J. Durrani, 2/28/89, (PB90-109885/AS).
- NCEER-89-0014 "Program EXKAL2 for Identification of Structural Dynamic Systems," by O. Maruyama, C.-B. Yun, M. Hoshiya and M. Shinozuka, 5/19/89, (PB90-109877/AS).
- NCEER-89-0015 "Response of Frames With Bolted Semi-Rigid Connections, Part I - Experimental Study and Analytical Predictions," by P.J. DiCorso, A.M. Reinhorn, J.R. Dickerson, J.B. Radzimirski and W.L. Harper, 6/1/89, to be published.
- NCEER-89-0016 "ARMA Monte Carlo Simulation in Probabilistic Structural Analysis," by P.D. Spanos and M.P. Mignolet, 7/10/89, (PB90-109893/AS).
- NCEER-89-P017 "Preliminary Proceedings from the Conference on Disaster Preparedness - The Place of Earthquake Education in Our Schools," Edited by K.E.K. Ross, 6/23/89.
- NCEER-89-0017 "Proceedings from the Conference on Disaster Preparedness - The Place of Earthquake Education in Our Schools," Edited by K.E.K. Ross, 12/31/89, (PB90-207895).

- NCEER-89-0018 "Multidimensional Models of Hysteretic Material Behavior for Vibration Analysis of Shape Memory Energy Absorbing Devices, by E.J. Graesser and F.A. Cozzarelli, 6/7/89, (PB90-164146/AS).
- NCEER-89-0019 "Nonlinear Dynamic Analysis of Three-Dimensional Base Isolated Structures (3D-BASIS)," by S. Nagarajaiah, A.M. Reinhorn and M.C. Constantinou, 8/3/89, (PB90-161936/AS).
- NCEER-89-0020 "Structural Control Considering Time-Rate of Control Forces and Control Rate Constraints," by F.Y. Cheng and C.P. Pantelides, 8/3/89, (PB90-120445/AS).
- NCEER-89-0021 "Subsurface Conditions of Memphis and Shelby County," by K.W. Ng, T-S. Chang and H-H.M. Hwang, 7/26/89, (PB90-120437/AS).
- NCEER-89-0022 "Seismic Wave Propagation Effects on Straight Jointed Buried Pipelines," by K. Elhadi and M.J. O'Rourke, 8/24/89, (PB90-162322/AS).
- NCEER-89-0023 "Workshop on Serviceability Analysis of Water Delivery Systems," edited by M. Grigoriu, 3/6/89, (PB90-127424/AS).
- NCEER-89-0024 "Shaking Table Study of a 1/5 Scale Steel Frame Composed of Tapered Members," by K.C. Chang, J.S. Hwang and G.C. Lee, 9/18/89, (PB90-160169/AS).
- NCEER-89-0025 "DYNA1D: A Computer Program for Nonlinear Seismic Site Response Analysis - Technical Documentation," by Jean H. Prevost, 9/14/89, (PB90-161944/AS).
- NCEER-89-0026 "1:4 Scale Model Studies of Active Tendon Systems and Active Mass Dampers for Aseismic Protection," by A.M. Reinhorn, T.T. Soong, R.C. Lin, Y.P. Yang, Y. Fukao, H. Abe and M. Nakai, 9/15/89, (PB90-173246/AS).
- NCEER-89-0027 "Scattering of Waves by Inclusions in a Nonhomogeneous Elastic Half Space Solved by Boundary Element Methods," by P.K. Hadley, A. Askar and A.S. Cakmak, 6/15/89, (PB90-145699/AS).
- NCEER-89-0028 "Statistical Evaluation of Deflection Amplification Factors for Reinforced Concrete Structures," by H.H.M. Hwang, J-W. Jaw and A.L. Ch'ng, 8/31/89, (PB90-164633/AS).
- NCEER-89-0029 "Bedrock Accelerations in Memphis Area Due to Large New Madrid Earthquakes," by H.H.M. Hwang, C.H.S. Chen and G. Yu, 11/7/89, (PB90-162330/AS).
- NCEER-89-0030 "Seismic Behavior and Response Sensitivity of Secondary Structural Systems," by Y.Q. Chen and T.T. Soong, 10/23/89, (PB90-164658/AS).
- NCEER-89-0031 "Random Vibration and Reliability Analysis of Primary-Secondary Structural Systems," by Y. Ibrahim, M. Grigoriu and T.T. Soong, 11/10/89, (PB90-161951/AS).
- NCEER-89-0032 "Proceedings from the Second U.S. - Japan Workshop on Liquefaction, Large Ground Deformation and Their Effects on Lifelines, September 26-29, 1989," Edited by T.D. O'Rourke and M. Hanada, 12/1/89, (PB90-209388/AS).
- NCEER-89-0033 "Deterministic Model for Seismic Damage Evaluation of Reinforced Concrete Structures," by J.M. Bracci, A.M. Reinhorn, J.B. Mander and S.K. Kunnath, 9/27/89.
- NCEER-89-0034 "On the Relation Between Local and Global Damage Indices," by E. DiPasquale and A.S. Cakmak, 8/15/89, (PB90-173865).
- NCEER-89-0035 "Cyclic Undrained Behavior of Nonplastic and Low Plasticity Silts," by A.J. Walker and H.E. Stewart, 7/26/89, (PB90-183518/AS).
- NCEER-89-0036 "Liquefaction Potential of Surficial Deposits in the City of Buffalo, New York," by M. Budhu, R. Giese and L. Baumgrass, 1/17/89, (PB90-208455/AS).

- NCEER-89-0037 "A Deterministic Assessment of Effects of Ground Motion Incoherence," by A.S. Veletsos and Y. Tang, 7/15/89, (PB90-164294/AS).
- NCEER-89-0038 "Workshop on Ground Motion Parameters for Seismic Hazard Mapping," July 17-18, 1989, edited by R.V. Whitman, 12/1/89, (PB90-173923/AS).
- NCEER-89-0039 "Seismic Effects on Elevated Transit Lines of the New York City Transit Authority," by C.J. Costantino, C.A. Miller and E. Heymsfield, 12/26/89, (PB90-207887/AS).
- NCEER-89-0040 "Centrifugal Modeling of Dynamic Soil-Structure Interaction," by K. Weissman, Supervised by J.H. Prevost, 5/10/89, (PB90-207879/AS).
- NCEER-89-0041 "Linearized Identification of Buildings With Cores for Seismic Vulnerability Assessment," by I.K. Ho and A.E. Aktan, 11/1/89, (PB90-251943/AS).
- NCEER-90-0001 "Geotechnical and Lifeline Aspects of the October 17, 1989 Loma Prieta Earthquake in San Francisco," by T.D. O'Rourke, H.E. Stewart, F.T. Blackburn and T.S. Dickerman, 1/90, (PB90-208596/AS).
- NCEER-90-0002 "Nonnormal Secondary Response Due to Yielding in a Primary Structure," by D.C.K. Chen and L.D. Lutes, 2/28/90, (PB90-251976/AS).
- NCEER-90-0003 "Earthquake Education Materials for Grades K-12," by K.E.K. Ross, 4/16/90, (PB91-113415/AS).
- NCEER-90-0004 "Catalog of Strong Motion Stations in Eastern North America," by R.W. Busby, 4/3/90, (PB90-251984/AS).
- NCEER-90-0005 "NCEER Strong-Motion Data Base: A User Manual for the GeoBase Release (Version 1.0 for the Sun3)," by P. Friberg and K. Jacob, 3/31/90 (PB90-258062/AS).
- NCEER-90-0006 "Seismic Hazard Along a Crude Oil Pipeline in the Event of an 1811-1812 Type New Madrid Earthquake," by H.H.M. Hwang and C.H.S. Chen, 4/16/90(PB90-258054).
- NCEER-90-0007 "Site-Specific Response Spectra for Memphis Sheahan Pumping Station," by H.H.M. Hwang and C.S. Lee, 5/15/90, (PB91-108811/AS).
- NCEER-90-0008 "Pilot Study on Seismic Vulnerability of Crude Oil Transmission Systems," by T. Ariman, R. Dobry, M. Grigoriu, F. Kozin, M. O'Rourke, T. O'Rourke and M. Shinozuka, 5/25/90, (PB91-108837/AS).
- NCEER-90-0009 "A Program to Generate Site Dependent Time Histories: EQGEN," by G.W. Ellis, M. Srinivasan and A.S. Cakmak, 1/30/90, (PB91-108829/AS).
- NCEER-90-0010 "Active Isolation for Seismic Protection of Operating Rooms," by M.E. Talbott, Supervised by M. Shinozuka, 6/8/9, (PB91-110205/AS).
- NCEER-90-0011 "Program LINEARID for Identification of Linear Structural Dynamic Systems," by C-B. Yun and M. Shinozuka, 6/25/90, (PB91-110312/AS).
- NCEER-90-0012 "Two-Dimensional Two-Phase Elasto-Plastic Seismic Response of Earth Dams," by A.N. Yiagos, Supervised by J.H. Prevost, 6/20/90, (PB91-110197/AS).
- NCEER-90-0013 "Secondary Systems in Base-Isolated Structures: Experimental Investigation, Stochastic Response and Stochastic Sensitivity," by G.D. Manolis, G. Juhn, M.C. Constantinou and A.M. Reinhorn, 7/1/90, (PB91-110320/AS).
- NCEER-90-0014 "Seismic Behavior of Lightly-Reinforced Concrete Column and Beam-Column Joint Details," by S.P. Pessiki, C.H. Conley, P. Gergely and R.N. White, 8/22/90, (PB91-108795/AS).
- NCEER-90-0015 "Two Hybrid Control Systems for Building Structures Under Strong Earthquakes," by J.N. Yang and A. Danielians, 6/29/90, (PB91-125393/AS).

- NCEER-90-0016 "Instantaneous Optimal Control with Acceleration and Velocity Feedback," by J.N. Yang and Z. Li, 6/29/90, (PB91-125401/AS).
- NCEER-90-0017 "Reconnaissance Report on the Northern Iran Earthquake of June 21, 1990," by M. Mehrain, 10/4/90, (PB91-125377/AS).
- NCEER-90-0018 "Evaluation of Liquefaction Potential in Memphis and Shelby County," by T.S. Chang, P.S. Tang, C.S. Lee and H. Hwang, 8/10/90, (PB91-125427/AS).
- NCEER-90-0019 "Experimental and Analytical Study of a Combined Sliding Disc Bearing and Helical Steel Spring Isolation System," by M.C. Constantinou, A.S. Mokha and A.M. Reinhorn, 10/4/90, (PB91-125385/AS).
- NCEER-90-0020 "Experimental Study and Analytical Prediction of Earthquake Response of a Sliding Isolation System with a Spherical Surface," by A.S. Mokha, M.C. Constantinou and A.M. Reinhorn, 10/11/90, (PB91-125419/AS).
- NCEER-90-0021 "Dynamic Interaction Factors for Floating Pile Groups," by G. Gazetas, K. Fan, A. Kaynia and E. Kausel, 9/10/90, (PB91-170381/AS).
- NCEER-90-0022 "Evaluation of Seismic Damage Indices for Reinforced Concrete Structures," by S. Rodríguez-Gómez and A.S. Cakmak, 9/30/90, PB91-171322/AS).
- NCEER-90-0023 "Study of Site Response at a Selected Memphis Site," by H. Desai, S. Ahmad, E.S. Gazetas and M.R. Oh, 10/11/90, (PB91-196857/AS).
- NCEER-90-0024 "A User's Guide to Strongmo: Version 1.0 of NCEER's Strong-Motion Data Access Tool for PCs and Terminals," by P.A. Friberg and C.A.T. Susch, 11/15/90, (PB91-171272/AS).
- NCEER-90-0025 "A Three-Dimensional Analytical Study of Spatial Variability of Seismic Ground Motions," by L-L. Hong and A.H.-S. Ang, 10/30/90, (PB91-170399/AS).
- NCEER-90-0026 "MUMOID User's Guide - A Program for the Identification of Modal Parameters," by S. Rodríguez-Gómez and E. DiPasquale, 9/30/90, (PB91-171298/AS).
- NCEER-90-0027 "SARCF-II User's Guide - Seismic Analysis of Reinforced Concrete Frames," by S. Rodríguez-Gómez, Y.S. Chung and C. Meyer, 9/30/90, (PB91-171280/AS).
- NCEER-90-0028 "Viscous Dampers: Testing, Modeling and Application in Vibration and Seismic Isolation," by N. Makris and M.C. Constantinou, 12/20/90 (PB91-190561/AS).
- NCEER-90-0029 "Soil Effects on Earthquake Ground Motions in the Memphis Area," by H. Hwang, C.S. Lee, K.W. Ng and T.S. Chang, 8/2/90, (PB91-190751/AS).
- NCEER-91-0001 "Proceedings from the Third Japan-U.S. Workshop on Earthquake Resistant Design of Lifeline Facilities and Countermeasures for Soil Liquefaction, December 17-19, 1990," edited by T.D. O'Rourke and M. Hamada, 2/1/91, (PB91-179259/AS).
- NCEER-91-0002 "Physical Space Solutions of Non-Proportionally Damped Systems," by M. Tong, Z. Liang and G.C. Lee, 1/15/91, (PB91-179242/AS).
- NCEER-91-0003 "Kinematic Seismic Response of Single Piles and Pile Groups," by K. Fan, G. Gazetas, A. Kaynia, E. Kausel and S. Ahmad, 1/10/91, to be published.
- NCEER-91-0004 "Theory of Complex Damping," by Z. Liang and G. Lee, to be published.
- NCEER-91-0005 "3D-BASIS - Nonlinear Dynamic Analysis of Three Dimensional Base Isolated Structures: Part II," by S. Nagarajaiah, A.M. Reinhorn and M.C. Constantinou, 2/28/91, (PB91-190553/AS).

- NCEER-91-0006 "A Multidimensional Hysteretic Model for Plasticity Deforming Metals in Energy Absorbing Devices," by E.J. Graesser and F.A. Cozzarelli, 4/9/91.
- NCEER-91-0007 "A Framework for Customizable Knowledge-Based Expert Systems with an Application to a KBES for Evaluating the Seismic Resistance of Existing Buildings," by E.G. Ibarra-Anaya and S.J. Fenves, 4/9/91, (PB91-210930/AS).
- NCEER-91-0008 "Nonlinear Analysis of Steel Frames with Semi-Rigid Connections Using the Capacity Spectrum Method," by G.G. Deierlein, S-H. Hsieh, Y-J. Shen and J.F. Abel, 7/2/91.
- NCEER-91-0009 "Earthquake Education Materials for Grades K-12," by K.E.K. Ross, 4/30/91, (PB91-212142/AS).
- NCEER-91-0010 "Phase Wave Velocities and Displacement Phase Differences in a Harmonically Oscillating Pile," by N. Makris and G. Gazetas, 7/8/91.
- NCEER-91-0011 "Dynamic Characteristics of a Full-Sized Five-Story Steel Structure and a 2/5 Model," by K.C. Chang, G.C. Yao, G.C. Lee, D.S. Hao and Y.C. Yeh," to be published.
- NCEER-91-0012 "Seismic Response of a 2/5 Scale Steel Structure with Added Viscoelastic Dampers," by K.C. Chang, T.T. Soong, S-T. Oh and M.L. Lai, 5/17/91.
- NCEER-91-0013 "Earthquake Response of Retaining Walls; Full-Scale Testing and Computational Modeling," by S. Alampalli and A-W.M. Elgarnal, 6/20/91, to be published.
- NCEER-91-0014 "3D-BASIS-M: Nonlinear Dynamic Analysis of Multiple Building Base Isolated Structures," by P.C. Tsopelas, S. Nagarajaiah, M.C. Constantinou and A.M. Reinhorn, 5/23/91.
- NCEER-91-0015 "Evaluation of SEAOC Design Requirements for Sliding Isolated Structures," by D. Theodossiou and M.C. Constantinou, 6/10/91.
- NCEER-91-0016 "Closed-Loop Modal Testing of a 27-Story Reinforced Concrete Flat Plate-Core Building," by H.R. Somaprasad, T. Toksoy, H. Yoshiyuki and A.E. Aktan, 7/15/91.

